Sukkur IBA Journal of Emerging Technologies (SJET) is the bi-annual research journal published by **Sukkur IBA University**, Pakistan. **SJET** is dedicated to serve as a key resource to provide applied engineering research associated with the Electrical, Electronics and innovations in Energy at the global scale. This Journal publishes manuscripts which are well written by highlighting development in emerging technologies. This Journal covers all branches of Engineering, Science & Emerging Technologies.

Disclaimer: The research material expressed in **Sukkur IBA Journal of Emerging Technologies (SJET)** is sole contribution of the authors. The research contribution of the authors does not reflect the management, advisory board, the editorial board, **Sukkur IBA University** press and the organization to which the authors are affiliated. Manuscripts published in **SJET** shall be processed through double-blind peer-reviewed by the two experts of field. The identities of the experts/reviewers shall remain anonymous to the authors. The Journal shall be published in June i.e. once a year. Neither the **Sukkur IBA University** nor the **SJET** shall be responsible for errors or any consequences highlighted by the reader. The errors and deficiencies in terms of research in manuscript can directly be reported to the authors.

Mission Statement

The mission of **Sukkur IBA Journal of Emerging Technologies (SJET)** is to provide a premier interdisciplinary platform to researchers, scientists and practitioners from the field of engineering in particular, electrical, electronics, renewable and emerging engineering fields for dissemination of their finding and to contribute in the knowledge domain.

Aims & Objectives

Sukkur IBA Journal of Emerging Technologies (SJET) will publish and encourage the submission of critically reviewed manuscripts on the cutting edge research in the field of emerging engineering technologies.

The objectives of **SJET** are:

1. To bring new engineering ideas, research and findings on a single platform.
2. To integrate interdisciplinary research for technological sustainable solution.
3. To provide scholarly platform to connect academia and industries for socio-economic development.

Research Themes

The research focused on but not limited to following core thematic areas:

Renewable Energy Sources and Storage:

- Solar Energy System
- Fuel cell Technology
- Hydro and Wind Energy
- Biomass and Bio-fuels
- Energy Management and Storage
- Energy Devices and Materials

Power Systems and Smart Grids:

- Power Quality Issues and solutions
- Micro grid systems and their Integration Problems
- Design Control and Management
- Energy Management and Environmental Issues
- Hybrid Power System
- Distributed and Co-Generation Systems

- Power Market and Power System Economics

Electrical Machines and Adjustable Speed Drives:

- AC and DC Machines and Drives
- Sensor-less Control
- PIEZO and Electrostatic Actuators
- Machine Design and Equipment Training
- Maintaininace and Fault Diagnosis
- Bearing less Driving Technologies

Power Electronics and its Application:

- Hard-switching and Soft-switching static converters
- Multi-level and Matrix Converters
- Emerging Topologies

- Simulation and Control Power Converters
- Power Factor Correctors
- Active Filters and Total Harmonics Distortions Analysis
- Optoelectronics and Photonic Devices
- Power Semiconductors, Passive Components, and Packaging Technologies
- Switch-mode power Supplies and Automotive
- Applications of Power Electronics in Home Appliance, Industry and Aerospace

High Voltage Engineering and Insulation Technology:

- Micro-electromechanical System (MEMS)
- Power Integrated Circuits (PIC)
- Power Engineering related Technologies
- Power System Stability and Control
- Power System transient Modeling, Simulation and Analysis
- Electromagnetic Transient Programs (EMTP)
- HVDC and FACTS Applications

Nanomaterials/Nanotechnology:

- Sensors and Actuators
- Electronic Thin Films and Integrated Circuits
- Nanogenerators
- Nanomaterials
- Nanotechnology

Communication and Signal Processing:

- Communication& Signal Processing
- Renewable Energy Sources and storages
- Power Systems and Smart Grids
- Electrical Machines and Adjustable Speed Drives
- Power Electronics and its application
- High Voltage Engineering and Insulation Technology
- RF, Microwave and Antenna Design
- Computer Vision, Machine Learning and Artificial Intelligence
- Embedded and VLSI System Design
- Analog and Mixed Signal Circuits
- Control Systems and Robotics
- Biomedical Engineering Systems and Circuits

Biomedical Electronics/ICT:

- Energy-efficient Wireless Body Sensor Networks
- Wireless Power/Energy Transfer in eHealth Applications
- Green and Battery-friendly Wireless Medical Networks
- Renewable Energy and Energy Harvesting for wireless and Body Sensor Networks.
- Telemedicine and Medical IoT
- Medical Video Transmission
- Energy Management for Medical Health Applications
- Role of 5G in Medical Health Applications

Patron's Message

Sukkur IBA University has been imparting education with its core values merit, quality and excellence since its inception. Sukkur IBA University has achieved numerous milestones in a very short span of time that hardly any other university has achieved in the history of Pakistan. The institute continuously being ranked as one of the best Institute in Pakistan by Higher Education Commission (HEC). The distinct service of Sukkur IBA University is to serve rural areas of Sindh and also underprivileged areas of other provinces of Pakistan. Sukkur IBA University is committed to serve targeted youth of Pakistan who is suffering from poverty and deprived of equal opportunity to seek quality education. Sukkur IBA University is successfully undertaking its mission and objectives that lead Pakistan towards socio-economic prosperity.

In continuation of endeavors to touch new horizon in the field of Engineering and Emerging Technologies, Sukkur IBA University publishes an international referred journal. Sukkur IBA University believes that research is an integral part of modern learnings ad development. **Sukkur IBA Journal of Emerging Technologies (SJET)** is the modest effort to contribute and promote the research environment within the university and Pakistan as a whole. SJET is a peer-reviewed and multidisciplinary research journal to publish findings and results of the latest and innovative research in the fields. Following the tradition of Sukkur IBA University, SJET is also aimed at achieving international recognition and high impact research publication in the near future.

Prof. Nisar Ahmed Siddiqui
Sitara-e-Imtiaz
Vice Chancellor
Sukkur IBA University
Patron **SJET**

Editorial

Dear Readers,

It is immense pleasure to present you the first issue of Sukkur IBA Journal of Emerging Technologies (SJET). Sukkur IBA University firmly believes in research environment and has provided a platform for the intellectuals and researchers to share knowledge and new findings on emerging trends in various research areas to solve the difficult technical problems related to the technological advancements in response to the demands of the times. The SJET provided interdisciplinary platform to researchers' community to collaborate, co-innovate and instigate efforts to break the technological barriers. This journal provides the opportunity to gain and present authentic and insightful scientific & technological information on the latest advances in the field of emerging technologies.

The SJET provides invaluable source of information and enables the interested researchers to access the original information they are seeking. The manuscripts submitted in SJET have been followed by double-blind peer-review process, which addresses key issues in the field of emerging engineering technologies. The SJET has endorsed highly standards which are prerequisite for publishing high quality research work. This journal manifests into eco-system for the academician and engineers work together in the pursuit of excellence & innovation, that is why the editorial board of SJET is comprises of academic and industrial researchers from various advanced countries. The journal has adopted Open access policy without charging any publication fees that will certainly increase the readership by providing free access to a wider audience.

On behalf of the SJET, I welcome the submissions for upcoming issue (Volume-1, issue-2, July-December, 2018) and looking forward to receive your valuable feedback.

I hope this journal will make a difference in our perspective and choice of research.

Sincerely,

Dr. Saeed Ahmed Khan
Chief Editor
SJET

Sukkur IBA University, Pakistan

Project and Production Management
Mr. Hassan Abbas, Ms. Suman Najam Shaikh, Mr. Akram Hussain

Contents

Automatic Positioned Controller Parabolic solar Dish Prototype

Asif A.Rahimoon[1], Izhar A.Sohu[1], M.Ishaque Junejo[1], Ali Abbas ,S.Nawaz Shah[1] ,Arslan Ahmed Sohu[2]

Abstract:

This paper discusses the development of dual axis parabolic dish tracker application for automatized position power system. This prototype tackles solar light in solar sterling design system or concentrated photovoltaic design by implementation of digitalize control circuit to enhance Concentrating solar power and Concentrating photovoltaic applications. A normally 121.92cm dish is designed with H-bridge controller technique & Slew drive actuator mode to capture solar irradiances. The surface of dish is polished with 12 aluminum bars to concentrate the solar irradiance in one reflective axis. Economic justification for Pakistan's industries would be possible if these automated based renewable prototypes are promoted in market in compare of single PV panel. This prototype controls the all weather conditions, utilizing real time flexible timing control strategy and photoelectric tracking scheme to provide cost effective product for industrial power generation applications. This locally adaptive material based prototype encouraged the result about 33% efficient with compared to photovoltaic panel.

Keywords: Pakistan Energy future; Solar concentrator; Thermal energy utilization.

1. Introduction

The world-wide rate of countries are utilizing decentralized power system to maintain the energy demand with small power energy system. These mini energy systems can be fabricated with renewable sources such as solar cooker, solar geyser, solar hydrogen productive devices and parabolic solar dish collectors [1, 2]. Utilization of parabolic reflector is proven to be effective through observation of different researchers that worked on heat collector by designing parabolic solar dish [3, 4]. The solar heat collectors are more reliable in operation when the suitable tracking scheme is installed with it. The different heat collectors are used from ancient times in bucolic sites as in 212 BC, Archimedes used sun light to burn roman fleet and in 10th century Ibn Sahl worked on parabolic mirror. The same trend is followed by new researchers on parabolic solar dish to capture heat and dispatch an economical and optimized prototype in market with different applications [5, 6, 7]. In proposed prototype the solar dish is fabricated with aluminum glass that is integrated with controller scheme of tracking with concerned measurement of Azimuth angle to gain efficient sun-light. As by researcher there are different scenarios of designing this prototype on small level application to commercial based with alteration of its tracking control techniques such as PLC, SCADA & Microcontroller to

[1] Faculty of Engineering, Science & Technology (FEST), Indus University Karachi, Pakistan
[2] Department of Electrical Engineering,Sukkur IBA University,Sukkur,Pakisan
Corresponding Email: asif.ahmed@indus.edu.pk

make parabolic heat collector efficient [8, 9, 10].The integrated technology of this proposed system that is comprised of Arduino based dual axis tracker, 12v operating power window motors and sensor fault control strategy to maintain elevation and tilt angles smoothly enhance the future work of power industries.

2. Proposed Dish Prototype

For Pakistan, in rural or desert areas where sunlight appears invariably under seasonal mode, the desired system is proposed to capture the solar irradiance in regular and seasonal mode. With high reflective glass material the heat collection is merged under a single focal point of parabolic dish [11, 12]. The maintenance of solar dish elevation angle and tilt angle is done through LDR actuators and power window motors. The whole tracking of proposed parabolic solar dish is based on Arduino based chip board that regulate the whole system in optimal and efficient mode. The power running actuators get their startup power service from an external battery to improve the remedies of sensor mechanism. The designed automated dual axis tracking prototype is capable to attained high temperature applications like as hot water & steam generation. As in previous research of dual axis the system rotates with their both operative modes which make the tracker slower in perception of heat measurement and sensor functioning so, to improve this state of sensor the optional mode is included in designed parabolic dish prototype that is tested at Indus University Karachi with Latitude 23.9207°N and Longitude 67.0882°E which gives you option to run your dish on single axis or both axis as suitable with your application area.

Fig. 1. Designed Prototype.

3. Hardware Development

The system is integrated with different parts to achieve the efficient output that is also calculated with some algorithms. The adoptive algorithm are included as parabola calculator2.0 for designing parameters of solar dish, solar angle meter for angle calculation of X-axis & Y-axis geometry, Arduino assembly for programming of controller chip, generalized equation are adopted with used of solar geometry tools that are as sun calculator & sun Earth tool for solar positioning and shadow effect rate.The arrangement of these integrated tools are shown in figure 3.
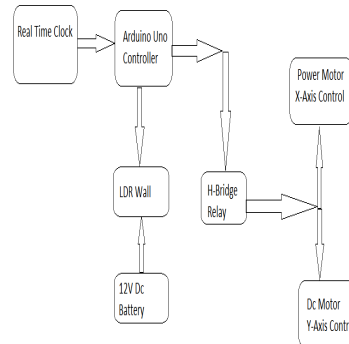
Fig. 2. Block Diagram.

3.1. Parabolic solar Dish design

TABLE I. Detailed sheet of dish.

Sr: No.	Parameters	Values	Units
1	Linear Diam.	14	Ft
2	Diameter	13.12	Ft
3	Depth	2.24	Ft
4	Focal Length	4.724	Ft
5	Volume	4.28	cubic ft
6	F Length/Diam	0.36	N/A
7	Area	134.43	ft^2

TABLE II. Automatic Tracking parameters.

Tracking Control	
Tracking	Dual axis Azimuth and elevation algorithm
Tracking Accuracy	$0.06^0 \cong 1mrad$
Control Scheme	*Arduino Uno based microcontroller*
Control apparatus	
X-axis control Motor with Pin #	180^0 limiting switch # 4
Y-axis control Motor with Pin #	55^0 limiting switch # 5
H-bridge	Relay Based Module
Motor Logical direction Controller	L298 module

3.2. Sensor Configuration

There are a lot of sensors used to run the trackers with opto-electronics technology. Here in this designed prototype we have installed LDR wall that will function with 12v output power. The designed wall is configured with H-Bridge drive module and power motor rotation. As by research mostly implemented motor are servo motor and DC gear motors, but due to misalignment and speed management challenges this prototype is designed with 12v DC gear with slew controller technique and 12v wiper motor. Slew controller technique is installed to tilt the dish with optimum speed rate according with input rated pulse of PWM generator. Each motor gets its input from H-Bridge dual axis module which had internal 5v AVR and 2 Pulse generators.

3.3. Arduino Controller

Arduino is an open source digital it that assemble the software and hardware designed projects with less complexity. The Omega controller Arduino is computationally installed with this prototype which is easy to program with in running project as compared of other technologies. As this prototype needs simple management to provide an optimum output result so the easy configurable controller is used to track and run the parabolic solar tracker.

3.4. Equations

a) *Hour angle*

$$H.A = \frac{no.\ of\ minutes\ past\ midnight}{\frac{4°}{min}}$$

b) *change in hour angle*:=$\frac{sin\infty - sin\delta.sin\emptyset}{cos\delta.cos\emptyset}$

c) *Declination angle*
D.A=
$sin^{-1} * [sin(Earth\ Tilt\ angle) * sin(earth\ eliptical\ position)]$

d) *Altitude Angle* = $sin \propto$ = $sin\delta * sin\emptyset + cos\delta * cosw * cos\emptyset$

e)
Azimuth angle. $= \frac{sin\alpha}{\frac{sinw.cos\delta}{cos\alpha}}$

f) *Shadow Length*= |OP|=**h/tanα**

4. Parabolic Dish Working

As concerned with dual axis solar heat collector from previous research work, different challenges were occur that are in sense of Cosine effect, Dish alignment, sensor actuation and MPPT technique(choice of controller). So, an automatic motorized control prototype is presented with 121.92cm diameter dish to enhance the solar irradiance application. The working is performed at Karachi, Sindh Pakistan with coordinate location of Latitude 23.9207°N and Longitude 67.0882°E .The whole implementation of solar designed dish with its all configured
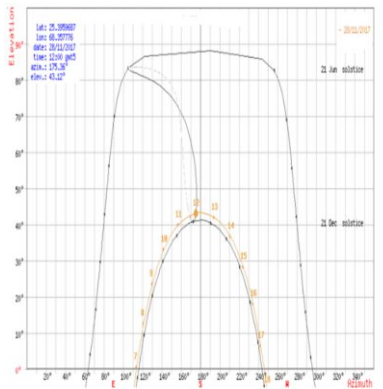
controller is accomplished on 4*4ft rectangular frame. The system perform its working when it get the input pulse from preset topology of controller to derive the motor in suitable direction either to tilt the dish or curve the dish with the help of DC-gear and power wiper motors. The output is performed with placement of 20w Solar panel on parabolic dish.

TABLE III. Result Analysis.

Change in hour angle	Angles measured		Time hour	Static solar PV			Prototype Result			Shadow length(ft)
	Altitude	Azimuth		Voc	Isc	power	Voc	Isc	power	
12.49^0	23.55^0	130.19^0	9am	19.7	0.15	2.95	20.3	0.29	5.88	7.51
25.09^0	32.9^0	141.91^0	10am	20.5	0.36	7.63	20.3	0.33	5.69	5.05
34.29^0	39.8^0	157.02^0	11am	20.1	0.16	3.22	19.2	0.36	6.91	3.93
38.67^0	43.15^0	175.18^0	12pm	20.1	0.34	8.33	19	0.69	13.11	3.51
37.15^0	42.04^0	194.12^0	1pm	20.4	0.42	8.57	19	0.94	17.86	3.64
30.19^0	36.80^0	210.9^0	2pm	20.2	0.43	8.68	20	0.67	13.4	4.39
19.1^0	28.5^0	224.2^0	3pm	20	0.36	7.2	20.5	0.51	10.45	6.03

Date	Time	Hour angle	Change in H.A	Yearly average Solar irradiance rate	Angles		Shadow length(ft)	Prototype LDR output volts			
					Altitude angle	Azimuth angle		y-axis		x-axis	
								LDR 1	LDR 2	LDR 3	LDR 4
28 .jan	Sunrise	0.46^0		1941							
	9.am	-45^0	12.49^0		23.73^0	130.10^0	7.51	0.723	0.567	3.631	3.783
	10am	-30^0	25.09^0		33.15^0	141.80^0	5.05	0.733	0.816	3.9	3.78
	11am	-15^0	34.29^0		40.07^0	157.02^0	3.93	3.211	2.297	3.910	3.696
	12pm	0^0	38.67^0		43.34^0	175.27^0	3.51	4.888	4.941	4.95	4.99
	1pm	15^0	37.15^0		42.19^0	194.28^0	3.64	3.830	3.910	4.985	4.990
	2pm	30^0	30.19^0		36.92^0	211.11^0	4.39	3.45	4.05	4.976	4.985
	3pm	45^0	19.1^0		28.58^0	224.4^0	6.03	3.93	3.846	4.941	4.892

Fig. 3. Sun Position Graph.

(a) Solar Dish   (b)Tracker frame   (c) controller chip

(d) Battery   (e) 12V Power Motor   (f) 12V Dc Motor

Fig. 4. Prototype Parts.

5. Conclusion

The tariff of electric price is become inverse proportion to oil and fossil fuel tariff that creates that hazard effect of load shading. So to provide a sustainable tool with development of power optimized techniques, we have to promote renewable energy applications with help of technical expertise. In this research an innovative low cost parabolic dish is analyzed optically to compensate the MPPT tracking issues. The thermally analyzed result is obtained with hour angle formulae tools and flux meter that is about $210 w/m^2$ on parabolic dish at $21.8℃$ temperature. This research concluded that the design and function of the prototype is proven to be efficient. Parabolic dish with single axis sun tracking mechanism upturns the magnitude of current, voltage and power of mounted solar panel is about 23.6% in compare of the static solar penal and Parabolic dish with dual axis sun tracking mechanism upturns the magnitude is about 33% in compare of the static solar penal.

REFERENCES

[1] A. Ahmed, P. Hameed, Z. A. Memon, A. K. Akhani, and P. Lohana, "Implementation of Design for efficiency enhancement of solar photovoltaic panel through parabolic solar dish tracker," *1st International Conference on Contemporary Sociology, Social Sciences and Sustainable Development,* March-22-24, 2018.

[2] A. Shaikh, M. H. Kabir, I. A. Sohu , A. Ahmed, A. Ahmed Sohu "Implementation of Design for Solar Tracking system Using FPGA" *International Conference On Emerging Trends In Telecommunication & Electronic Engineering, (ICET),* Feb-27-28, 2018.

[3] I. Gopang, P. Hameed, and Z. A. Memon, "Parabolic dish solar system for increased power effeciency," *The First International Conference on Industrial Engineering and Management Applications,* (Feb-2017).

[4] K. Das, H. Ghosh, M. Sengupta, "Single Axis Solar Tracking System using Microcontroller (ATmega328) and Servo Motor," *International Journal of Scientific and Research Publications,* vol. 6, no. 6, June 2016.

[5] H. Hijazi ,O. Mokhiamar, and O. Elsamni, "Mechanical design of a low cost parabolic solar dish concentrator," *Alexandria Engineering Journal,* vol. 55, pp. 1–11, 2016.

[6] S. Danial and M. Boroushaki, "Design analysis and optimization of Solar Dish," *Int. Journal of Renewable Energy.*

[7] M. Navin, K. Magar, A. Abhishek, J. Fernandes, P. Kulkarni, "Solar steam

power generator," *International Conference on Technologies for Sustainable Development (ICTSD-2015),* Feb. 04 – 06, 2015.

[8] SafaSkouri, Salwabouadila, Sassi Ben Nasrallah, "Estimating intercept factor of a solar parabolic dish with photogrammetric equipment," 6th International Renewable Energy Congress (IREC), 2015.

[9] S. Povlovic, V. Stefanovic, D. Vasiljevic, and E. Petrovic, "Optical Design of solar parabolic concentrating collector based on Trapezoidal reflective petals," *Journal of energy and power Engineering,* April-2015.

[10] N. M. Arago, T. M. Amado, and J. W. F. Orillo, "Utilization of Cassegrain Feed Parabolic Antenna Design in Increasing the Efficiency of Photovoltaic Module," *7th IEEE International Conference humanoid, nanotechnology,information technology communication and control environment and management (HNICEM),* Nov-2014.

[11] B. Anak Sup, M. Farid, T. Zanariah, R. A. Bakar, and G. Ming, "Effect of rim angle to the flux distribution diameter in solar parabolic dish collector," *2nd Int. conference on Sustainable energy engineering and Application,* 2014.

[12] M. A. Soderstrand, S. B. Lee, and P. Chung, "Mini-dish based hybrid concentrated solar power system for home use," *IEEE 56th Int. Midwest symposium on circuit and system (MWSCAS),* Aug-2014.

Analyzing the impact of Temperature on Proton Exchange Membrane Fuel Cell performance Using Matlab

Aftab Ahmed Khuhro[1] ,Intizar Ali[2] ,Safiullah[2]

Abstract:

The Proton Exchange Membrane Fuel cell (PEMFC) is a device that converts the chemical energy of hydrogen into electrical energy. It receives hydrogen at anode and oxygen at the cathode side, due to chemical reaction at electrodes electronic current, along with that water and heat is also produced. Heat produced causes problem for current produced, cell performance and may lead to a phase change of water produced. Heat produced may also cause melting of the sensitive membrane and increase losses in a fuel cell. Water produced causes flooding at Electrodes and membrane which requires a specific amount of water only. This study used Mat lab to analyze the impact of temperature on different parameters which have a significant effect on heat and mass flow. The results showed that the performance of Proton Exchange Membrane fuel cell reduces with increase in temperature significantly during operation of the cell. The performance of fuel cell can be enhanced if the temperature of the fuel cell is controlled and kept within limits. Proton Exchange Membrane fuel cell is suitable for transport, automobile, and other applications.

Keywords: *Heat; Mass; Fuel Cell; Transport; Management; Issues; Mass flow; Temperature; Matlab.*

1.Introduction

In the beginning of this century, the world has realized the shortage of fossil fuels which include mainly coal, gas, and oil. Most of worlds energy demand is dependent on these natural resources. It is predicted that these resources will be very close to depletion in 2060. Nuclear, Solar, Wind and other resources are considered as best option to replace the fossil fuels needed in future. However, still there will be a need for fuel to run high speed and heavy-duty vehicles of future and fuel cells are a suitable option for such a need [1].

William Grove is considered to be first to invent fuel cell in 1839. In 1960 NASA first commercialized the fuel cell by using them in their space missions [2]. After that, this technology was less discussed among researchers due to its shortcomings such as high cost and low efficiency. Nonetheless, improving fuel cell performance by improving its design, material and optimizing performance has found new interest among researchers.

Proton Exchange Membrane Fuel cells are the power source of future. Many researchers are working on this technology to improve its performance and make it compatible with
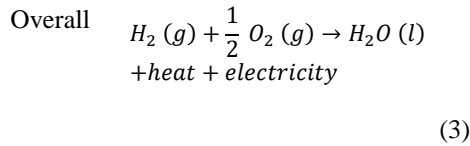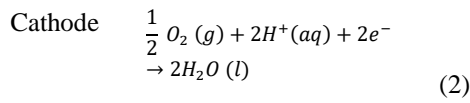
[1] Energy system Engineering, Sukkur IBA University, Sukkur, Pakistan
[2] Department of Mechanical Engineering Technology, The Benazir Bhutto Shaheed University of Technology and Skill Development, Khairpur, Pakistan
Corresponding Email: aftab.mere17@iba-suk.edu.pk

other fossil fuel technologies. PEMFCs use pure hydrogen as fuel which can be produced using solar or wind power. Hence this technology becomes clean, sustainable and emission-free technology [1].

PEMFCs consist of a membrane, electrodes, gas diffusion layer, bipolar plates, and current collectors [2]. Hydrogen at anode breaks into proton and electron. The membrane allows proton only to pass through and electrons flow through the external path to do some work. When hydrogen breaks at anode due to catalyst action, it is exothermic reaction hence heat is released [3]. Water is produced at cathode when proton from membrane and oxygen through flow channels combine at cathode [4]. The reaction that occurs on both sides of the membrane is given below.

Anode $\quad H_2$ (g)$\rightarrow 2H^+(aq) + 2e^-$ $\quad$ (1)

Cathode $\quad \dfrac{1}{2} O_2 (g) + 2H^+(aq) + 2e^-$
$\rightarrow 2H_2O (l)$ $\quad$ (2)

Overall $\quad H_2 (g) + \dfrac{1}{2} O_2 (g) \rightarrow H_2O (l)$
$+heat + electricity$

(3)

Heat and water produced are required in specific amount only [5]. If there is excessive heat, it will melt sensitive membrane and affect the efficiency drastically. And if water produced is in the excessive amount, it will cause flooding at electrodes, reducing the active area for reaction and reduce cell performance [6]. Hence this study aims to analyze different fuel cell parameters which can affect heat and mass transfer phenomenon directly or indirectly. The connection of several fuel cell units in series and parallel will add up voltages and current which might be utilized in electric vehicles. This shows the importance of fuel cell electricity generation for the automobile industry.

In order to optimize the performance of fuel cell, optimizing heat and mass problem is necessary. Most of fuel cell performance

parameters depend on heat and mass transfer phenomenon [9].
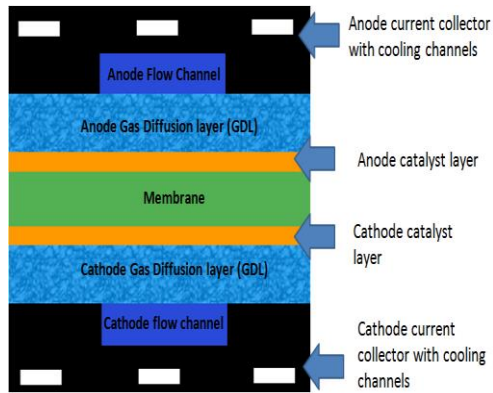
Fig. 1. PEM Fuel Cell diagram [3].
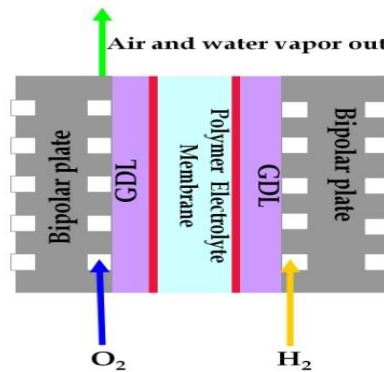
Fig. 2. Flow channels and flow directions [5].
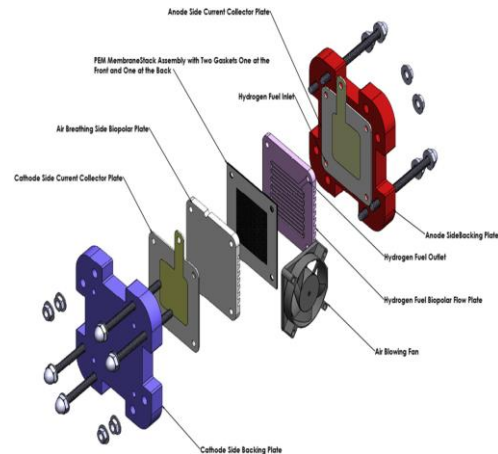
Fig. 3. Exploded view of PEM Fuel cell [16].

2.Methodology

This study is based on Numerical analysis of heat and mass transfer issues due to variation of different parameters during operation of the fuel cell. This paper focuses on the impact of temperature variation during cell working and observes the impact on the performance of cell by choosing a different range of operating parameters and analyzed them using the available commercial software. Rather choosing many parameters and observing their effect cell this study is focused on the temperature of the cell which is considered as a most important factor of fuel cell performance. Thus, understanding the fuel cell temperature and its behavior becomes very important.

2.1. Mass transport and Water Management

In order to produce the continuous power, we need a continuous supply of fuel at the anode side of the cell. Added with that excessive surplus water produced as the output of reaction should be removed continuously. Voltage and current reduction may be caused due to three kind of losses of fuel cell activation, concentration and ohmic losses [10].

Mass transport is a flow of species within the cell and by optimizing flow and analyzing their effect on cell performance we can predict cell behavior. Water produced may cause the membrane to rupture or occupy active places where reaction needs to take place [11].

$$\sum(m_i)\ in = \sum(m_i)\ out \qquad (4)$$

Mass balance of cell system should be mass that goes into system equals that leaves the system.

$$w_{el} = n_{cell}V_{cell}\ I \qquad (5)$$

However, cell power can be expressed as given in equation above where n_cell represents the number of cells, V_cell represents cell voltage and I is current of cell.

The higher flow rates cause the better distribution of reactants. If the flow rate is too high that may rupture sensitive membrane. There are basically two types of flow within the cell. One is by convection that occurs in flow channels and the other is diffusive which is due to pores of diffusion layer and electrodes [12].

Hence the study of mass transport and water management become important to properly design fuel cell. Different parameters and constants are used to study the behavior of cell performance when temperature changes with time of operation.

TABLE I. The parameters and constants used in this study to analyze the effect of temperature on fuel cell performance.

Parameters symbol	Constant value
Thermal conductivity (k)	Depends on material
Heat transfer rate (q)	-------
Ideal gas constant (R)	8.314
Faraday's constant (F)	96487
Transfer coefficient (α)	0.5
Enthalpy	Depends on temperature
Thermal Resistance (R)	------

2.2. Heat Management

The temperature in PEMFCs is always unsteady even if flow rate at both electrodes is kept constant. Temperature variations within the cell due to water phase change, heat produced by the chemical reaction, water flooding within the cell and air convection [13].

Determining heat distribution within the cell is key to determine temperature variations and predict them properly. Operating temperature is an important parameter that can affect the efficiency of the cell. Temperature control, distribution and dynamic response are very important to understand for better performance of the cell. It is necessary for proper operation of fuel cell stack that optimum values should be known for parameters such as temperature. Some researcher has shown that temperature has the greatest effect on cell performance [14].

Operation of fuel cell stack is an uncertain process and the temperature is a parameter that has the highest uncertainty during operation. Water transport is directly affected by operating temperature of the cell. It also affects flow species, removal of water, and flooding at electrodes [15].

Heat distribution can be determined using energy balance on the system. The energy balance depends on several factors such as power produced, reactions and heat loss on walls of the cell [16].

The enthalpy of a system that enters the system is equal to the enthalpy of products plus heat generated. The rate of heat transfer with cross-section area A is given below.

$$q_x = -kA \frac{dT}{dx} \qquad (6)$$

Where k is thermal conductivity and $\frac{dT}{dx}$ is a temperature gradient. L represents the length and T_1 and T_2 are initial and final temperatures.

$$q_x = k \frac{T_1 - T_2}{L} \qquad (7)$$

Thermal resistance associated with conduction in the plane wall is given as

$$R_{cond} = \frac{T_1 - T_2}{q_x} = \frac{1}{kA} \qquad (8)$$

Heat transfer through conduction between two adjacent materials in contact is given as

$$q = h_{tc} A \Delta T \qquad (9)$$

Where h_{tc} is convective heat transfer co-efficient. Thermal resistance associated with heat transfer by convection is given as

$$R_{conv} = \frac{T_1 - T_2}{qx} = \frac{1}{hA}$$

Where *h* is enthalpy. Since conduction and convection are in series they can be written mathematically as

$$R_{total} = \frac{1}{h_1 A} + \frac{L}{kA} + \frac{1}{h_2 A}$$

$$q = UA\Delta T$$

The considering fuel cell walls as composite and in series total heat transfer can be written as equation above where U is overall heat transfer coefficient.

The fuel cell system runs efficiently when there is precise control of temperature. At higher temperature, the kinetics will be faster and reduce activation losses. But higher temperature may damage the membrane so it is required at an optimum level. Higher temperature will also cause water to vaporize and change its phase from liquid to gas. Small fuel cell stack does not require cooling but larger stack requires cooling for homogenous temperature distribution and control [17].

Heat distribution can be controlled by properly designing flow channels and bipolar plates. Introducing cooling channels with bipolar plates additional heat can be removed.

3. Results and discussion

The objective of this study is to analyze and observe the impact of temperature on fuel cell Losses, Performance, Entropy, Current produced, Consumption of fuel and Reversible cell potential.

Temperature is an important parameter that has an effect on heat and mass parameters. Temperature has a low impact on the entropy of mass species during operation of the cell.

The entropy of H_2, O_2, and water does not show significant change while temperature increases during operation.

Water management at Membrane in cell stack is very important because Ionic current flows through the hydrated membrane. Heat is generated at anode which causes dehydration of membrane. On the other hand, water generated at cathode may cause flooding if generation rate is higher than transport rate. Both the hydration and flooding at cathode depends on heat generated by fuel cell reaction and both dehydration of electrolytic membrane and flooding of cathode must be avoided to get optimum performance of cell stack.
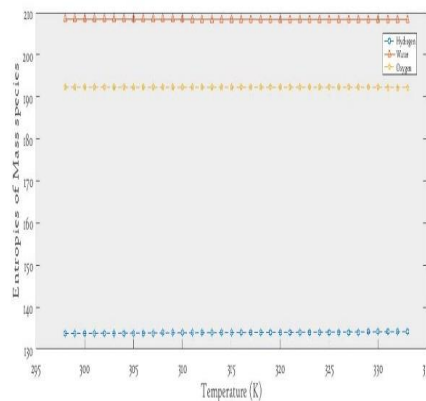
Fig. 4. The impact of temperature on the entropy of mass species.
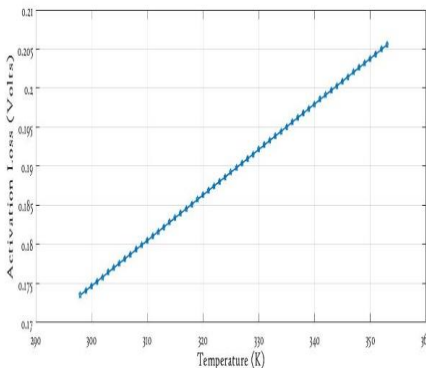
Fig. 5. The impact of temperature on activation losses.

However, the temperature has a significant impact on activation losses of the cell. If temperature increases the activation losses increases with that exponentially. Hence temperature control during operation of the cell becomes very important to limit activation losses. Heat and mass species play an important role in cell performance and are related to temperature directly or indirectly.

Temperature also plays an important role in current produced by the cell, hydrogen consumed at the anode and total electricity produced by the cell. This study shows that if temperature increases with that current produced by cell decrease significantly. The significant loss in total electricity produced is also observed. Due to increase in temperature number of moles consumed at the anode side of PEMFCs also reduces. The less current produced and moles at anode show that performance of cell reduces with increase in temperature. The results show that reversible cell potential also reduces with increase in temperature. Hence temperature has a negative impact on reversible potential which will add further loss in fuel cell performance and efficiency to operate at high temperature.

Temperature has a positive impact on cell current density.

If temperature increases cell electrode kinetics increases along with electrode kinetics limiting current density increases.

The key findings of this study would be following.

1. Temperature has less impact on Entropy but it accelerates the kinetic reaction at first along with an increase in activation losses.

2. Reversible cell potential values reduced with increasing temperature.

TABLE II. Effect of temperature on cell current, electricity produced and H_2 consumed at the anode.

Temperature (K)	Current produced (A)	Electricity produced	No of moles consumed (H_2)
298.15	1.9733	1.70×10^5	0.8835
303.15	1.9467	1.67×10^5	0.8689
308.15	1.9092	1.64×10^5	0.8548
313.15	1.8788	1.62×10^5	0.8412
318.15	1.8492	1.59×10^5	0.8280
323.15	1.8206	1.57×10^5	0.8151
328.15	1.7929	1.54×10^5	0.8027
333.15	1.7660	1.52×10^5	0.7907
338.15	1.7399	1.50×10^5	0.7790
343.15	1.7145	1.48×10^5	0.7676
348.15	1.6899	1.46×10^5	0.7566
353.15	1.6660	1.43×10^5	0.7459

TABLE III. Effect of temperature on reversible cell potential.

Temperature (K)	Reversible cell potential
298	1.2289
303	1.2247
308	1.2205
313	1.2163
318	1.2120
323	1.2036
328	1.1993
333	1.1909
343	1.1902
353	1.1824
363	1.1740
373	1.1655
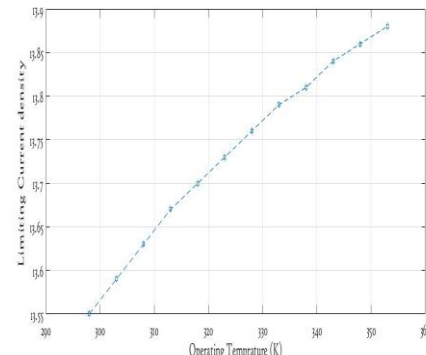
Fig. 6. The impact of Temperature on limiting current density.

3. The less fuel was consumed due to increase in temperature which is not good for the overall performance of the cell.

4. Conclusion

This paper shows that temperature has a significant impact on current produced within fuel cell stack compared to Entropy of mass species. As the temperature rises due to heat released during reaction taking place at Electrodes, current and electricity produced

are reduced. There was a continuous drop in hydrogen consumption at Electrodes due to rise in temperature. The lesser consumption of hydrogen fuel at anode leads to the minimum amount of current and electricity production.

Temperature also affects the activation losses of the cell, the increase in temperature active places at anode and cathode of cell show more resistance for reaction. The operation time to calculate cell current and other parameters was chosen 24 hours. During this period number of moles calculated and converted in liters at 25oC are 19.79 liters.

The number of liters consumed at 80oC ware 16.70. It can be concluded that with higher temperature cell tends to consume less fuel as compared to low temperature, which will eventually result in low performance and reliability of PEMFCs.

ACKNOWLEDGMENT

REFERENCES

[1] S. Shafiee, & E. Topal, "When will fossil fuel reserves be diminished?," *Energy policy,* vol. 37, no. 1, pp. 181-189, 2009.

[2] A. Arvay, A. Ahmed, X.-H. Peng, and A. Kannan, "Convergence criteria establishment for 3D simulation of proton exchange membrane fuel cell," *International journal of hydrogen energy,* vol. 37, pp. 2482-2489, 2012.

[3] C. Siegel, "Review of computational heat and mass transfer modeling in polymer-electrolyte-membrane (PEM) fuel cells," *Energy,* vol. 33, pp. 1331-1352, 2008.

[4] A. Arvay, Proton exchange membrane fuel cell modeling and simulation using Ansys Fluent. *Arizona State University,* 2011.

[5] J. Carton and A. Olabi, "Three-dimensional proton exchange membrane fuel cell model: comparison of double channel and open pore cellular foam flow plates," *Energy,* vol. 136, pp. 185-195, 2017.

[6] R. B. Ferreira, D. Falcão, V. Oliveira, and A. Pinto, "Numerical simulations of two-phase flow in proton exchange membrane fuel cells using the volume of fluid method–A review," *Journal of Power Sources,* vol. 277, pp. 329-342, 2015.

[7] S. Cano-Andrade, A. Hernandez-Guerrero, M. Von Spakovsky, C. Damian-Ascencio, and J. Rubio-Arana, "Current density and polarization curves for radial flow field patterns applied to PEMFCs (Proton Exchange Membrane Fuel Cells)," *Energy,* vol. 35, pp. 920-927, 2010.

[8] X.-D. Wang, Y.-X. Huang, C.-H. Cheng, J.-Y. Jang, D.-J. Lee, W.-M. Yan, et al., "Flow field optimization for proton exchange membrane fuel cells with varying channel heights and widths," *Electrochimica Acta,* vol. 54, pp. 5522-5530, 2009.

[9] D. Spernjak, A. K. Prasad, and S. G. Advani, "In situ comparison of water content and dynamics in parallel, single-serpentine, and interdigitated flow fields of polymer electrolyte membrane fuel cells," *Journal of Power Sources,* vol. 195, pp. 3553-3568, 2010.

[10] M. Zhukovsky, L. Fomina, and S. Beznosyuk, "Computer modeling of hydrogen fuel cell subsystems: Carbon nanogel electrodes and fractal nanoparticle catalysts," *International Journal of Hydrogen Energy,* vol. 36, pp. 1212-1216, 2011.

[11] L. Karpenko-Jereb, P. Innerwinkler, A.-M. Kelterer, C. Sternig, C. Fink, P. Prenninger, et al., "A novel membrane transport model for polymer electrolyte fuel cell simulations," *International*

journal of hydrogen energy, vol. 39, pp. 7077-7088, 2014.

[12] A. Manso, F. Marzo, J. Barranco, X. Garikano, and M. G. Mujika, "Influence of geometric parameters of the flow fields on the performance of a PEM fuel cell. A review," *International journal of hydrogen energy,* vol. 37, pp. 15256-15287, 2012.

[13] P. K. Sinha, C.-Y. Wang, and U. Beuscher, "Transport phenomena in elevated temperature PEM fuel cells," *Journal of The Electrochemical Society,* vol. 154, pp. B106-B116, 2007.

[14] A. Bıyıkoğlu, "Review of proton exchange membrane fuel cell models," International Journal of Hydrogen *Energy,* vol. 30, pp. 1181-1212, 2005.

[15] J.-H. Jang, W.-M. Yan, and C.-C. Shih, "Effects of the gas diffusion-layer parameters on cell performance of PEM fuel cells," *Journal of power sources,* vol. 161, pp. 323-332, 2006.

[16] T. Wilberforce, Z. El-Hassan, F. Khatib, A. Al Makky, J. Mooney, A. Barouaji, et al., "Development of Bi-polar plate design of PEM fuel cell using CFD techniques," *International journal of hydrogen energy,* vol. 42, pp. 25663-25685, 2017.

[17] A. A. Khuhro, Y. Ali, M. Najam-Uddin, and S. Khan, "A Technological, Economical and Efficiency Review of Direct Methanol Fuel Cell,".

Solar Concentrator's Effect on Solar Panel Efficiency

Manoj Kumar Panjwani[1,2], Li Meicheng[2], Idris Khan [2], Zulfiqar Ali[2], Mohan Menghwar[2], Zulqarnain Arain [1,2], Danish Khan[2]

Abstract:

   Given the current energy emergencies, the existing emphasis is increasing on the renewables as researchers predict near the end to fossils. In the light of the current renewable energy resources, the solar energy is seen to be one of the most reliable ones for the third world countries. Moreover, the efficiency of current commercial photovoltaics hardly touches 30 %. This paper studies the mechanism of empowering solar concentrators to collect higher solar irradiation to concentrate on the solar panel and study the variations in the amount of power received and the temperature constraints. The study utilises the use of solar concentrators in regions under and over the mentioned standard temperature ranges by the manufacturer on the specification sheet, and thoroughly studies the variations observed in output parameters.

Keywords: Solar Concentrator; Efficiency; Temperature; Renewable energy.

1. Introduction

   The energy that is received directly from the sun is approximately near to 1413 W/ m2. However, the actual utilisation which is indicated on the ground scale is near to 1050 W/m2 as reported by the United States Branch of Agriculture, Portland USA. In general, the

   Earth's top layer is nearly 30% more extreme than the one which is received on the ground. Most studies report that the real solar energy that is being utilised for the normal operation of the solar panel is nearly 70% of the total energy that is received directly from the sun on planet Earth. In other words, current photovoltaics utilises 70% of the energy received on the earth to satisfy our current energy demands [1-2].

   The manufacturers of the Solar Panel are always required to display a specification list on the back of the Solar Panel. The specification list consists of the various parameters that the Solar Panel is going to respond. Most of the commercial Solar Panel manufacturers are reporting that their Panels would respond to the standard when exposed to irradiations of 1000W/m2 and 25*C. In the case where the standard ranges are violated contribute to the irregular response from the Solar Panel, thus arising stability issues for the photovoltaic systems. More specifically, the Solar Panel is allowed to operate in areas which exceed the standard ranges of any parameter, which ultimately lead to increasing issues for the systems stability [3].

[1] Department of Energy Systems Engineering, Sukkur IBA University Pakistan
[2] Renewable Energy School, North China Electric Power University, Beijing China
Corresponding Email: manoj.panjwani@iba-suk.edu.pk

If considering areas in most South Asian countries, the concern mostly raised by the manufacturer highlights the insights where there is an issue of increasing temperatures and most of the cities located in lower South Asian regions touches 50*C+. Given the current situation, the temperature ranges offered by the regions allowed most of the Solar Panels to deviate from the standard performance[3-4].

It is very important to know the temperature of the solar panel before we could design the system to respond to certain energy demand from the community. It is also important to highlight that the behaviour of the Solar Panel concerning environmental parameters is irregular. Thus it allows the higher risk of instability issues for the systems which are off-grid and on-grid [5]. Considering the Polycrystalline Solar Panel, it indicates that when the temperature is decreased by one degree Celsius above 25*C, the output power will also simultaneously affect. Moreover, it indicates a standard range where it maintains its temperature coefficient. However, it also indicates that the temperature coefficient values also appear differently when the temperature ranges enter into ranges higher than the critical range for the Solar Panel [6].

With an increasing demand of utilising the Solar concentrators in fulfilling the daily energy demands, the solar concentrators are also being utilised to allow a higher amount of Solar irradiations to concentrate on a particular area and could lead to the higher amount of power output from the existing Photovoltaic Plant. It's a matter of the fact that it's the solar irradiations that ultimately are converted into power output in photovoltaic's and not the heat. With empowering Solar concentrators on concentrating the number of irradiations can help the system to operate in a certain range, and once the standard temperature is crossed, it appears to display negative impact on the overall output of the Photovoltaic system. Moreover, utilising the Solar Panel in ranges above the standard

ultimately lead to an unreliable response of the Panel on a longer run [7-8].

Pearson correlation coefficient is mostly utilised to understand the linear behaviour/connection between any two variables. It can also be used to carefully understand the behaviour of the system if there is any change in a specific variable(s) [9].

During experimental analysis, solar trackers were utilised to assure that the concentrator could respond to the peak hours to assure maximum power conversion for the system. The system comprised a controlled laboratory environment where it was directed to bring expansion of the temperature with increasing amount of irradiation from a light source. In corresponding, the behaviour of the solar panel was carefully studied and reported.

2. Experimental Analysis

Experimental setup included a controlled test bench which included a 50W BP Solar Panel (Polycrystalline) with specification Vamp(17.3V),Imp(2.9A),temperature coefficient of Isc(0.065 ± 0.015)%/ °C, Temperature coefficient of Voc(-80 ±10) mv/°C and Temperature coefficient of power(-0.5 ± 0.05)%/°C. It also includes Hygrometer, Thermometer, six tungsten filament bulbs acting as load (50,100,500,1000W), and 12 Millimeters for point to point calculations. The readings were carefully monitored with every increase in humidity and temperature ranges. Later the Solar Concentrator was employed to see the variations on the parameters affected. Results were carefully monitored, and Karachi,Pakistan (Latitude: 24.8934', Longitude: 67.0281') was taken as a reference for experiments.

2.1. Humidity's effect on Solar Panel

The values of voltage, current, and power continue to depreciate as there is an increase in the amount of humidity as can be referred from Figure 1-3. Linear depreciation range could be seen from humidity range 25-30% as can be referred from Table 2. With an increase

in the temperature in the room, the range of humidity was found decreasing. There was a decreasing trend which was followed by the voltages and currents when a variation was brought in the temperature. Concerning Figure 4, few parameters were getting disturbed when it comes to utilising the Solar Panels. A significant decrease in the voltage and humidity were noticed as there was a linear increase in the temperature ranges. Figure 4 reflects the effect of temperature increase on the produced current. The current follows an unusual behaviour when there is a variation on the temperature.

With an increasing level of humidity ranges, there is a decrement noticed on the number of voltages produced which also appears to cause various issues on the system's stability and overall performance as can be referred from Equation 1 [10].

The similar trend could be referred to the amount of current produced with the variation brought in the amount of humidity. Thus the similar trend would also lead to increased stability issues for the system. The interesting fact noticed in the experiment shows that there is no constant trend followed by the current when there is variation brought on the system.

With the current trend followed on the amount of power produced by the solar panel concerning variations brought from the variations in the humidity, various instability issues are ultimately leading to the unreliability of the photovoltaic systems as can be referred from Table 1.

2.2. Usage of Solar Concentrator

Solar concentrators are employed for various reasons including one for heating water and thermal energy production. Moreover, they are currently employed to study their contribution to the increasing energy productions for the Solar Panel. Solar Concentrators could help in collecting higher intensities for the efficient energy conversion. The concentrators that were utilized in the experiment setup had a dimension of 850 x 565 x 50mm which was utilized to cover the area of a 50W solar panel. The side angle was kept 30 degrees for a reasonable tilt to encourage maximum power conversion.

It can be easily noticed that with the increasing pattern of solar intensity over Solar Panel, there is a consequent increase in the amount of surface temperature on the Solar Panel. With increasing temperature, various issues can be associated with the temperature coefficient mentioned in the manufacturer's specification list. Ultimately, it starts deviating from the standard range, and hence there are stability issues that arise. Moreover, the increasing temperature though somehow contribute positively as the amount of humidity that appears on the surface of solar panel starts decreasing making Solar Panel easy to convert the irradiations into electrical energy as can be referred from Table 2.

Concerning the decreasing humidity because of the increasing temperature on the panel, despite the fact that humidity negatively affects the performance of Solar Panel, there is a decrease noticed in the current produced by the system. In result of a decrease in the amount of current from the system, various issues lead to unstable behaviour of the system as can be referred from Table 3.

Due to continuous increment in the temperature ranges due to increase in the solar intensity, there is an irregular pattern followed by the power output. There are various reasons due to which it follows irregular behaviour, and most of them reflect the internal material characteristics of the material used in the manufacturing of the Solar Panel. The respective reading of irregular behaviour could be referred from Table 4 and 5 and can be related from Equation 2 and 3 [10].

From Table 6, the Pearson correlation value as stated in Equation 4 is used for a default value under the range of parameters listed by the manufacturer. It can be seen that in the range of (6.85*C – 36.85*C), correlation of the photovoltaic power and solar radiation is greater than 0.85 which indirectly states that the solar radiation is the main factor that affects the output power from

the Solar Panel. Moreover, the temperature has a positive effect which means that the temperature increase in the region under the region specified can positively affect the power output of the panel. The results can also be verified referring the value of the power and the temperature in table 4. However, the humidity range can be seen portraying a negative value which states that the humidity negative impacts the overall power output from the Solar Panel. Moreover, the value of the wind also has a little positive impact in a sense that the wind would provide the ventilation effect to the solar panel which varies from region to region.

From Table 7, The Pearson correlation value is used for a default value over the range of parameters listed by the manufacturer. It can be seen that in the range of (36.85*C-58.70*C), correlation of the photovoltaic power and solar radiation is greater than 0.85 which also validates the importance of the solar radiation in the overall power output of the Panel. However, the interesting aspect of it lies in the temperature where the coefficient

shows a negative value. The negative value shows that the temperature in a range higher than those indicated by the manufacturer has a negative impact on the power produced by the Solar Panel. The aspect could be seen validating the results obtained in Table 5. The same aspect can be seen from the humidity's part also that it also portrays a negative impact on the power produced by Solar Panel. However, wind factor could be seen positive so that the Solar Panel is exposed to need of ventilation for the said aspect.

The results indicated after various attempts on the Solar Panel with variations from in the solar intensities from temperature range 6.85*C – 36.85*C shows a positive change in the output power output. However, once the temperature of 36.85*C is crossed, it starts portraying negative effect on the power output from the photovoltaic system. With an increasing trend from 36.85*C-56.70*C, the power output could be seen decreasing and arising many concerns over the stability of the installed photovoltaic system.

3. Tables, Figures, and Equations

3.1. Tables

TABLE 1. Experimental Values of Voltage (V), Current (A) and Power (W) with increasing trend in Humidity (%) on constant Solar Irradiance [9].

Solar Irradiance (W/ m2)	Temperature (C)	Humidity (%)	Voltage (V)	Current (Amp)	Powers (watts)
800	31.85	40	17.1	2.41	41.21
800	31.85	45	16.89	2.34	39.52
800	31.85	50	16.75	2.21	37.08
800	31.85	55	16.54	2.14	35.39
800	31.85	60	16.45	2.02	33.22
800	31.85	65	16.35	1.92	31.39
800	31.85	70	16.32	1.84	30.02

TABLE 2. Solar irradiance calculated with and without concentrator with percent increase.

Solar Irradiance (W/ **m2)** Without Concentrator	Solar Irradiance (W/ **m2)** with Concentrator	Percent Increase
650	693	6.20
730	786	7.12
820	869	5.63
915	962	4.88
985	1037	5.01
1028	1086	5.34
1134	1197	5.26

TABLE 3. Power output calculated with Solar Concentrator.

Solar Irradiance (W/ **m2)**	Humidity (%)	Temperature at the Panel (C)	Voltage (V)	Current (Amp)	Powers (watts)
650	25	31.85	16.3	2.12	34.56
730	25	32.35	16.9	2.24	37.86
820	25	32.85	17.1	2.31	39.50
915	24	33.15	17.11	2.37	40.55
985	23	33.85	17.14	2.42	41.48
1028	22	34.55	17.15	2.49	42.70
1134	21	35.33	17.15	2.51	43.04

TABLE 4. Calculated parameters with Solar Concentrator in the temperature range (6.85*C – 36.85*C).

Solar Irradiance (W/ m2)	Concentrated Irradiations(W/ m2)	Temperature at the Panel (C)	Humidity (%)	Voltage (V)	Current (Amp)	Powers (watts)
650	693	6.85	25	16.5	2.14	35.31
730	786	11.85	25	16.9	2.24	37.85
820	869	16.85	25	17.1	2.31	39.50
915	962	21.85	24	17.15	2.42	41.50
985	1037	26.85	23	17.16	2.48	42.55
1028	1086	31.85	22	17.16	2.52	43.24
1134	1197	36.85	21	17.18	2.61	44.83

TABLE 5. Calculated parameters with Solar Concentrator in the temperature range (26.85*C-58.70*C).

Solar Irradiance (W/ m2)	Concentrated Irradiations(W/m2)	Temperature at the Panel (C)	Humidity (%)	Voltage (V)	Current (Amp)	Powers (watts)
650	693	26.85	25	16.85	2.04	34.37
730	786	31.85	25	16.9	2.08	35.15
820	869	36.85	25	16.7	2.12	35.40
915	962	41.85	23	16.32	2.13	34.76
985	1037	46.85	21	15.37	2.14	32.89
1028	1086	51.85	19	14.8	2.16	31.97
1134	1197	58.70	16	14.25	2.19	31.21

TABLE 6. Pearson correlation coefficient for PV power with meteorological factors in the temperature range (6.85*C – 36.85*C).

Weather Type	Radiation	Temperature	Humidity	Wind speed
Sunny	0.915436	0.389721	-0.35921	0.22321
Foggy	0.909706	0.365947	-0.34865	0.21479
Rainy	0.889801	0.301972	-0.32875	0.16826

TABLE 7. Pearson correlation coefficient for PV power with meteorological factors in the temperature range (36.85*C-58.70*C).

Weather Type	Radiation	Temperature	Humidity	Wind speed
Sunny	0.92443	- 0.31891	-0.24334	0.21551
Foggy	0.91704	-0.278663	-0.32654	0.20267
Rainy	0.89501	-0.299886	-0.27752	0.14722

3.2. Figures
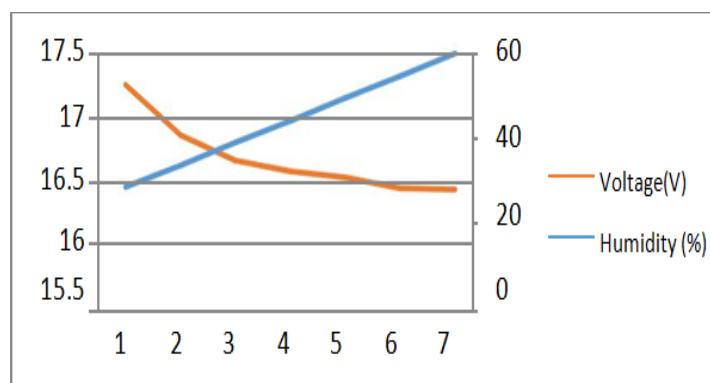
Fig. 1. Figure portrays the effect of Humidity on Voltage Produced.
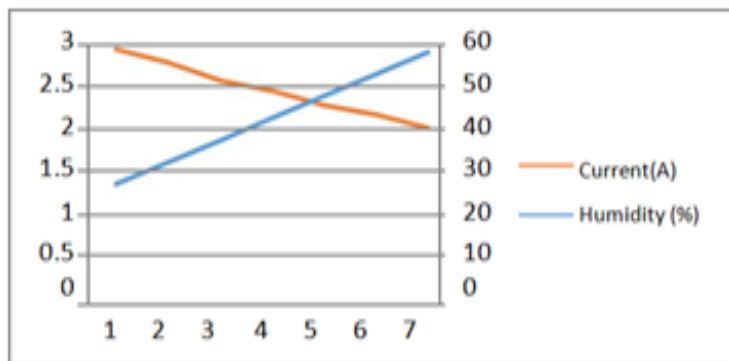
Fig. 2. Figure portrays the effect of humidity on the Current produced.
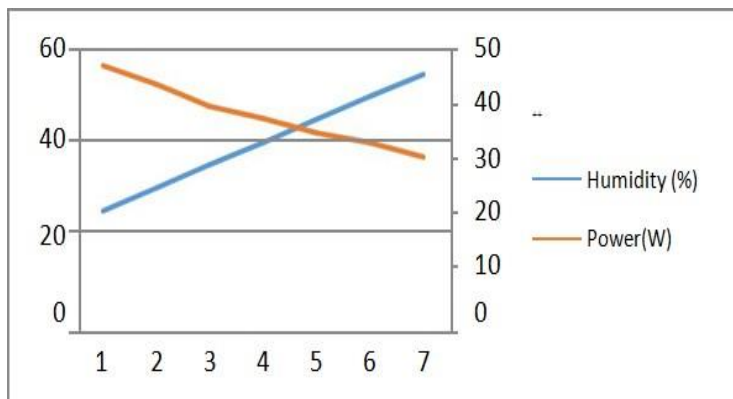
Fig. 3. Figure portrays the effect of Humidity on Power Produced.
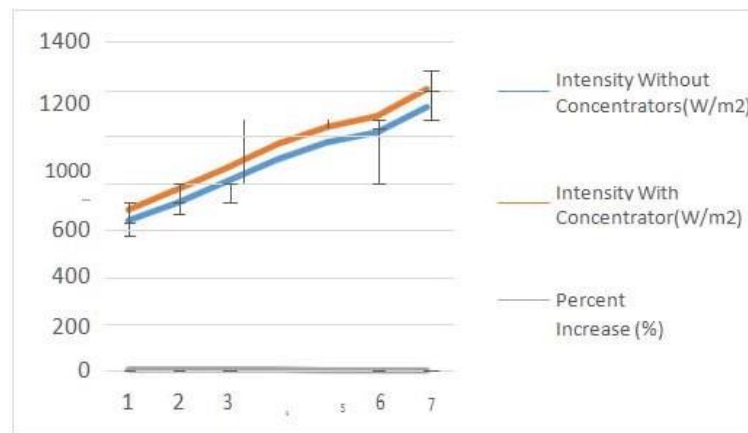
Fig. 4. Graph is portraying an increase in the solar intensity collected at the surface of the Solar Panel due to Solar Concentrator.
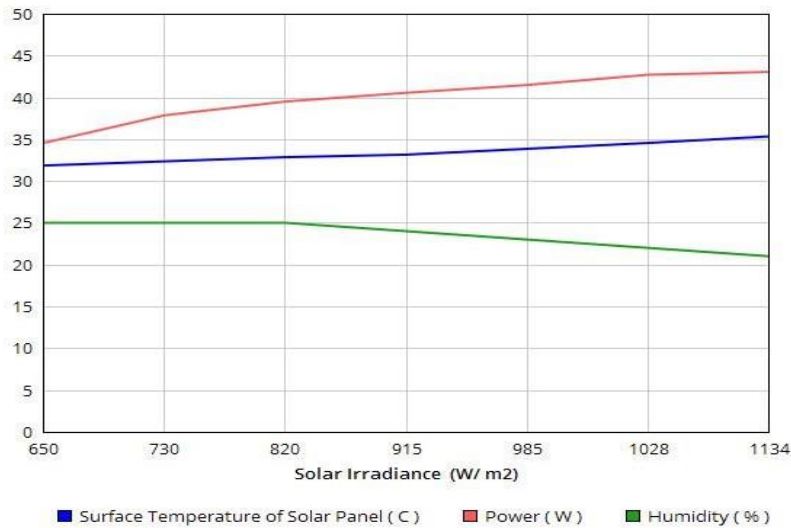
Fig. 5. The graph is portraying the effect of increase in the solar irradiations on Panel's Power Output, Humidity and Surface Temperature.
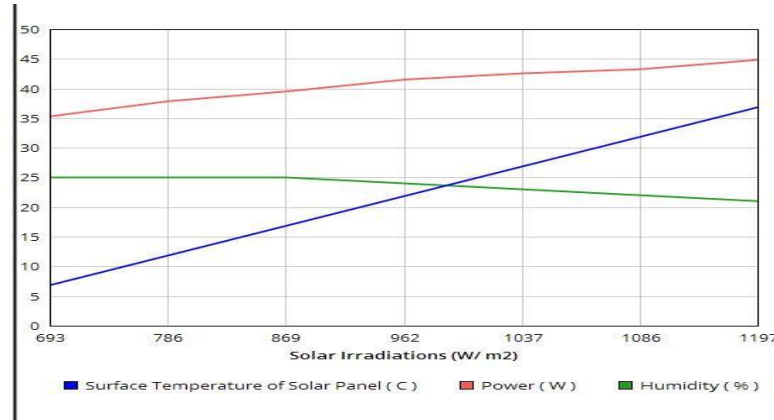
Fig. 6. Graph portraying the effect of an increase in the solar irradiations on Panel's Power Output, Humidity and Surface Temperature in Temperature ranges (6.85*C-36.85*C).
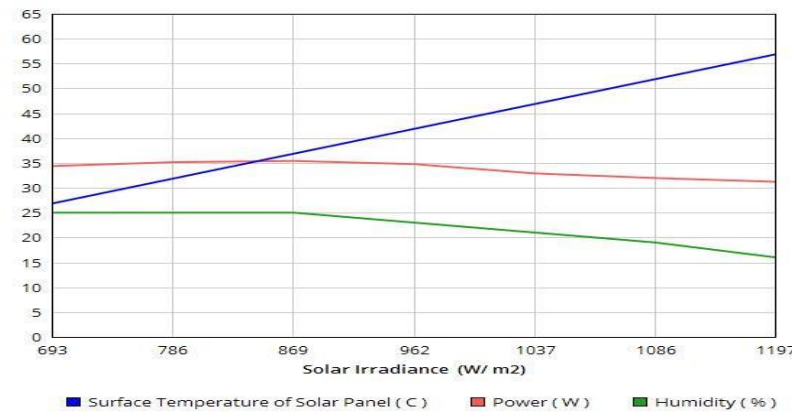
Fig. 7. Graph portraying the effect of an increase in the solar irradiations on Panel's Power Output, Humidity and Surface Temperature in Temperature ranges (26.85*C-58.70*C).
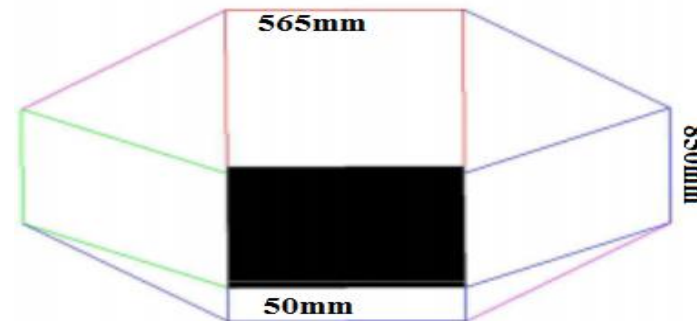
Fig. 8. Shows the solar concentrator used for the experimental analysis (850 x 565 x 50mm).
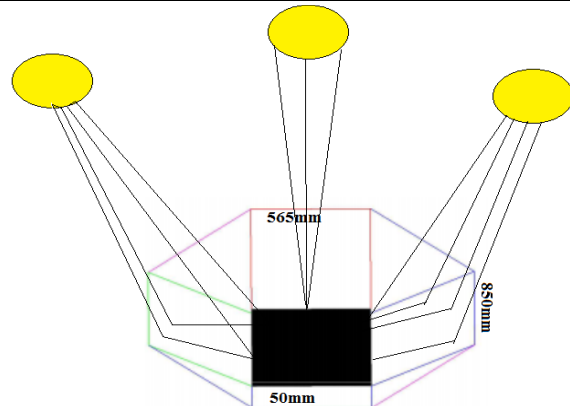
Fig. 9. Design of the static solar concentrator mechanism utilizing the peak hours.
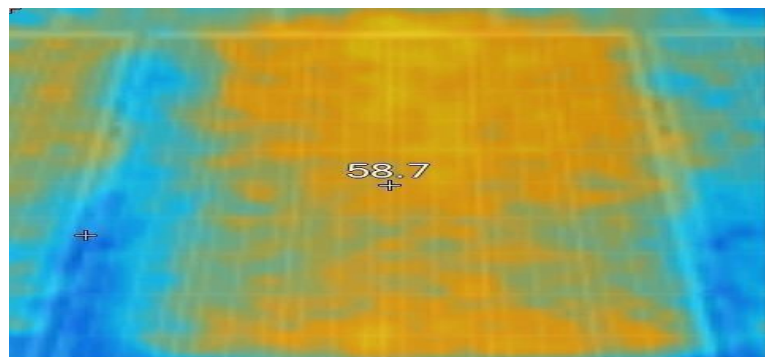
Fig. 10. Portrays areas which are under high temperature because of the solar concentrator at 58.7*C.
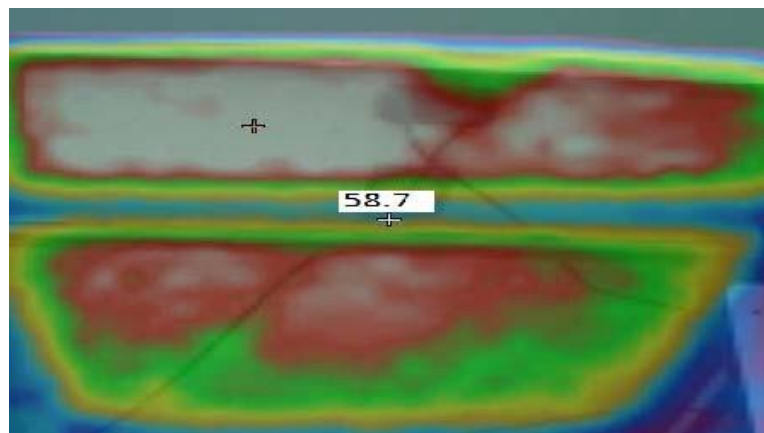
Fig. 11. Portrays areas at the backside of the Solar Panel at 58.7*C.

3.3. Equations

Voc module = Temp coefficient $*$ (Tstc - T ambient) + Voc rated   (1)

Where:

Voc, mod = open circuit voltage at module temperature

Tstc [°C] = temperature at standard test conditions, 25 °C, 1000 W/m2 solar irradiance

Tambient [°C] = Module temperature Voc,rated = open circuit voltage at STC.

$$P_i = \int_0^\infty E(\lambda)\, d\lambda \qquad (2)$$

$$J_{sc} = \int E(\lambda)\, SR(\lambda)\, d\lambda \qquad (3)$$

$$\rho_{A,B} = \frac{\text{cov}(A,B)}{\sqrt{\text{cov}(A,a)}\sqrt{\text{cov}(B,b)}} \qquad (4)$$

4. Results and Discussions

As per the results validated and investigated, it's well understood that the photovoltaic systems appear to be working efficiently if there is solar concentrator's used within the specified region mentioned by the manufacturer on the specification list. The solar concentrator is successful in collecting a significant amount of radiation to be converted.

It can be referred from Figure 4 and Figure 5, that with an increase in the irradiations, there is a considerable increase in the temperature noticed and there is an irregular behaviour of the system noticed when the temperature ranges are brought to variant as specified on the specification list.

It can be referred from Figure 6 that when operating the Solar Panel from the range 6.85*C-36.85*C, the system is seen to deliver a higher amount of Power Output. However, referring to Figure 7, when the specified range is surpassed, there appears decrement in the Power Output which indirectly makes the system more unstable and unreliable.

The Solar Concentrator's specification is specified in Figure 8 which are incorporated in the experimental setup. From Figure 9, it can be deduced that the solar concentrators can be incorporated to cover a specified angle to cover and utilize the peak hours for the photovoltaic system.

Referring Figure 10, it can be observed that when the Solar Panel is exposed to Solar Concentrator, the centre of the Solar Panel is studied to have been exposed to increasing temperature which indirectly leads to irregular behaviour of the Solar Panel when the specified temperature range is surpassed. Moreover, in the view of Figure 10, the sides of the Solar Panel could be seen experiencing lesser temperature effect as compared to the centre part because of utilising the Solar Concentrators.

Moreover, referring Figure 11, the impact of the Solar Concentrator could be seen at the back of the Panel which is also experiencing a shift in the temperature ranges and is indicated by reddish colour.

Considering the facts mentioned above and figures utilising Solar Concentrator in ranges

below mentioned could help in enhancing the power efficiency by utilising the Solar Concentrators. Various experiments were conducted to validate the idea of increasing and decreasing of Power Output concerning solar radiations concentrated and allowed to hit the Solar Panel.

5. Conclusion

The thorough investigation was carried out to properly study and validate the idea of incorporating the Solar Concentrator on the Solar Panel to enhance the Power Efficiency. There is significant need to allow few changes to the Photovoltaic System to allow a stable and reliable response. The proposed idea was seen working effectively in ranges identified as 6.85*C-36.85*C where in response to increasing solar intensity, the power output was seen increasing. However, the studied range from 36.85*C-58.70*C was seen negatively contributing to the Power Output and hence it was seen decreasing with increasing of Solar Intensity and Surface Temperature of the Solar Panel. Therefore, predefined measures are to be considered before utilising the Solar Concentrators in areas that are hot and humid.

6. Future Recommendations

Given the irregular response of the Solar Panel with incorporating Solar Concentrator, heat sinks could help to control the overall temperature ranges of the Solar Panel. Moreover, there could be additional ventilation factor that could be studied before incorporating the Solar Concentrators in areas under and above the standard range as specified by the specification list. Additional ventilation could help effectively in increasing the overall stability and long-run durability of the Photovoltaic System. Additionally, there is a prompt need for self-cleaning of the Solar Panel that could also positively help in utilizing the proper conversion of the irradiation as there is a mixture of water and dust that forms a layer on the Solar Panel. However, there could be different Solar Panels

that could be manufactured to be exposed to areas which are hot and humid.

REFERENCES

[1] M. Chegaar and P. Mialhe, "Effect of atmospheric parameters on the silicon solar cells performance" *Journal of Electron Devices,* vol. 6, pp. 173-176, 2008.

[2] R. Gottschalk, D. G. Infield, and M. J. Kearney, "Influence of environmental conditions on the outdoor performance of thin film devices," *In 17th European Photovoltaic Solar Energy Conference,* 2001.

[3] Raghunathan, Vijay, A. Kansal, J. Hsu, J. Friedman, and M. Srivastava, "Design considerations for solar energy harvesting wireless embedded systems," *In Proceedings of the 4th international symposium on Information processing in sensor networks,* pp. 64. IEEE Press, 2005.

[4] Zeller, Peter, and H. M. Libati, "Utilization of solar energy for electrical power supply in rural African areas," *In AFRICON 2009 (AFRICON'09,)* pp. 1-6. IEEE.

[5] Ahmed, M. Mohamud and M. Sulaiman, "Design and proper sizing of solar energy schemes for electricity production in Malaysia," *In Power Engineering Conference,* 2003. *PECon 2003,*

Proceedings. National, pp. 268-271. IEEE, 2003.

[6] Omubo-Pepple, V. B., C. Israel-Cookey, and G. I. Alaminokuma, "Effects of temperature, solar flux and relative humidity on the efficient conversion of solar energy to electricity," *European Journal of Scientific Research*, vol. 35, no. 2, pp. 173-180, 2009.

[7] G. Mostafa and F. Khan, "An efficient method of the solar panel energy measurement system," *1st International Conference on the Developments in Renewable Energy Technology (ICDRET), 2009,* pp. 1-3, IEEE.

[8] M. C. Alonso-Garcia, J. M. Ruiz, and F. Chenlo, "Experimental study of mismatch and shading effects in the I–V characteristic of a photovoltaic module," *Solar Energy Materials and Solar Cells* vol. 90, no. 3, pp. 329-340, 2006.

[9] Karl Pearson (20 June 1895), Notes on regression and inheritance in the case of two parents. *Proceedings of the Royal Society of London,* vol. 58, pp. 240–242.

[10] M. K. Panjwani, S. K. Panjwani, F. H. Mangi, D. Khan, and L. Meicheng, "Humid free efficient solar panel," *In AIP Conference Proceedings,* vol. 1884, no. 1, p. 020002. AIP Publishing, 2017.

Low Loss Transmission Circular Polarizer for KU Band Application

Farman Ali Mangi[1], Nafessa Shahani[2], Deedar Ali Jamro[1]

Abstract:

Low loss transmission circular polarizer is proposed for Ku band applications. The designed structure consists of two closely cross metallic strips which are based on FSS for 15.25 GHz and 15.28 GHz applications. The right hand circular polarization (RHCP) and left handed circular polarization (LHCP) are obtained at 15.25 GHz and at 15.28 GHz. The transmission loss through polarizer is important issue for high frequency applications. Due to transmission loss, new techniques are required to reduce the transmission loss of transmitted wave and achieve pure circular polarization. Meanwhile, low loss transmission has been achieved by using dual layer of strips to obtain perfect circular polarization at certain mentioned resonant frequencies. Theoretically, it is found that the outgoing waves through polarizer are perfect circular polarization at the distinct frequency ranges.

Keywords: Polarizer; Circular Polarization; Frequency selective surface; Quarter wave plate; Metamaterial.

1. Introduction

In modern microwave communication, circular polarization has received great interest in recent years. Precise, manipulation and detection of circular polarization of electromagnetic waves is important in modern technology. Artificially generating circular polarization is significantly more challenging in microwave communication technology. For instance, circular polarization is widely used in microwave communication and satellite communication systems. In addition, the CP achieves reflection effect, atmospheric absorption and lower susceptibility and intrinsically lower cross polarization discrimination.

An electronically steerable CP antenna array is more efficient for the inter-aircraft communication in terms of mobile nodes and wireless communication. The common application of antenna arrays is complex due to reduced level of practically-achievable output for extended millimetre wave communication network [1]. The CP antenna array approach was introduced for the use of a linearly polarised antenna array and electromagnetically coupled polarising wave plate. Dielectric polarisers [2], meander-line [3-5] and grid-plate [6] polarisers have been proposed to convert linear polarised electromagnetic waves to circular. CP antenna array is the combination of individual antenna elements which realize the directivity requirement and gain for the long distance [7-

[1] Department of Physics, Shah Abdul Latif University Khairpur, Sindh, Pakistan
[2] Institute of Chemistry, Shah Abdul Latif University Khairpur, Sindh, Pakistan
Corresponding Email: farman.mangi@salu.edu.pk

8]. In previous research contribution, the transmission type circular polarizers were proposed, such as U-shape split ring resonators, metallic helices, parallel plates, twisted Q-shaped metasurface, split ring resonator [9-10]. The four patch antennas were selected to produce 90º phase shift and [11] introduces an elliptical CP dielectric resonator antenna array. In [12, 13], the thin dual-band polarizer was designed for satellite applications and meta-device with different functionalities is integrated.

The several known CP antennas composed of different multi-pot feed networks and radiation elements which makes them inefficient for practical application. The end fire antenna array are introduced to date [14, 15] which are constructed of seamless integration with linearly polarized. Polarization state of electromagnetic waves affect our daily life in order to consumer products to high technology applications [16]. The characteristics of a non-isotropic transparent material based on the electromagnetic waves incident upon a birefringent material.

If E field converted in two orthogonal components of E_x and E_y having same amplitude, the phase shift of any one component will result in circular polarization and satisfy the phase shift 90º is known as quarter wave plate. The intensity of the incident electromagnetic wave does not change after propagating through a wave plate (only the polarisation state is changed). Wave plates are mostly considered as linearly birefringent, which means that the index of refraction differs along the two principal axes, which affects the phase shift of the orthogonal components differently [17].

Quarter wave plate possesses intriguing property to convert linear-to-circularly polarized waves when it is twisted at 45º to the impinging polarizing plane. The unique characteristics of quarter wave plate is to change EM waves from linear-to-circularly polarized states. Most often, the manipulation or polarization control can be obtained with quarter wave plate [18]-[24]. The phase difference between outcome two orthogonal transmitted waves is quarter of the wavelength 90º when impinged wave is linearly polarized at 450 and quarter wave plate has ability to change the impinged wave to circular polarization [25].

Frequency selective surface (FSSs) are developed as special filter and polarization transformer for microwave and millimetre waves. They are considered for many applications such as telecommunication, dichroic reflectors, waveguides and wireless security. [26-28]. FSSs can also be considered as polarizer [29-31] which has overall good performance and ease fabrication. The structure based on 15 x15 arrays of dual split ring resonators to demonstrate the transmission phase [32].

2. Structure of Single Layer Polarizer

First of all we have proposed single strip polarizer that operate at 13.20 GHz is designed and fabricated to produce perfect right hand circular polarization. This single strip acts as a quarter-wave plate that transforms a linearly polarized incident wave into a circularly polarized transmitted wave. A single strip oriented at 45° with λ/4 arm length along the x-y plane in simple unit cell. Whereas, the lengths of the single strip in x-y directions is 7.5 mm and width is 2 mm. Perfect Electric Conductor (PEC) material is used to the strip. The periodicity positions of the unit cell in three axes are X=28, Y=, 28 and Z= 25.25, respectively.
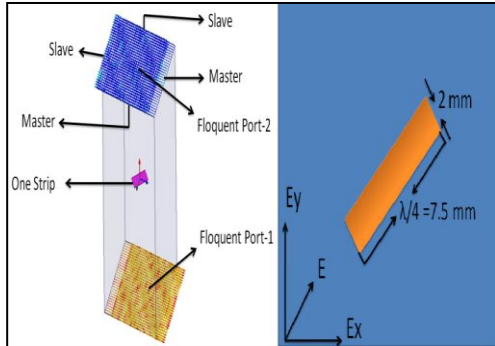
Fig. 1. View of circular polarizer based on single strip.

3. Structure of Circular Polarizer

Circular polarizer using FSS design for 15.25 GHz and 15.28 GHz applications. Using this FSS to obtain CP at resonant frequencies. In this structure, two metallic strips are placed perpendicular at angle +45º and -45º along x-y directions and separated at the distance of 7.2 mm perpendicularly from each other. The FSS polarizer is depicted in Fig.2. The proposed structure is constructed as cross dipole with $\lambda/4$ arm length along x-y axis. The length of each strips are selected 7.5 mm and 2mm wide, respectively. The Perfect Electric Conductor (PEC) material is used to strips. The periodicity positions of the unit cell in three axes are X=33, Y=, 33 and Z= 54, respectively.
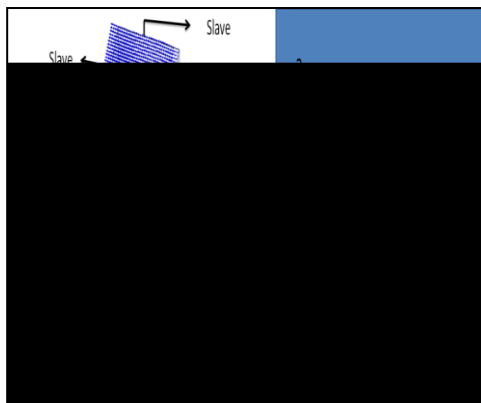
Fig. 2. View of Circular Polarizer based on two metallic strips.

4. Simulation Analysis

For simulation purpose, the HFSS software is used in terms of periodic boundary conditions. The impinged wave through floquet port one converted into circular polarized waves. The incident EM wave slanted at 45º and emerge in to two decomposed orthogonal waves $E_x$ and E_y to realize pure CP as shown in Fig.1. It can be observed that the transmission loss of designed structure -3.2 dB at the 13.2 GHz as depicted in Fig. 4. The axial ratio is 1.1 corresponds to phase difference of 90º at resonant frequency of 13.2 GHz mentioned in Fig.3 & 5. The RHCP wave and LHCP wave are generated at distinct resonant frequencies. The transmission loss of dual Polarizer at the RHC polarization is -1.8 dB and at LHC polarization is -2.6 dB with respect to resonant frequencies 15.25 GHz and 15.28 GHz. Meanwhile, corresponding phase differences between outcome waves E_x and E_y are depicted in Fig. 5 and 8. The simulated phase differences of outcome waves are satisfied at 90º to achieve pure CP at resonant frequencies.
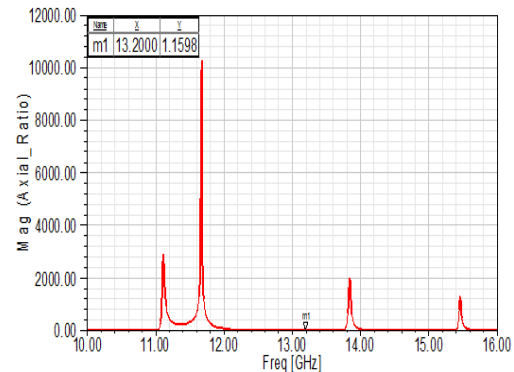
Fig. 3. Axial ratio at 13.20 GHz.

5. Theoretical Results

The HFSS software is used to analyze the obtained phase difference and magnitudes of output orthogonal components through designed low loss transmission circular polarizer. While, phase difference and transmission magnitudes of outcome waves

can be directly calculated by formula E_x/E_y and $\Delta\phi = E_x\phi - E_y\phi$.

In Fig.1, the unit cell structure is depicted in Fig.1 which is oriented at 45° in x-y direction. The transmitted of two orthogonal waves is same at 13.20 GHz which converts linear-to-circularly polarized wave. The calculated axial ratio of outcome two waves is 1.1 at 13.20 GHz depicted in Fig. 3. The low loss transmission of the generated waves is noticed due to reflection of polarized constructed by single metallic strip. The generated orthogonal waves are same at 13.20 GHz but transmission loss about -3.2 dB is observed. Obviously, the calculated transmission loss impact on the transmission power through single layer structure. The calculated phase difference of CP is 90° at the 13.20 GHz which corresponds to axial ratio between two outcome waves as mentioned in Fig. 3.
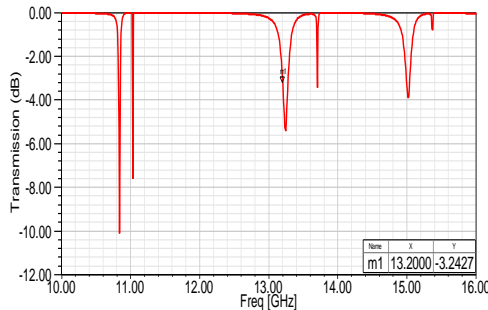

**Fig. 4.** Transmission magnitudes at 13.20 GHz.
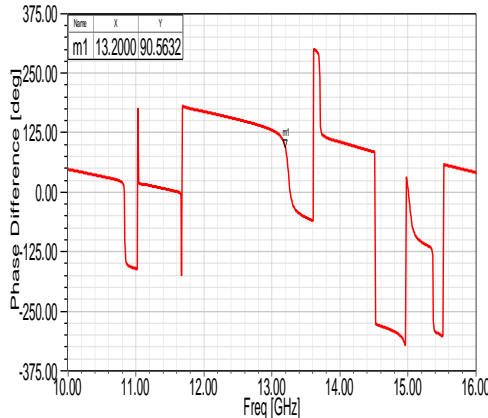
Fig. 5. Phase difference at 13.20 GHz.

The transmission loss of single-layer polarizer oriented at 45^0 in x-y direction is -3.2 dB as shown in Fig. 4. Furthermore, a innovative technique has been proposed to reduce transmission loss of single polarizer based on introducing the dual layer polarizer mounted perpendicularly to each other in the x-y direction as shown in Fig. 2.

The magnitudes of output orthogonal components are similar at the frequency of 15.25 GHz and 15.28 GHz to obtain the RHCP and LHCP. Nevertheless, it is necessary to obtain the circular polarization the phase difference of two orthogonal components E_x and E_y of E field must be satisfied at 90^0 .The transmission axial ratio between two orthogonal components is 1.4 and 1.2 at 15.25 GHz and 15.28 GHz as shown in Fig. 6. Whereas, the phase difference between two orthogonal components E_x and E_y is calculated by the phase difference formula of circular polarization.

The transmission loss after reflection from the Polarizer surface as shown in Fig.7 indicates the transmission magnitude of E components E_x and E_y in dB are -1.8 at 15.25 GHz and -2.60 at 15.28 GHz as shown in Fig. 7. It means that the magnitude of both orthogonals E_x and E_y components are same. The transmission loss is observed -1.8 and -2.6 dB that effect the transmission of waves through polarizer. It is observed that the transmission loss of dual layer polarizer has been reduced against single polarizer as shown in Fig. 7. The circular polarization can be calculated by the following expression.

$$\Delta\emptyset = \emptyset\mathbf{y} - \emptyset\mathbf{x}$$
$$= \begin{cases} +\left(\dfrac{1}{2} + 2\mathbf{n}\right)\pi, \mathbf{n} = 0, 1, 2, \ldots \ldots \ldots \ldots \\ +(\left(\dfrac{1}{2} + 2\mathbf{n}\right)\pi, \mathbf{n} = 0, 1, 2, \ldots \ldots \ldots \ldots \end{cases} \quad (\mathbf{1})$$

It is observed circular polarization achieved when axial ratio value of two orthogonal components is satisfied 1.2 at certain mentioned frequencies and correspond to 89.9^0 phase difference of two components.

Therefore, we have achieved at about 99% RCP and LCP at the frequencies of 15.25 GHz and 15.28 GHz as shown in Fig.6 and 7. The phase difference is calculated by deducing the value form Fig. 8 and verified by above equation 1.
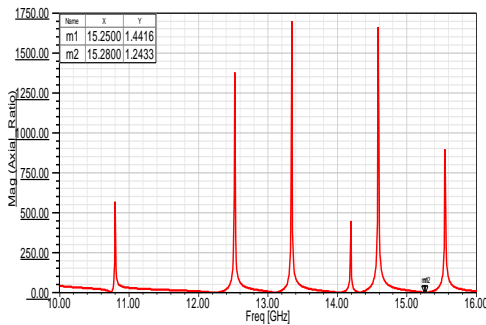
Fig. 6. Axial ratio is at 15.25 GHz and 15.28 GHz.
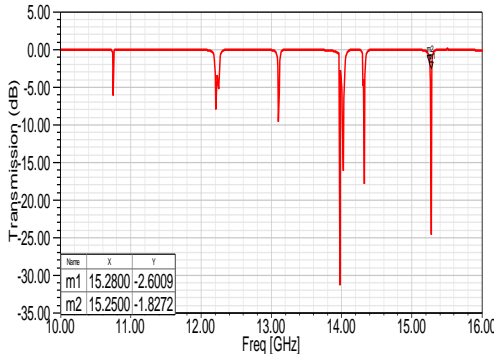
Fig. 7. Transmission magnitude at 15.25 GHz and 15.28 GHz.
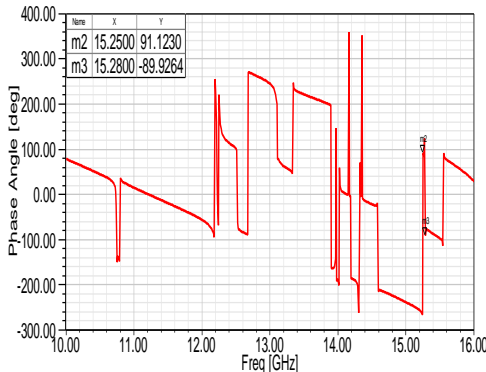
Fig. 8. Phase difference at 15.25 GHz and 15.28 GHz.

6. Conclusion

In conclusion, we proposed the low loss transmission circular polarizer using two metallic strips to investigate the transmission characteristics with pure circular polarization at 15.25 GHz and 15.28 GHz. The designed structure is based on FSS which generates the THCP wave and LHCP wave at resonance frequencies. The constructed model is simple and could be designed and fabricated easily by using HFSS software with high precision. The reflection and transmission characteristics are good features of the designed structure. In addition, the design techniques can be employed to construct the polarizers using double layer polarizers based on metallic strips or split ring resonators for millimetre, micrometre and terahertz frequencies. In future, this research can be carried out to compose polarizers using FSSs to extend the bandwidth and reduce the transmission loss.

REFERENCES

[1] V. Dyadyuk and Y. J. Guo, "Towards multi-gigabit ad-hoc wireless networks in the E-band", *IEEE Global Symposium on Millimeter Waves,* Sendai, Japan, 2009.

[2] L. Goldstone, "MM wave transmission polariser," *In Antennas and Propagation Society International Symposium,* 1979, vol. 17, pp. 606–609.

[3] L.Young, L. Robinson, and C. Hacking, "meander-line polarizer*," IEEE Transactions on Antenna and propagation,* vol. 21, pp. 376-378, 1973.

[4] R. S. Chu and K. M. Lee, "Analytical method of a multilayered meander-line polarizer plate with normal and oblique plane-wave incidence," *IEEE Transactions on Antenna and Propagation,* vol. 35, pp. 652-661, 1987.

[5] M. Mazur and W. Zieniutycz, "Multi-layer meander line polarizer for Ku band," *13th International Conference on*

Microwaves, Radar and Wireless Communication, vol. 1, pp. 78-81, 2000.

[6] Z. Chen , X. Li, "Novel mixed grid-plate circular polarizers," *4th International Conference on Microwave and Millimeter Wave Technology (ICMMT 2004), Proc.* pp. 66 – 69, Aug. 2004.

[7] W. Zhou, N. H. Noordin, N. Haridas, A. O. El-Rayis, A. T. Erdogan and T. Arslan, "A WiFi/4G compact feeding network for an 8-element circular antenna array," *Loughborough Antennas and Propagation Conference (LAPC2011),* pp. 1-4, 14-15 Nov. 2011.

[8] M. K. A. Rahim, T. Masri, O. Ayop and H. A. Majid, "Circular polarization array antenna," *Asia-Pacific Microwave Conference, APMC* 2008, pp. 1-4.

[9] M. Fartookzadeh and S. H. Mohseni Armaki, "Enhancement of Dual-Band Reflection-Mode Circular Polarizers Using Dual-Layer Rectangular Frequency Selective Surfaces," *IEEE Transactions on Antennas and Propagation,* vol. 64, no. 10, 2016.

[10] H. Cao, J. Liang , X. Wu and et al, "Dual-band polarization conversion based on non-twisted Q-shaped metasurface," *Optics Communications,* vol. 370, 2016.

[11] S. L. S. Yang, R. Chair, A. A. Kishk, K.-F. Lee and K.-M. Luk, "Study on sequential feeding networks for subarrays of circularly polarized elliptical dielectric resonator antenna," *IEEE Transactions on Antennas and Propagation,* vol. 55, pp. 321-333, 2007.

[12] N. J. G. Fonseca and Cyril Mangenot, "High-Performance Electrically Thin Dual-Band Polarizing Reflective Surface for Broadband Satellite Applications," *IEEE Transactions on Antennas and Propagation,* vol. 64, no. 2, 2016.

[13] H. X. Xu, S. Sun, S. Tang and et al., "Dynamical control on helicity of electromagnetic waves by tunable metasurfaces," *Sci. Rep,* vol. 6, 2016.

[14] H. Uchimura, N. Shino, K. Miyazato, "Novel circular polarized antenna array substrates for 60GHz-band," *IEEE MTT-S International Microwave Symposium Digest,* 12-17 June 2005 Page(s):4.

[15] S. W. Wang et al., "A circular polarizer designed with a dielectric septum loading," *IEEE Transactions on Microwave Theory and Techniques,* vol. 52, no. 7, pp. 1719-1723, 2004.

[16] N. K. Grady et al., "Terahertz Meta Material for linear polarization conversion and anomalous refraction," *Science* vol. 340, no. 14 June 2013, pp. 1304,

[17] G. I. Kiani, and V. Dyadyuk, "Quarter-wave plate polarizer based on frequency selective surface," *European Microwave Conference,* pp. 1361–1364, 28-30 Sept. 2010.

[18] D. Lerner, "A wave polarization converter for circular polarization," *IEEE Trans. Antennas Propag.,* vol. AP-13, no. 1, pp. 3–7, Jan. 1965.

[19] L. Young, L. Robinson, and C. Hacking, "Meander-line polarizer," *IEEE Trans. Antennas Propag.,* vol. AP-21, no. 3, pp. 376–378, Mar. 1973.

[20] R.-S. Chu and K.-M. Lee, "Analytical method of a multilayered meander-line polarizer plate with normal and obliqueplane-wave incidence," *IEEE Trans. Antennas Propag.,* vol. AP-35, no.6, pp. 652–661, Jun. 1987.

[21] A. K. Bhattacharyya and T. J. Chwalek, "Analysis of multilayered meander line polarizer," *Int. J. Microw. Millimeter-Wave Comput.-Aided Eng.,* vol. 7, no. 6, pp. 442–454, 1997.

[22] M. Euler, V. Fusco, R. Cahill, and R. Dickie, "Comparison of frequency-selective screen- based linear to circular split-ring polarisation convertors," *IET Microw., Antennas, Propag.,* vol. 4, no. 11, pp. 1764–1772, 2010.

[23] M. Euler, V. Fusco, R. Cahill, and R. Dickie, "325 GHz single layer sub-millimeter wave fss based split slot ring linear to circular polarization convertor," *IEEE Trans. Antennas Propag.,* vol. 58, no. 7, pp. 2457–2459, Jul. 2010.

[24] M. Joyal and J. Laurin, "Analysis and design of thin circular polarizers based on meander lines," *IEEE Trans. Antennas Propag.,* vol. 60, no. 6, pp. 3007–3011, Jun. 2012

[25] C. Pfeiffer and A. Grbic, "Millimeter-Wave Transmitarrays for Wavefront and Polarization Control," *IEEE Transactions on Microwave Theory and Techniques,* vol. 61, no. 12, pp, 4407, december 2013,

[26] B. A. Munk, Frequency Selective Surfaces, Theory and Design, *John Wiley & Sons Inc,* 2000.

[27] G. I. Kiani, A. R. Weily, and K. P. Esselle, "A novel absorb/transmit FSS for secure indoor wireless networks with reduced multipath fading," IEEE Microwave and Wireless Components Letters, 16, pp. 378-380, 2006.

[28] G. I. Kiani, K. L. Ford, K. P. Esselle, A. R. Weily, and C. J. Panagamuwa, "Oblique incidence performance of a novel frequency selective surface absorber," *IEEE Transactions on Antennas and Propagation,* vol. 55, pp. 2931-2934, 2007.

[29] A. Strikewerda et al., "Comparison of birefringent metamaterials and meaderline structure as quarter-wave plates at terahertz frequencies," *Optics Express,* 17, pp. 136-149, 2009.

[30] K. Karkkainen, and M. Stuchly, "Frequency selective surface as a polarisation transformer," *IEE Proceedings on Microwaves, Antennas and Propagation,* vol. 149, pp. 248-252, 2002.

[31] S. A. Winkler, W. Hong, M. Bozzi, and K. Wu, "A novel polarization rotating frequency selective surface based on substrate integrated waveguide technology," *In Proceedings of the 39th European Microwave Conference,* Rome, Italy, 2009.

[32] H. X. Xu, S. Tang, G. M. Wang and et al., "Multifunctional Microstrip Array Combining a Linear Polarizer and Focusing Metasurface," *IEEE Transactions on Antennas and Propagation,* vol. 64, No. 8, (2016).

A Comparative Analysis of Different Commercial Lights

Shoaib Ahmed Shaikh[1], Hamza Ali[1], Mansaf Ali Abro[1], M Talha Iqrar[1], Abdul Manan Memon[1]

Abstract:

There is a huge amount of financial losses due to usage of inefficient appliances in domestic, commercial and industrial sectors. A common appliance which occurs in the domestic, industrial and commercial loads is the lighting. This paper represents the study of different types of lights used in shopping malls by focusing on the different parameters of lights as Lumens, efficiency, power consumption, temperature. A survey was conducted in the shopping mall and measurements were also taken which shows the negative impact on the economic, power sector and environment. The proposed system was initiated by using the other types of lights with the help of DIALUX software which shows the improved results of cost, Lumens, temperature, power consumption and environmental benefits.

Keywords: *Lighting overview; Lighting comparision; Shopping Mall survey; Environmental impacts; Power quality scenario.*

1.Introduction

There are different types of loads used in the buildings as; inductive, capacitive and resistive. Lighting system consists of different lights which again comprises in the above-mentioned load categories. This most common system keeps vital role and is crucial for ensuring its product, safety and luxury of the residents in the buildings. However, proper designing of the lighting is necessary for getting the desired requirement of output of illumination with least quantity of electricity use. From the report the Artificial Lighting consumption is up to 20-30% of the total commercial loads electricity consumption in a building [1]. As per guidance of IEA the lighting consumption from Global electricity consumption is distributed in percentage form as depicted in the pie chart in figure 1[2].

- Service sector 48%
- Residential sector 22%
- Industrial sector 16%
- street & other lighting 8%
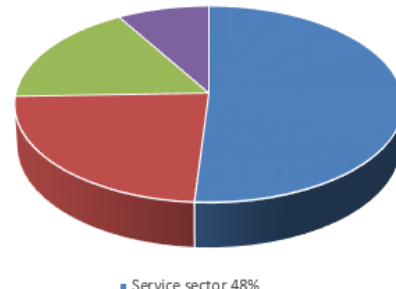
Fig. 1. Global electricity consumption of light [2].

[1] FEST, Hamdard University Karachi, Pakistan
Corresponding Email: skshaikh@outlook.com

There is a huge gap in developing countries between demand and supply, surveys is being conducted and measures are being taken to reduce the consumptions of electricity as their demand side (DM) management part. It is estimated that by switching energy efficient technologies the reduction of energy up to 27% in residential side and 30% in commercial side could be received [3]. This has increased the usage of power electronic or non-linear energy saving devices. By extensive usage of these electronic equipment's, negative harmful impacts on the quality of power in the distribution system may arise. With extravagance one problem's solution will generate several other technical problems. Experiments and measurements have proved and clarified that preventation is more profitable and economical after the fact being known, rather than initiative of other problem's solution findings [4].

So many techniques occur to reduce the power consumption limit. Among these techniques replacement of inefficient energy lamps with the other efficient lamps is one of the best techniques.

Replacing the incandescent lights with standard energy efficient lights is economical in the summer season by the reduction of cooling needs in the building as well as reducing the lightning power consumption [5]. Surveys, Studies and measures have proved that there is a significant portion of lighting constitution in the country's total electricity consumption. In accordance with the Swedish Energy Agency report, around 23 % of the country's total consumption of electricity occurs for lighting [6].

There is a momentous quantity of lighting consumption of the total energy resources in the world. In accordance with 2011 statistics, there are about 7.2% of lightning consumption of the developed and advanced world's primary energy assets which is accountable for the huge amount i.e. 430×10^9 kg of carbon emission [7]. With such a huge amount of CO_2 emission and energy use, increasing the lightning efficiency by taking surveys and measurements is mandatory [8-9].

Electricity Rational consumption in buildings has become very essential and pertinent subject, particularly when growth of energy is becoming costlier and climate change may be initiated due to immoderate use through high release of greenhouse (CO_2) gases [10].

Energy consumption growth and emission of greenhouse (CO_2) gases in urban surroundings have made policies for energy saving and improving efficiency a prime concern in the energy plans of almost all countries [11]. Particularly in building, energy utilization for lightning is an extensive contributor to CO_2 release, and its estimation has been taken which accounts for 20 to 40% of total energy utilization in buildings [12-13].

This paper represents the comparison of lights used in a shopping mall with its performance characteristics as power consumption, its temperature, Lumens, efficacy, etc., Environmental impacts due to lighting usage and some other power quality issues. We have designed a wooden box on a DIALUX software to check all the mentioned parameters with the help of instruments as watt meter, Lux meter and infra-red thermometer.

2. Overview of Lights

There are various types of lights used as indoor and outdoor applications. At a recent time, the opinion of utilizing the more eminent and enduring Light Emitting Diode (LED) in the applications which were consistently the province of inefficient and short life Compact Fluorescent Lamps (CFLs) and incandescent Lamps (ILs) has given the result of the development of LED lights. Relatively,

in the general lightening system, LED technology is new and is developing continuously which have made it exigent for assessing its environmental aspects. LED lamps primarily are planned for domestic and commercial consumers. Moreover, LED lamps are environmentally affable as compared to other lamps like CFL has mercury inside it [14].

Each appliance has their own pros and cons. Despite this, it is necessary to use the standardized and efficient appliances as lights. In the selection of lights, the following important factors are considered shown in figure 2.
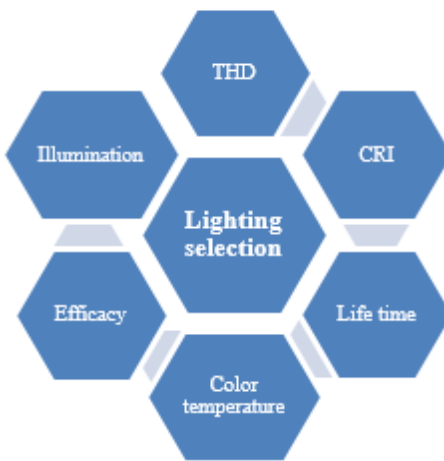

Fig. 2. Factors for the selection of lights.

Following are some types of lights which are familiar and mostly used for domestic and commercial purpose:

2.1. Incandescent Lamp:

This is a common household light bulb. It's simple yet brilliant. It was invented in late 1800s and amazingly it has hardly changed at all. In early it had on the top priority and in high usage due to lack of other lights inventions.

Heat is the main drawback of incandescent lamp and considered as highly inefficacious light bulb because loss of input energy is about 90% as heat

output [15]. The efficacy range of IL is 10-20lumen/watt, which depends on their construction features and temperature of the filament during operation [16]. Generally, the rated life period of IL is less (<) around 1000hrs as compared to other lamps [17-18]. Halogen gas keeps vital role in incandescent lighting, special by adding this gas in incandescent lamp glass that has made the lifetime range higher.

According to the US market report 2010, higher consumption (62%) of ILs has lowered the value of efficiency i.e. 19.1lumen/watt in the residential sector. This value could be improved by replacing the inefficient IL with other durable and energy efficient lights [19].

Researchers and experts tried to increase efficiency of IL and they asserted that the efficacy of HL may be increased to a value 45lumen/watt, but verification has not been achieved [20].

In European Union countries, due to above so many cons, EU commission had emphasized for the installation of IL to be banned from Sep 2012 on priority basis. It was not a proper solution to ban the product rather to give the alternate solution of making it an efficient. As this issue could be resolved by the usage of inert gases having emptiness CO_2 emissions or other harmful gases which increased the cost due to high consumption. It is also estimated that electrical energy consumption in houses can be reduced up to 10-15% [21].

2.2. Fluorescent Lamp:

The common type of discharge lamp is a fluorescent lamp (FL) or tube used today in many sectors. This type of light is further classified as CFL and LFL. Inside a CFL or IFL, a UV light is produced due to passing of electrical charge through mercury gas. This light then results in the excitement of coated phosphorescent on the inner side of the tube for the production of the light. In fluorescent lighting, ballast is required for supplying an amount of current to start up. This can be attached on lighting fitting and

can be integrated in the bulb's design. A fluorescent is a more efficient lamp as an incandescent lamp at present has been eliminated due to inefficiency and other drawbacks. Typically, the lamp's surpassing initial cost is neutralized by smaller energy cost [22]. Many shapes and sizes occur for Fluorescent Lamps. The Fluorescent Lamps (FLs) are recognized by their standard coding system which specifies the parameters and operating typical features with their relevant information. 'T' is a key factor which denotes tabular and shows the diameter of tube, e.g. 1inch diameter itemizes T8 tube [23].

Due to less power consumption and more luminous, CFLs is accredited as Cost-effective "Energy Saving Lamps" as compared to IL [24]. Equivalence of CFL and IL can be done with the ratio 4:1; this means that for the same light 80W IL could be replaced by 20W CFL [25].

2.3. LED Lamp:

A new type of device for lighting spreads over the planet the LED. It isn't a new device some way or another it has been used for years all around the world. What is new however, is being achieved greater power emission than a few years ago and making it provide white light. Their advantage that it consumes less energy ($<$) as the traditional incandescent lamps (IL) uses high energy. A traditional lamp i.e. IL needs to be heated to emit light and a lot of energy is emitted and wasted in the heat form. Moreover, the materials suffer this heating problem at high temperature values. Recently, several types of energy-saving lamps have become popular. The first energy saving lamps that replaced incandescent ones is fluorescents, which contain gases inside. On the other hand, LEDs can be made very small and solid elements are used in LEDs. In addition, LEDs are familiar due to their easily control, allow new applications such as generation of any light spectrum visibility of demand, optimizing energy costs and information transmission, this is known to be smart lighting.

A more efficacious, long lived LED lamp is also an environmentally friendly lamp than other light sources due to the empty mercury composition material. Today the high power white LED has increased luminous efficacy value reached up to 231lumen/watt in a laboratory [26].

From the Measures being taken and tests being conducted in the lab, it is shown that in domestic LED light and CFLs will not initiate any harmonic problem in the future of the network as compared to classic light bulbs [27-28].

3. Methodology

We have taken the measurands and counting of various lights used in shopping mall. The shopping mall consists of basement, ground floor and other four floors. There are so many shops in a shopping mall as shown in figure 3.

Fig. 3. Different shops in a shopping mall.

The most common lights used in a shopping mall are FL. CFL, IL, Halogen, HQI-TS, HPI-T, HPI-TS and HCI-T for different locations. As above mentioned that the lights performance can be observed by checking its parameters as; power rating, temperature, lumen etc. The existed data of lumen of different portions and shops of

building is given in the form of bar charts in figure 4, figure 5 and figure 6 respectively.
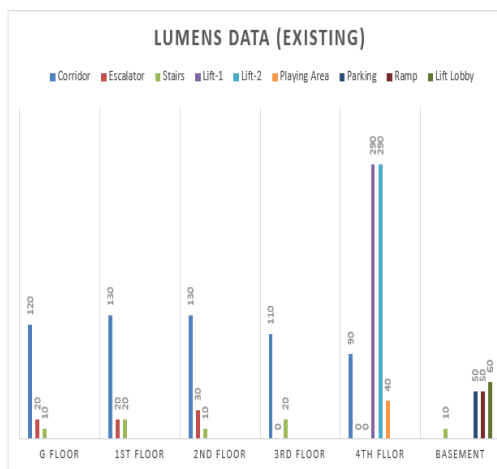

Fig. 4. Lumens data of the shopping mall.
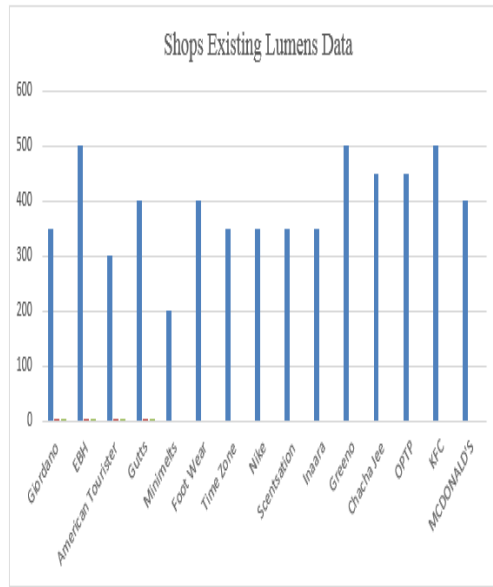
Fig. 5. Lumens data of shops in a mall.

Fig. 6. Existed power rating of the lights (53767 or 53.767kw).

We have checked the data of lighting used in a mall. Now we are going to select the other lights which are recommended as efficient and cost-effective lights. A wooden box is set which is designed by using the DIALUX software to check the results of exiting lights and recommended lights as shown in figure 7. Our focus is to check the Lumens, temperature and power rating by using the instruments as Lux meter, infra-red thermometer and wattmeter.

For experiments, we take three existed lights and three recommended lights to check their performance in a designed box as shown in figure 8.

The rating of existed lights is given as:

A_1 = FL = 36W, 56lumens, 37°C

B_1 = CFL = 24W, 50lumens, 38°C

C_1 = Halogen = 50W, 270lumens, 60.5°C

The rating of recommended lights is given as:

A_2 = FL = 16W, 60.8lumens, 32°C

B_2 = CFL= 11.7W, 65.2lumens, 34.5°C

C_2 = Halogen = 7.8W, 470lumens, 35.3°C
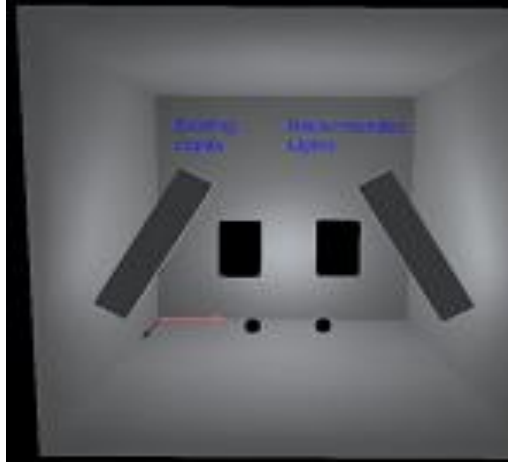
Fig. 7. Box selection on DIALUX software.
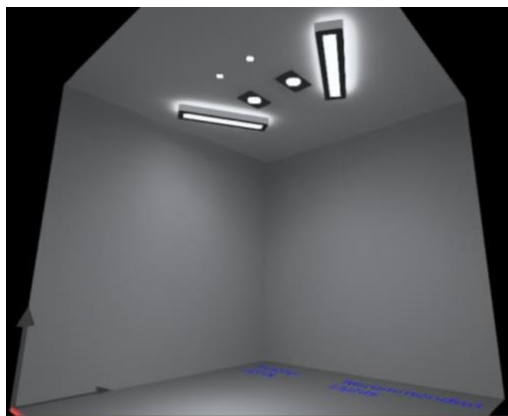
Fig. 8. Lights comparison.

After replacing the lights, we got the power rating result in the form bar chart as shown in figure 9, which clearly shows the improved results. It is an obvious that there is a direct relationship of power consumption with power rating and operating time. So, a positive result of the graph also depicts the recommended lights are cost-beneficial, high Lumens value and low temperature rating.

Fig. 9. Recommended power rating of lights.

The next comparison is of the Lumens and temperature mentioned in the charts given below in figure 10 and figure 11 respectively.
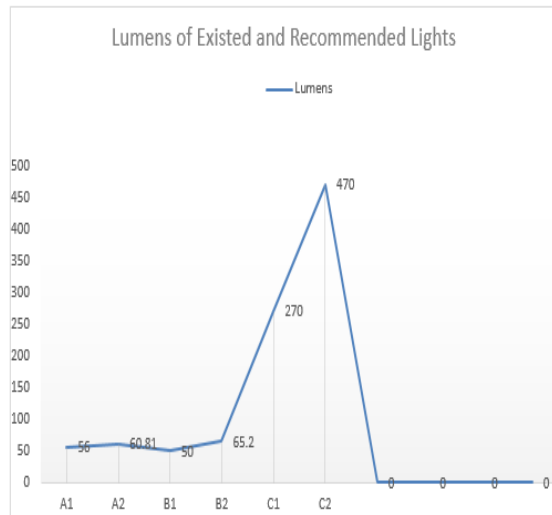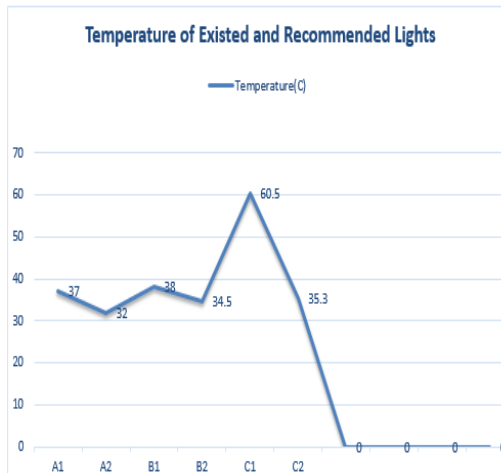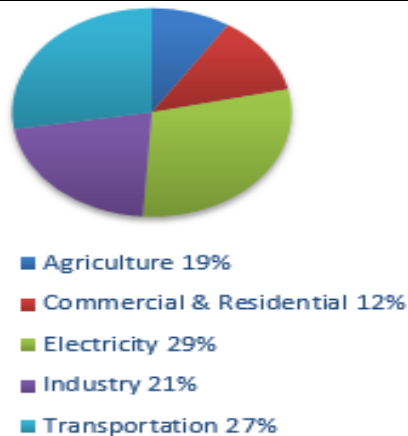
Fig. 10. Lumens of different lights.
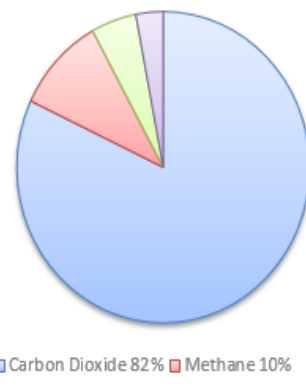
Fig. 11. Temperature of different lights.

Fig. 12. US greenhouse gas emission by economic sector 2015.

4. Energy and Enviromnetal impacts:

A greenhouse gas is not a particular gas, but consists of other different gases. Greenhouse gases in an atmosphere trap heat and keep the planet warmer. Human beings, their activities and liveliness are the responsibility for all of the growth in greenhouse gas emission from the last 150years. The primary greenhouse emission sources in United States (US) are electricity, transportation, industry, commercial/residential, agriculture and land use for forestry. In figure 12, total US greenhouse gas emission by Economic sector 2015 are presented in percentage form according to the US Environment protection agency [29].

Total emission in 2015 was equal to 6,587 Million Metric Tons of CO_2 equivalent. The greenhouse (GH) gases comprise of CO_2, N_2O, CH_4 & Fluorinated gases. A Pie chart of the total emission is given in figure 13.

Fig. 13. Greenhouse gases emission.

The energy we utilize in our homes, mainly dependent on the atmosphere where we live and the different type devices that consume energy which are in our usage. Figure 14 shows the pie chart of residential energy consumption in percentage for the year 2009 [30].
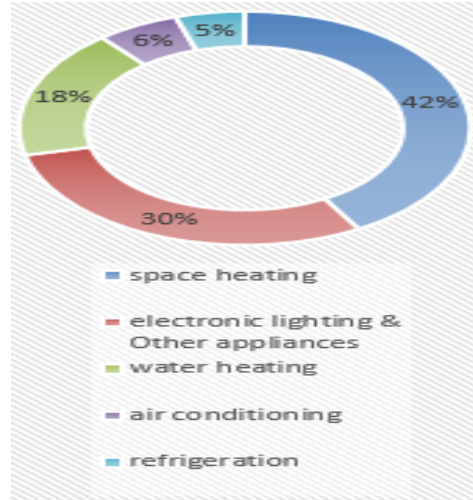
Fig. 14. Residential energy consumption survey (RECS) 2009.

It is not widely considered and focused that the biggest and main reason of greenhouse gas emission is lighting. The energy consumed to supply lighting necessitates greenhouse gas emission of 19×10^2 megatons of CO_2/year throughout the world [31]. As each of us are producing CO_2 gas from our daily activities as by turning the lights and it is already discussed above that lightning is one of the main sources of producing CO_2 gas. We can reduce the CO_2 emission gases with the usage of advanced lighting technology. Light bulbs are not associated with carbon dioxide but when we switch on the lights in our homes, this deadly CO_2 gas in initiated in the generation of electricity on which those light bulbs powers. Changing our incandescent light bulbs or other types to new, more efficient and high environmental friendly LED lamp is the best for an ease reduction of carbon emissions.

Vitae Energy Consulting claims in his recent report that saving could be £1.4 billion a year on its energy spend industry in the UK and 10 million tons (MTs) of CO_2 emissions annually by updating and modernizing the lighting stock on the usage of today's energy-efficient and advanced lighting technologies.

The study and survey was carried over 500 companies in the warehousing and manufacturing sector and concluded that, a quarter of the companies in around surveyed and observed, the lighting system accelerated in the 1950s and consumed almost inefficient light bulbs that were sheltered in fittings not ameliorated for efficient light radiation. The study also showed that energy usage of industrial lighting energy could be cut relatively 60% if the fittings were optimized for using the specially designed reflectors for increasing the overall light.

5. Power Quality Scenario

Incandescent light has unity power factor as it is a purely resistive load type lamp. The main advantage of this lamp is that it does not need any electronic driver to start thus no any harmonic issue occurs. Whereas other lamp types such as LED lamps and discharge lamps require special drivers for the operation purpose, hence produces harmonic distortions in the supply current wave which disturbs the sinusoidal waveform [32-33].

Inductance in ballast in case of discharge lamps has low lagging power factor which disturbs the power triangle, so it is necessary to compensate. A capacitor for compensation is the best solution to be connected in parallel with blast to increase the value the power factor (P.f) in a florescent lamp. In new T5 Fluorescent lamp (FL) luminaire, there is improved P.f of a good value 0.9 and improved THD value (<15%) due to usage of electronic ballast [33]. Whereas CFL of low rating with electronic ballasts have low leading power factor (0.5-0.6). Due to weight and space issues, low rating CFLs cannot be compensated individually [34]. Thus, power factor can be improved centrally in a given location if low rated CFLs with large quantity are used [35]. LED lamps designed as a source of voltage with a low rating of series resistance to limit the line current I_L, have usually much higher power factor than other

lamps (discharge lamps). According to the United states Dept. of the energy star program, the acceptable range of power factor (P.f) 0.7-0.9 has been mandated for domestic and commercial Light Emitting diode Lamps [36], also UK Energy Saving Trust has mandated a minimum acceptable power factor (P.f) of 0.7 with a prolonged objective having power factor of 0.9 for integral Light emitting diode lamps [34].

6. Conclusion

A common load which is always on peak usage in each season is of lighting. It is very important to select the proper lights for domestic, commercial and industrial usage. This paper focus on the profile of all types of lights specifically FL, CFL, IL and halogen. A survey of a shopping mall was being conducted for different types of light on different locations. There were lot of impacts due to existed lights as lumens, efficacy, temperature, power losses etc. Then other types of light with different parameters were recommended by selecting a wood box with a usage of DIALUX software which showed the improved results in this research work. This is not only important for the performance of lights but very much cost beneficial from economic point of view. On the other hand, it is also seen from consumption and environmental point of view that the IL lamp has the CO_2 emissions issues and high energy consumption. Halogen lamp was better than IL due to inert gases existed inside it which are not so worse than IL lamp. FL and CFL lamp was much better than IL lamp and Halogen due to low consumption of energy and environmental friendly. Furthermore, the above lights can also be replaced with the new technology of lights as "LED" which have led all types of lights due to several advantages. Our next task is to work on the LED lights and on the cons of above lights to give the improved techniques.

REFERENCES

[1] JC. Lam, DHW. Li, and S. Cheung, "An Analysis Of Electricity End-Use In Air-Conditioned Office Buildings In Hong Kong," *Building Environ*, vol. 38, no. 3, pp. pp. 493–8, 2003.

[2] Energy Conservation In Buildings And Community Systems Program (Ecbcs) Annex 45 Guidebook On Energy-Efficient Electric Lightingfor Buildings, Edited By Liisa Halonen, Eino Tetri & Pramod Bhusal, *International Energy Agency,* 2010.

[3] J. Trifunovic, J. Mikulovic, Z. Djurisic, M. Djuric, and M. Kostic, "Reductions in Electricity Consumption And Power Demand in Case of the Mass use of Compact Fluorescent Lamps," *Energy* vol. 34, pp. 1355–1363, 2009.

[4] N. R. Watson, T. L. Scott, S. Hirsch, "Implications For Distribution Networks of High Penetration Of Compact Fluorescent Lamps," *IEEE Transactions On Power Delivery,* vol. 24, pp. 1521–1528, 2009.

[5] R. Saidur, "Energy Consumption, Energy Savings, and Emission Analysis in

Malaysian Office Buildings," *Energy Policy* vol. 37, pp. 4104–4113, 2009.

[6] M. Bladh and H. Krantz, "Towards A Bright Future? Household Use Of Electric Light: A Microlevel Study," *Energy Policy,* vol. 36, pp. 3521–3530, 2008.

[7] K. Powell, "Panel4: Lessons From The Field. Solid-State Lighting Program: U.S. Department Of Energy," 2011. Available From:/Http://Apps1.Eere.Energy.Gov/B uildings/Publications/Pdfs/Ssl/Powell_L essons_Sslmiw2011.Pdfs (Access On:3 August 2012).

[8] J. R.-M. Belizza, S. –P. Claudia, "Electricity Sector Reforms In Four Latin- American Countries and Their Impact On Carbon Dioxide Emissions and Renew- Able Energy," *Energy Policy* vol. 38, pp. 6755–6766, 2010.

[9] Sheinbaum, C., Rui´Z, B.J., Ozawa, L., 2011.Energy Consumption And Related Co2 Emissions In Five Latin American Countries: Changes From 1990 To 2006 And Perspectives. *Energy*, vol. 36, 3629–3638.

[10] Linhart F, Scartezzini J-L. Minimizing Lighting Power Density In Office Rooms Equipped With Anidolic Daylighting Systems. Solar Energy 2010; 84(4):587–95.

[11] Pérez-Lombard L. A Review On Buildings Energy Consumption Information. Energy Build 2008; 40:394–8.

[12] Energy Information Administration. Commercial Buildings Energy Consumption Survey; 2003

[13] Brunner, E.J., Ford, P.S., Mcnulty, M.A., Thayer, M.A., 2010. Compact Fluorescent Lighting And Residential Natural Gas Consumption: Testing For Interactive Effects. Energy Policy 38, 1288–1296.

[14] Beth Daley, "Mercury Leaks Found As New Bulbs Break: Energy Benefits Of Fluorescents May Outweigh Risk," The Boston Globe, February 26, 2008

[15] Brunner, E.J., Ford, P.S., Mcnulty, M.A., Thayer, M.A., 2010. Compact Fluorescent Lighting And Residential Natural Gas Consumption: Testing For Interactive Effects. Energy Policy 38, 1288–1296.

[16] Doe, 2012a. 2010 U.S. Lighting Market Characterization. Solid-State Lighting Program:U.S. Department Of Energy. Available From: /Http://Apps1.Eere.Energy.Gov/Building s/Publications/Pdfs/Ssl/2010-Lmc-Final-Jan-2012.Pdfs(Access On:1august2012).

[17] Osram, 2009. Life Cycle Assessment Of Illuminants A Comparison Of Light Bulbs, Compact Fluorescent Lamps And Led Lamps.

[18] Simpson, R.S., 2008. Lighting Control—Technology And Applications. Focal Press.

[19] Doe, 2012a. 2010 U.S. Lighting Market Characterization. Solid-State Lighting Program:U.S. Department Of Energy.Available From: /Http://Apps1.Eere.Energy.Gov/Building s/Publications/Pdfs/Ssl/2010-Lmc-Final-Jan2012.Pdfs(Accesson: 1august2012).

[20] Eceee, 2011. Evaluating The Potential Of Halogen Technologies. European Council For An Energy Efficient Economy.Available From: /Http://Www.Eceee.Org/ Eco_Design/Products/Directional_Lighti ng/Halogen_Technologies_Report/ Eceee_Report_Halogen_Technologiess (Access On:27 July 2012).

[21] Europa, 2009. Phasing Out Conventional Incandescent Bulbs (Faq-Press Release). Available From: /Http://Europa.Eu/Rapid/Pressreleasesact ion.Do?Reference= Memo/09/368s (Access On:20 September2012).

[22] Onaygil S, Güler Ö. Determination Of The Energy Saving By Daylight

Responsive Lighting Control Systems With An Example From Istanbul. Building And Environment 2003; 38(7):973–7.

[23] Roisin B, Bodart M, Deneyer A, D'herdt P. Lighting Energy Savings In Offices Using Different Control Systems And Their Real Consumption. Energy And Buildings 2008;40(4):514–23

[24] Simpson, R.S., 2008.Lighting Control—Technology And Applications. Focal Press.

[25] Vito, 2007. Eco-Design Study Lot 19-Domestic Lighting. Preparatory Studies For Eco-Design Requirements Of Eups. Available From: /Http://Www.Eup4light.

[26] Cree: Cree 231 Lumen Per Watt Led Shatters Led Efficacy Records. [Online]. Available: Http://Www. Cree.Com/Press/Press_Detail.Asp? I=1304945651119. [Accessed November 17, 2011].

[27] S.K. Ronnberg, M.H.J. Bollen, Et. A! Harmonic Emission Before And After Changing To Led And Cfl - Part I: Laboratory Measurements For A Domestic Customer, 14th International Conference On Harmonics And Quality Of Power, P. 1-7,2010.

[28] S.K. Ronnberg, M. Wahlberg, Et. A! Harmonic Emission Before And After Changing To Led And Cfl - Part Ii: Field Measurements For A Hotel, 14th International Conference On Harmonics And Quality Of Power, P. 59-67, 2010.

[29] Https://Www.Epa.Gov/Ghgemissions/Inventory-Us-Greenhouse-Gas-Emissions-And-Sinks

[30] Https://Www.Eia.Gov

[31] Key World Energy Statistics 2007 (International Energy Agency, Paris, France, 2007).

[32] Philips, 2009. The Abc's Of Electronic Fluorescent Ballasts: A Guide To Fluorescent Ballasts. Available From: /Http://Www.Advance.Philips.Com/Doc uments/Uploads/ Literature/Rt-8010-R03_Abc.Pdfs (Accesson:3 August2012).

[33] Akashi, Y.,2002.T5 Fluorescent Systems. The Lighting Research Center, National Lighting Product Information Program(Nlpip). Available From: /Http://Www.Lrc.Rpi.Edu/Programs/Nlp ip/Publicationdetails.Asp?Id=284&Type =2s (Access On: 5august2012).

[34] CIE, 2012. Led Bulb Placement Meeting New Challenges. Components In Electronics. Available From: /Http://Content.Yudu.Com/A1wimc/Ciea pril12/Resources/52.Htms (Accesson:5 August2012).

[35] Sehat Sutardja, 2009. Green Opportunities. Marvell Semiconductor,Inc. Available From: /Http://Www.Marvell.Com/Environment /Assets/Marvell-Green-Opportu Nities.Pdfs (Access On:20july2012).

[36] ECN Magazine, 2011. Power Factor Correction Techniques Inled Lighting. Available From: /Http://Www.Ecnmag.Com/Products/201 1/08/Power-Factor-Correction-Techniques-Led-Lightings (Access On:22 September2012).

Fuzzy Logic Based Speed Controller For a Container Ship

Abdul Qadir[1], Dur Muhammad, Mukhtiar Unar[2], Jawaid Doudpoto[2], Mahmood Khatak[2]

Abstract:

Speed control of marine ships is one of the leading problems in terms of safety and economy. This research aims at designing a fuzzy logic-based speed controller for a marine ship. The dynamic model of container ship is considered. Fuzzy logic-based approach is employed to control the variations and to maintain the controller performance under the ideal conditions as well as during rough weather. MATLAB is used for simulation. The results show that the proposed controller has enhanced control performance compared to conventional controllers, efficiently confine the influence of the environmental disturbance, ensure perfectly control, and have good robustness.

Keywords: Container ship, Speed control, Fuzzy logic, Disturbances.

1.Introduction

It is essential for the marine ships to have some sort of speed controller to control and govern the speed of the ship to improve stability and maneuverability of ship during course keeping, course changing and pitching motion. Because while the ship is under the sea conditions, in very short span of time the propeller load will change during the pitching motion of the ship as the propeller may be close to or above the surface of water. Various researchers have contributed in this area. Le Luo et al. worked on electric propulsion system of ship [1]. His work is based on development of PID controller. Y. Luo et al. also worked on electrical propulsion system and tested PI control mode for combined power and speed control of marine ship [2]. Rigatos et al. presented the fuzzy control for

adaptive ship steering problems [3]. W Meng et al. presented the Fuzzy Logic technique for dynamic positioning of ship [4]. Tadeusz et al. worked on the effect of wind, waves and loading conditions on speed of ship [5]. The abovementioned research is based on the design of PID or PI controller for electric propulsion, speed and power control, However the speed control of ship under sea is a non-linear and time varying and PID controller is not effective in dynamic behavior, robustness and control. The mass of the container ship, hydrodynamic force and moments also require complex mathematical modelling, whereas the design of Fuzzy logic controller is expert knowledge-based system and widely used by control researchers for ship steering control, dynamic positioning of ship and electric propulsion control. Published studies have never considered Fuzzy logic-

[1] Mechanical Engineering, Faculty of Engineering and Management sciences Isra University Hyderabad
[2] Mechatronics Engineering, Institute of Information and communication Technologies MUET Jamshoro
Corresponding Email: aq.channa@isra.edu.pk

based speed control design for a marine ship. Considering Fuzzy logic in marine ships will be useful in regulating and advancing the speed control of marine ships. This study thus proposes a fuzzy logic-based speed controller which maintains the desired performance in both ideal conditions as well as in presence of disturbances.

2. Dynamics of a Ship

A rigid body can be completely defined by six coordinates as shown in Fig. 1 Therefore, six degrees of freedom are necessary to describe the motion of a ship [6] as mentioned in TABLE 1, where the *x, y* and *z* coordinates represent the linear motion along *x, y* and *z*, and the ϕ, θ and ψ represent the angular motion.

TABLE 1. Notation of ship motion.

Motion	Forces & moments	linear & angular vel.	Positions & Euler angles
Surge	X	u	X
Sway	Y	v	y
Heave	Z	w	z
Roll	K	p	ϕ
Pitch	M	q	θ
Yaw	N	r	ψ

2.1. Container Model

The mathematical model for a container ship has been presented by Son and Nomoto [8]. The parameters of the container model are given in TABLE 2 [8].

TABLE 2. Container ship parameters.

Parameter	Value	Unit
Length	175	Meter (m)
Breath	47.17	Meter (m)
Volume	21,224	$Meter^3$ (M^3)
Block co-efficient	0.558	No unit
Ship speed	16	Knots
Propeller speed	80	rev/m

State vector of a container ship can be defined as

$$x = [\ u\ v\ r\ x\ y\ \psi\ p\ \phi\ \delta\ n]' \qquad (1)$$

The definitions of all elements of state vector in Eq.1 are given in TABLE 1. The speed of ship can be specified by surge velocity 'u' and actual shaft velocity 'n' from Eq. 1 Therefore, the sub-model may be presented as in Eq. 2

$$x\_prop = [\ x\,(1)\quad x\,(10)] \qquad (2)$$

Where

- u = x (1)   x (1) = 7.
- n = x (10)/60   x (10) = 80.

2.2. Propeller Model

The mathematical expression which governs the propulsion speed of the propeller is given in Eq. 3 [7]

$$\dot{n} = \frac{1}{T_m}(n\_c - n) \qquad (3)$$

Where 'ṅ' is the output of the propeller as shown in Fig 4, 'n_c' and 'n' are command shaft velocity and actual shaft velocity. T_m is the time constant for shaft dynamics.
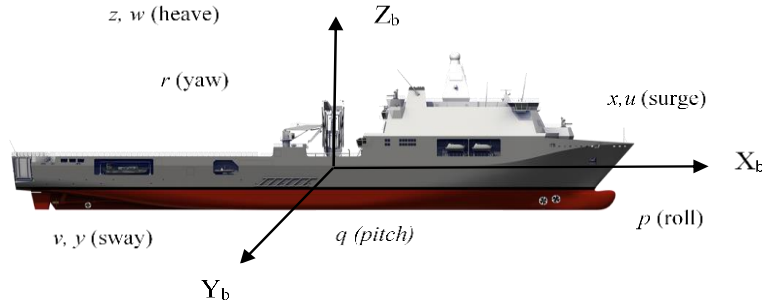
Fig. 1. Body fixed reference frame.

3. Fuzzy Logic Controller (FLC)

The fuzzy logic controller is a method of mapping the input states against the output [10]. Fuzzy interface system (FIS) as shown in Fig. 2 is used to map the given input to required output and this mapping provides basis for decision making [9, 11]. A FLC has three stages namely Fuzzifier, Interface system and Defuzzifier. The fuzzifier is a stage where membership functions are mapped, and a truth value is assigned [13]. In interface system stage set of rules is developed and results are generated by each rule, which are then further processed in defuzzifier, where results from rule base are combined to obtain a crisp output [12, 14].

Fig. 2. Fuzzy interface system.

The design of fuzzy logic controller is carried through following steps.

3.1. Inputs and Outputs for Controller

The speed of a ship is the function of the shaft speed. The other parameters which are affected by shaft speed are surge velocity 'u' and actual shaft velocity 'n'. Therefore, the inputs are speed error (u_error) and shaft speed error (n_error) whereas the output is selected as command shaft velocity (n_c). Fuzzy logic controller uses the expert knowledge in the form of linguistic rules. The ranges are tuned by trial and error method. Finally, the ranges given in TABLE 3 yielded the satisfactory performance and the values of fuzzified variables are given in TABLE 4, TABLE 5 and TABLE 6 respectively.

TABLE 3. Ranges of Input and Output.

Input vector (X_{error})	Speed error	u_error	-0.07 to 0.01
	Shaft speed error	n_error	-0.03 to 4.6
Output (n_c)	Command shaft speed	n_c	-0.09 to 155

3.2. Fuzzification of Inputs and Outputs

Fuzzification is the method of translating the fixed single in fuzzy variables. During the process of fuzzification the inputs and output defined by a linguistic word are divided into subsets. All the input and output subsets are mapped into fuzzy sets taking definite membership functions as shown in Fig. 3. In

this research 5 sub-sets are defined for input and output, labelled as: big negative (BN), small negative (SN), Zero error (ZE), big positive (BP) and small positive (SP).
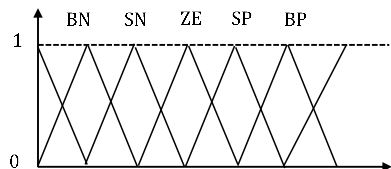
Fig. 3. Mapping of subsets.

Each of these subsets is presented in a way that their values intersect each other as given in TABLE 4, TABLE 5 and

TABLE 6. Each of subsets is mapped into triangular membership function.

TABLE 4. Fuzzy variables and subsets of (u_error).

Fuzzy Subsets	(u_error)		
	A	B	C
BN	-0.2	-0.0798	-0.06005
SN	-0.0798	-0.06005	-0.04003
ZE	-0.06005	-0.04003	-0.01995
BP	-0.04003	-0.01995	0.00028
SP	-0.01995	0.00028	0.02

TABLE 5. Fuzzy variables and subsets of (ṅ_error).

Fuzzy Subsets	(n_c)		
	A	B	C
BN	0.5	24.98	49.96
SN	24.98	49.96	74.96
ZE	49.96	74.96	99.98
BP	74.96	99.98	124.8
SP	99.98	124.8	140

Fuzzy Subsets	(ṅ_error)		
	A	B	C
BN	-0.05	0.8006	1.633
SN	0.8006	1.633	2.49
ZE	1.633	2.47	3.334
BP	2.47	3.334	4.158
SP	3.334	4.158	4.5

TABLE 6. Fuzzy variables and subsets of (u_c).

3.3. Defuzzification

Defuzzification is a method to convert the collected output of the linguistic rules into single output value [12]. The maximum degree, average of weight or center of gravity method of defuzzification can be used. For this work centroid defuzzification method is used due to its simplicity and less computation. The mathematical representation of centroid defuzzification method is given in Eq. 4 [9,10]

$$u\_c = \frac{\int \mu_C(n).n.dn}{\int \mu_c(n)dn} \qquad (4)$$

where u_c is the single output value, $\mu_c(n)$ is the combined membership function and n is the output variable.
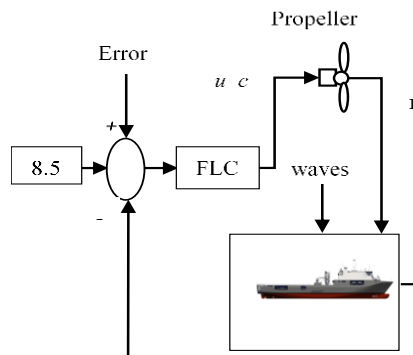

Fig. 4. Fuzzy logic controller.

4. Simulation of FLC

The simulations are carried out by a close lope control as shown in Fig. 4. The performance of controller was tried in calm sea ideal conditions as well as with disturbances (wind generated waves). The simulation results are presented in the Fig. 5 and Fig. 6.

4.1. Performance of Controller without Disturbances

The container ship speed controller designed in this research is asked to track the set speed value 8.5 m/s as the input signal for the FLC controller with propeller speed (n) of 80 rpm. In ideal conditions (without disturbances) the actual speed (blue line) tracking the desired speed (dashed red line) value with minimal steady state error up to -1 and within 350 seconds the actual speed overlaps desired speed value as steady state error becomes 0. The simulations are carried out on MTALB software and the results are presented in **Error! Reference source not found.**.
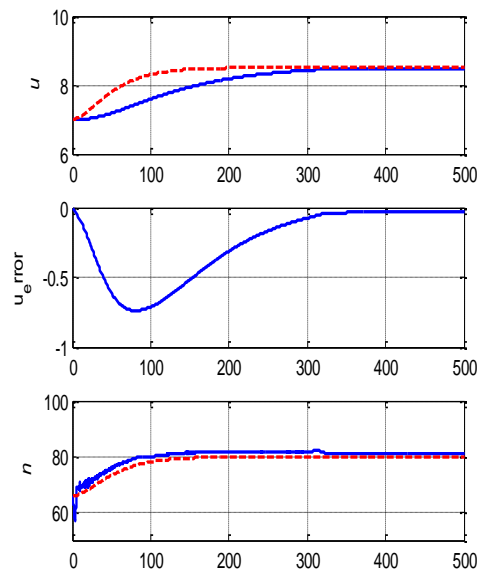
Fig. 5. Simulation of controller in ideal calm se conditions.

4.2. Performance of Controller with Disturbances

The Sea conditions are highly dynamic and time variant. There are many disturbances acting on sea ships, i.e, sea currents, depth of water, density of water and wind generated waves etc. in this research wind generated waves are taken as disturbances and the response of controller is tested. The effect of waves can be seen on propeller speed in terms of oscillations, where propeller is trying to overcome the effect of waves to maintain the ship speed. The controller has successfully maintained the ship speed with less than -0.1 error and the propeller speed is stable within 350 seconds. The simulation results are presented in Fig. 6.
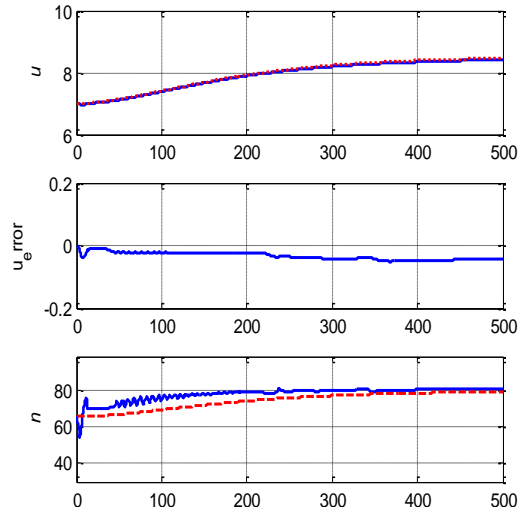
Fig. 6. Simulation of controller with disturbances.

5. Conclusion

Due to the complex and non-linear behavior of sea, mathematical modeling of ship maneuvering is difficult. Therefore, expert knowledge based fuzzy logic control system is designed for container ship speed. The controller is tested with calm sea (ideal) conditions and with wind generated waves as disturbances. The designed controller has remained robust and successfully traced the

desired speed values with and without disturbances.

REFERENCES

[1] L. Luo, L. Gao, and H. Fu, "The Control and Modeling of Diesel Generator Set in Electric Propulsion Ship," *International Journal of Information Technology and Computer Science (IJITCS),* vol. 3, pp. 31, 2011.

[2] Y. Luo, S. Lv, S. Kang, and X. Duan, "Combined power and rotating speed control of ship electrical propulsion system in waves," *International Conference on Information and Automation (ICIA),* 2012, pp. 200-205.

[3] G. Rigatos and S. Tzafestas, "Adaptive fuzzy control for the ship steering problem," *Mechatronics,* vol.16, pp. 479-489, 2006.

[4] W. Meng, L. H. Sheng, M. Qing, and B. G. Rong, "Intelligent control algorithm for ship dynamic positioning," *Archives of Control Sciences,* vol. 24, pp. 479-497, 2014.

[5] T. Szelangiewicz, B. Wiśniewski, and K. Żelazny, "The influence of wind, wave and loading condition on total resistance and speed of the vessel," *Polish Maritime Research,* vol. 21, pp. 61-67 10.2478/pomr-2014-0031.

[6] M. N. Farouk, S. Enzhe, M. A.Xiuzhen, " D6114 Diesel Engine Speed Control: A case Between PID Controller and Fuzzy Logic Controller," *Proceedings of 2014 IEEE International Conference on Mechatronics and Automation,* August 3 - 6, Tianjin, China.

[7] Q. Sun, J. Chen, "Speed governor design based on fuzzy self-tuning PID method for marine diesel engine," *5th International Conference on Advanced Design and Manufacturing Engineering (ICADME 2015).*

[8] T. I. Fossen, Guidance and control of ocean vehicles. John wiley and sons., 1994, ISBN 0 471 94113 pp.445.

[9] B. Purwahyudi and H. A. Saidah, "fuzzy logic controller for volts/hz induction motor control used in electrically driven marine propeller," ISSN-L: 2223-9553, ISSN: 2223-9944 Vol. 4 No. 5 September 2013.

[10] Y. Yang and C. Zhou, "Adaptive Fuzzy control of ship autopilot with uncertain nonlinear systems," *Proceedings of IEEE Conference on Cybernetics and Intelligent Systems,* Singapore, 2004.

[11] S. Dick, "Toward complex fuzzy logic, Fuzzy systems," EEE Transactions on Fuzzy Systems, vol. 13, no. 3, pp. 405 – 414, 2005.

[12] M. Jamshaid, A. Titli, L. A. Zadeh, and S. Boverie, "Application of Fuzzy logic," *Environmental and Intelligent Manufacturing series,* 1997.

[13] M. Santos, R. Lopez, and Cruz de la J.M., "A neuro-fuzzy approach to fast ferry vertical motion modelling," *Artificial Intelligence,* 2006, vol.19, pp. 313-321.

Estimating News Coverage Patterns using Latent Dirichlet Allocation (LDA)

Batool Zehra[1], Naeem Ahmed Mahoto[1], Vijdan Khalique[1]

Abstract:

The growing rate of unstructured textual data has made an open challenge for the knowledge discovery which aims extracting desired information from large collection of data. This study presents a system to derive news coverage patterns with the help of probabilistic model – Latent Dirichlet Allocation. Pattern is an arrangement of words within collected data that more likely appear together in certain context. The news coverage patterns have been computed as number function of news articles comprising of such patterns. A prototype, as a proof, has been developed to estimate the news coverage patterns for a newspaper – The Dawn. Analyzing the news coverage patterns from different aspects has been carried out using multidimensional data model. Further, the extracted news coverage patterns are illustrated by visual graphs to yield in-depth understanding of the topics which have been covered in the news. The results also assist in identification of schema related to newspaper and journalists' articles.

Keywords: *News Coverage Pattern; Probabilistic Model; data visualization; Multi-dimensional Data Model.*

1. Introduction

The rapid growth of the Web technologies has resulted in number of websites. According to statistics, there are 1800,047,111 active websites recorded in 2017 [1]. That means, tremendous volume of data is produced on these websites, which paves the way for information processing in order to extract knowledge and meaningful patterns. It can assist in decision-making regarding a number of scenarios and problems.

Out of total number of active websites, there are many e-news websites with a large share of visitors who regularly check news and read articles on these websites. For example, in US, around 70% of the population refer to the Internet for keeping up-to-date with news [2]. In addition, a large number of news articles are published on the daily basis covering various current topics. There exists a huge platform that can be explored with modern computing and data processing tools to find out interesting and useful knowledge.

In this research study, useful knowledge is extracted from the e-newspaper articles to obtain the news coverage patterns. News coverage pattern refers to finding issues or topics being discussed over a certain period of time. The aim is to find out the coverage given to a specific topic or issue in news. The coverage patterns would reveal that what topics or issues remained under discussed and trending subject in a newspaper. The news

coverage patterns have been obtained by means of Latent Dirichlet Allocation (LDA), which is a probabilistic model for collection of discrete data [3]. LDA is a modeling technique, which automatically develops topics based on patterns of co-occurrence of words. LDA finds out a set of ideas or themes that well describe the entire corpus. The scope of this research is focused on the daily news and newspaper articles published on the website of a popular newspaper-The Dawn. During the course of this research, an application prototype as the proof of concept has been developed that performs the task of estimating the news coverage patterns. Text mining and analysis is performed to check coverage of certain news. Precisely, the goal of this research is to identify and highlight the topics or issues under discussion in numerous articles of the Dawn newspaper. Furthermore, the trending topics are statistically represented as knowledge to end-users. The information visualization has been considered an emerging field for the several application domains; for instance, structural information by injecting parameters of location has been represented in visual formats [7]. The paper is organized as follows: Related studies are discussed in section 2; the working principle of extracting news coverage patterns is reported in section 3; the outcomes of the study are described in the discussion section 4; finally, section 5 presents conclusions.

2. Literature

Maintaining the integrity of the specifications reference [4] described way to utilize LDA to journalism. The study [5] evaluated two novel approaches, one by using a video stream and second by using the closed caption data. An LDA approach has been used to detect the text stream and the person shots. The research concluded that the individual system gave comparable results, however; a combination of the two systems provided a significant improvement as compared to the individual system.

Reference [6] treated groups of objects together as spatial visual words and investigated configurations of regions using LDA and invariant descriptors. In this research, computation of invariant spatial signatures for pairs of objects was based on a measure of their interaction inside the scene. A simple classification was used to define spatial visual words to extract new patterns of similar object configurations. The modeling of the scene into a finite mixture was in accordance with the spatial visual words by the use of latent dirichlet model. Statistical analysis was done to better understand the spatial distributions inside the discovered semantic classes. One case study for synthetic imagery and for real imagery was experimented using LDA and the results proved that this model has good performances with the small amount of training data. It has been concluded that scene level analysis can be done through LDA with minimal human interaction leaving behind the traditional approaches of pixel or region level analysis [6]. The reference [8] unearthed significant components, for instance, nouns and verbs given broadcast transcript. It further computed weights of components with the help of their frequency in the text.

The study under consideration applies LDA in order to get news patterns for better understanding of trends of news topics/issues.

3. News Coverage Patterns Extraction Workflow

The workflow of identifying news coverage patterns is explained in this section that comprises of four steps. The steps are explained in the order of their execution as illustrated in Fig. 1. The workflow intends to find out the coverage of various issues/topics in multiple news articles and news. Following are the steps and their explanations.

3.1. Web Crawler

The primary source of data is online news websites. In order to fetch data from these websites, a crawler has been designed and

developed. However, crawler targeted only one website – The Dawn (*www.dawn.com*). The crawler gathered daily news and news articles, which needed preprocessing before determining news coverage patterns. These collected news and news articles are stored in documents referred to as document database or corpus.

3.2. Data collection and preprocessing

Preprocessing stage involves the rectification of data such that the subsequent processes can be done. The refinement of data leads to better results, since unnecessary data gets removed and useful data elements are left behind. The data refinement procedure during preprocessing performs activities: *Tokenization, Stop word removal, Stemming and Vector Space Model.*

3.2.1. Tokenization

Tokenization is the process to partition the sentences contained in the textual data into its tokens (i.e., words). For example, consider a sentence 'This study aims at extracting news coverage patterns'; the tokenization results into tokens: {'This', 'study', 'aims', 'at', 'extracting', 'news', 'coverage', 'patterns'}.

3.2.2. Stop word removal

News and articles are read one-by-one by the system. The system removes stop words from the given document. Stop words are commonly used words in language such as *is, at, a, on, of etc*. Their presence can mislead the text search and text analysis. Therefore, stop words are removed from text during preprocessing stage.

3.2.3. Stemming

In the next stage of preprocessing, stemming takes place. Stemming is the procedure of determining the base word or root word of a given word. For example, *extract* is the root word of *extracting*. During stemming, each word is traced to its basic root word. This is an important process as it can help remove noise from data.

3.2.4. Vector Space Model

Vector space model represents text documents as vectors. Vector(s) corresponds to the dimension of the vector space. The text data of news and news articles has been represented in the form of bag-of-words.
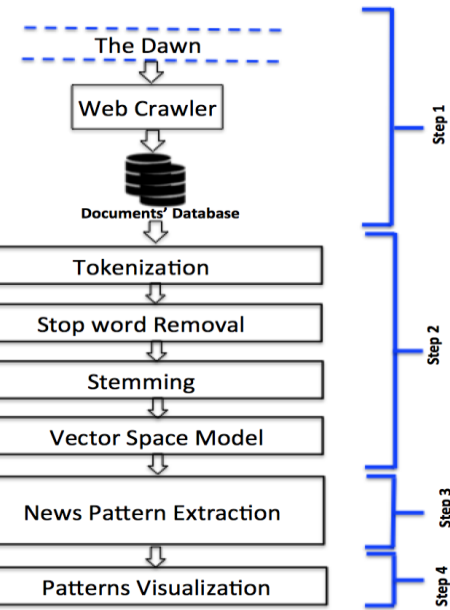
Fig. 1. Workflow of news pattern extraction and visualization.

3.3. News Pattern Extraction

News pattern extraction refers identifying patterns about coverage of certain topics in news and articles. LDA finds out what topics are discussed in a given article by observing processed news data (i.e., vector space model – bag-of-words) and produces a topic distribution. A prototype application developed in this study has implemented LDA for the news coverage pattern extraction.

Latent Dirichlet Allocation (LDA) – LDA algorithm reported in [3] presents the mathematical model. The principle concept of LDA describes that documents' database (or corpus) contains words referring to latent topics and thus relate to the overall theme of the documents.

Consider a set of **M** documents' database (**DD**) or corpus such that $DD = \{d_1, d_2, ..., d_m\}$ $\sum n = \{p_1, ..., p_k\}$, where d_i represents set of documents in the corpus **DD** and each document **d** is a vector of **N** comprises of words w_i such that $d = \{w_1, w_2, ..., w_n\}$.

LDA accomplishes steps as reported below for each **w** in corpus **DD**.

    i.   Select N from Poisson Probability (ξ)

    ii.   Select q from Dir(a), where a shows per-document topic distribution

    iii.   For each of the **N** words w_n:

        a.   Select a topic $z_n \sim$ Multinomial(θ)

        b.   Select a word w_n from $p(w_n \mid z_n, b)$, a multinomial probability conditioned on topic z_n; $b_{ij} = p(w^j = 1 \mid z^i = 1)$ probability of w_n towards the topic z_n

Having parameters a, b, the joint distribution of a topic mixture q, a set of N topics **z**, and a set of N words **w** is given by:

$$p(q, z, w \mid a, b) = p(q \mid a) \bigcirc_{n=1}^{N} p(z_n \mid q) p(w_n \mid z_n, b)$$

3.4. News Pattern Extraction

Visualization is the final output of this study. The extracted news patterns are presented statistically using graphs, line charts and bar charts. The statistical representation gives a comprehensive view of how certain topics are discussed in news and articles in a newspaper.

4. Discussion

LDA helps to find the main theme of an article and discover the coverage of specific news theme. The discovered theme is then chronologically ordered and presented in this section as bar graphs and line charts in order to show the trend of various patterns of news issues and topics.

Figure 2 and 3 show the trends of topics mentioned in newspaper. These topics are frequently discussed and have been in news for the given period of time. The frequencies are plotted on y-axis while x-axis possesses timings. Each topic has its own line with different colors to indicate the change in trends. For instance, the topic named *NAB* in Fig. 2 remained top in news during 15 days. Similarly, trends about *corruption* and *politicians* have been the most frequent topics during the given dates. It can also be observed that these topics have almost similar trend with slight variations. This trend leads to understanding the media coverage in newspapers. In other words, media targets news about *NAB*, *corruption* and *politicians*. The similar trends are depicted in Fig. 3.

In Fig. 4, the topics (i.e. army, military, Pakistan) discussed in news articles by different columnist of The Dawn newspaper are depicted. The topics being covered by these writers show a trend of certain issues. These trends represent that who among the considered writers focuses which of the issues and topics in their writings.
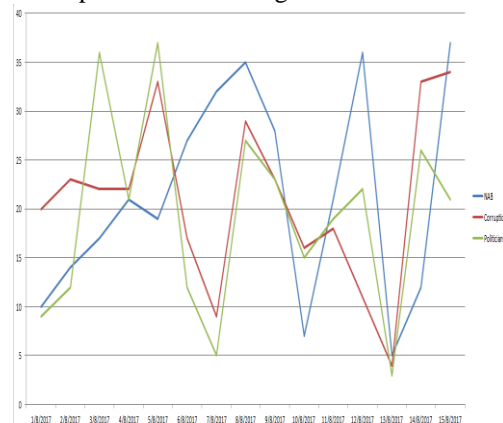
**Fig. 2.** News coverage trend of 3 topics - 15 days.
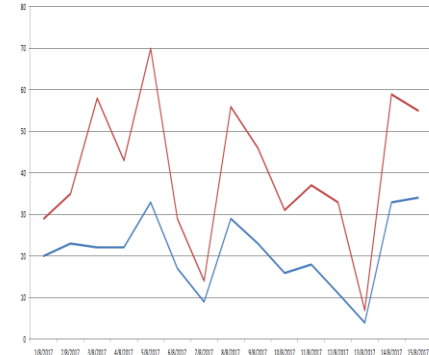
Fig. 3. Number of news regarding certain topics.

For example, referring to Fig. 4, Cyril Almeida mostly talked about Pakistan, military and army in his news articles. These news coverage patterns and topics covered by the writers in their writings clearly yield the direction and mindset of the media personnel, since media has been considered as opinion maker for the societies.

Fig. 5 provides information regarding available collected news and news articles in the database. The prototype application offers to search for the topics or terms in the specified range of time within news or in news articles of columnists.
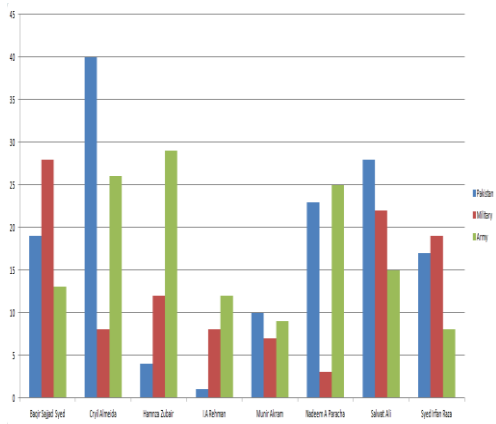

Fig. 4. Frequency of topics covered in articles written by news analysts.

For instance, Fig. 6 represents that term *PPP (Pakistan People's Party)* has been trending more in the news on 5th March 2017 as compared with rest of the days of March

2017 in the available database of the prototype application. The news coverage patterns and their trend helps in understanding the behavior and mindset of media personnel, who play an essential role in building opinions of the people. The patterns not only will serve government officials to have in-depth information about directions of media and its agenda. Likewise, the writings of certain columnists will help in understanding the targets and their priorities in building the nation.
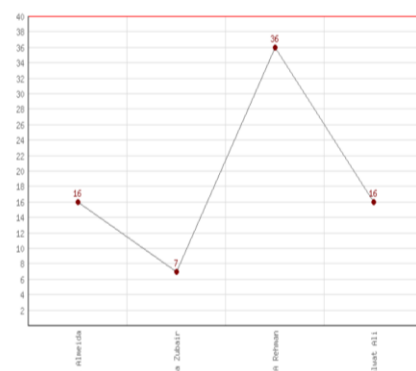

**Fig. 5.** The news and news articles in the corpus.
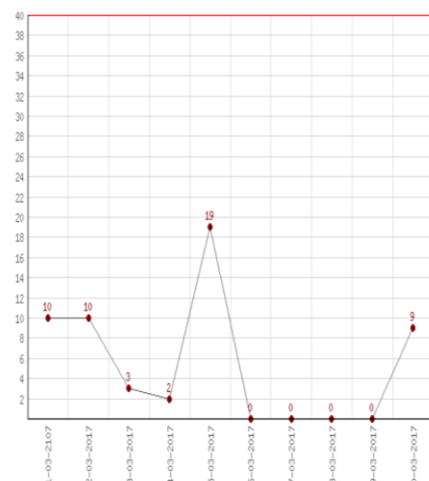
Fig. 6. Term PPP (Pakistan People Party) coverage trend.

5. Conclusion

This paper presents an approach to apply Probabilistic Topic Model (i.e., LDA) in finding significant patterns from newspapers. The data, crawled from The Dawn newspaper's official website, has been processed to uncover the news coverage in certain time limits. To validate the potential of understanding news coverage patterns, a prototype application has been built, which performed the necessary steps to reveal the patterns. These patterns have been presented with the help of visualization methods.

It has become a fact that media influences perception of general public and mold their sentiments and thinking about certain issues and events. This research would assist in identifying the narrative of media groups regarding certain issues and events. The point of view of article writers can be stipulated by applying the analytical approach presented in this study. Consequently, the inclination of a newspaper can be judged based on the coverage they are giving to various issues. The in-depth knowledge about media groups and their news coverage patterns may assist government authorities like PEMRA (Pakistan Electronic Media Regulatory Authority) to regulate the electronic print media.

As future works, we plan to compare the applied approach with the state-of-the-art methods and included other newspapers as well as research articles to determine the topical coverage of the scientific research articles.

REFERENCES

[1] D. S. Fowler, "Tek Eye How Many Websites Are There In The World?," Online: tekeye.uk/computing/how-many-websites-are-there (Accessed 30-1-2018).

[2] Fuller, Steve, "Topic: News Industry", Online: www.statista.com/topics/1640/news/ (Accessed 20-1-2018).

[3] D. M. Blei, Y. Ng. Andrew, and Michael I. Jordan, "Latent dirichlet allocation," *Journal of machine Learning research,* pp. 993-1022, Jan 2003.

[4] C. Jacobi, W. V. Atteveldt, and K. Welbers, "Quantitative analysis of large amounts of journalistic texts using topic modelling", *Digital Journalism,* vol. 4, no. 1, pp. 89-106, 2016.

[5] H. Misra, F. Hopfgartner, A. Goual, P. Punitha, and J. M. Jose, "News Story Segementation Based on Semantic Coherence and Content Similiarity", *In MMM,* pp.347-357, January 2010.

[6] C. Vaduva, I. Gavat, and M. Datcu, "Latent Dirichlet Allocation for spatial analysis of satellite images," *IEEE Transactions on Geoscience and Remote sensing,* vol. 5, no. 15, pp. 2770-2786, 2013.

[7] S. Shah, V. Khalique, S. Saddar, and N. A. Mahoto, "A Framework for Visual Representation of Crime Information," *In Indian Journal of Science and Technology,* vol. 10, no. 40, pp. 1-8. ISSN: 0974-6846, 2017.

[8] M. J. Pickering, L. Wong, and S. R̈uger, "ANSES: Summarisation of news video," Image and Video Retrieval, LNCS 2728, pp.425-434, 2013.

Power Quality Analysis of Controlled Rectifiers and their Impact on Input Power System

Abdul Ghaffar[1],Engr. Jahangir Badar Soomro[1],Altaf Hussain[1], Dr. Faheem A. Chachar[1]

Abstract:

This paper introduces the power quality analysis of AC-DC converter topologies and discusses their impact on input power system. Due to latest advancement in the technologies and power semiconductor devices, it is impossible to put barriers for the applications of power electronics topologies. These topologies are of different structure and causes harmonics when connected to the power system, these harmonics affects not only the power quality of the system network but also increase conductor overheating and core losses in motor applications. Due to their wide usage of rectifiers, it is necessary to observe its impact on the input power system, which includes THD (total harmonic distortion) and distortion in the input power factor etc. This research work focuses on the power quality analysis of the input power system due to AC-DC converters. In this paper input THD of single-pulse, two-pulse and six-pulse controlled rectifiers are examined using FFT analysis in MATLAB its effect on input power system are also observed.

1.Introduction

The AC-DC converter is by far the largest group of power switching circuits applied in industrial applications [1-3]. Usually rectifiers are developed using diodes and thyristors to provide uncontrolled and controlled DC power at the output with unidirectional and bidirectional power flow [4]. The drawback that comes with these rectifiers is that they cause non-linearity in the system which causes the harmonics to be injected in the system. These harmonics cause current distortion as well as poor power factor at the input side.

The difference between a linear and non-linear load is that a linear load is a load which draws current from the supply which is proportional to the applied voltage, whereas a load is considered non-linear load when its impedance changes with the applied voltage, due to that change in impedance current drawn by the load is non-linear and that non-linear current carries harmonics with it. The power electronics converters also lie in the family of non-linear load.

"IEEE 519-1992 defines harmonics as a sinusoidal component of a periodic wave or quantity (e.g. voltage or current) having a frequency that is an integral multiple of the fundamental frequency" [5].

Harmonics causes many unwanted effects in the system network. The most saviour effect

---

[1] Dept. of Electrical Engineering, Sukkur IBA University, Sukkur, Pakistan
Corresponding Email: aghaffar.es14@iba-suk.edu.pk

is the heating of equipment caused by iron losses and copper losses. A simple three phase nonlinear load is six-pulse rectifier and this type of load produces a significant amount of harmonics in the system network. Harmonics are not only generated by the non-linear loads but also the linear loads like rotating machines or transformers but their magnitude is quite low.

Increasing the number of pulses of rectifiers like six-pulse, twelve-pulse decreases the effect of harmonics by the formula
$$h = np \pm 1$$

where n is the number integer.

p is the number of pulses.
h is the harmonics order.

This paper comprises the comparative analysis of the harmonics effect of rectifier topologies (i.e. single-pulse, two-pulse, six-pulse and twelve-pulse) and their effect on input supply as well as on input power factor at different power factor using different loads.

2. Methodology

For performing the experimental study and analysis of Harmonics Generation Rectifiers the approach would be as designing of different topologies of rectifiers. For each configuration, the simulation would be done through MATLAB/Simulink. The simulated waveforms of current and voltage in case of different loads would be obtained by taking different firing angles and then correlate the effectiveness of different model and its configurations. Due to switching operations of AC-DC converters non-linearity is produced in the input current due to which harmonics are generated [6] which not only disturb the performance of converters but also quality of input power system is badly affected. The power quality factor would be observed by the Fluke Power Quality Analyzer that can monetize the cost of energy waste due to poor quality.

The implementation of different rectifiers circuits i.e. single pulse, two pulse, six pulse

and twelve pulse would be done on simulation on MATLAB/Simulink using different techniques over different loads.

3. Single Phase Half Wave Rectifier

Power Converters are used whenever there is mismatch between power supply available and load requirement. The Thyristor can be triggered at any angle α in positive half cycle as well as in negative half cycle so that the output voltage can be controlled. The thyristor acts as an open during the negative half cycle [7].

3.1. Single Phase Half Wave Controlled Rectifier with R Load

Fig. 1. shows half wave controlled rectifier with resistive load. This topology is also known as 1-pulse rectifier.
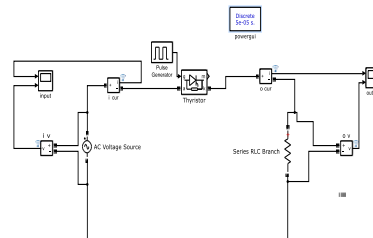

Fig. 1. Half Wave Controlled Rectifier with R load.
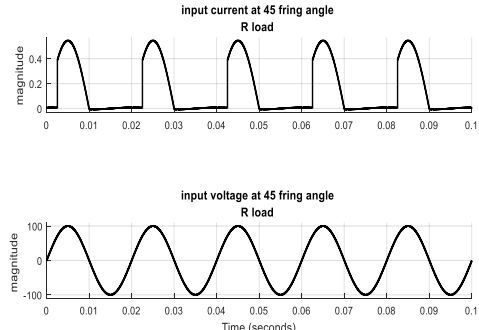
**Fig. 2.** Input Current and Voltage with R load at firing angle of 45°.

Input voltage and current waveform at firing angle of 45° is shown in Fig. 2. Input current is no more a pure sinusoidal and Fig. 3 shows input current harmonics at firing angle of 45°.
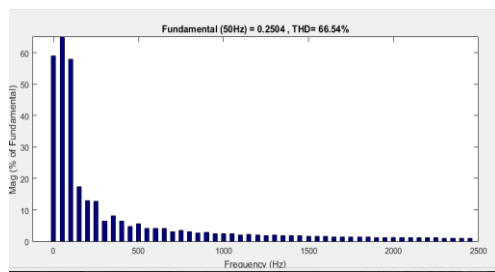
Fig. 3. Input Current THD with R load at firing angle of 45º.

Output current and voltage with resistive load is shown in Fig. 4. It can be seen from waveform that output is not pure DC and it contains AC components along with DC components.
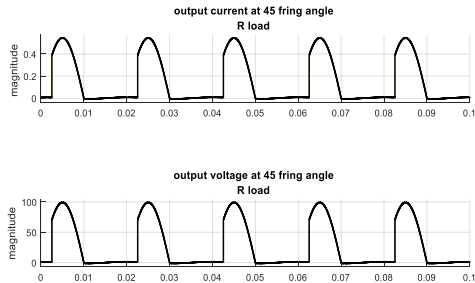

Fig. 4. Output Current and Voltage with R load at firing angle of 45º.

TABLE I. input, output, voltage thd, current thd and power factor with r load at different firing angles.

Firing Angle	Input Current THD %	Output Current THD %	Output Voltage THD %	Input Power factor
30º	55.38	55.38	55.38	0.69
45º	66.54	66.54	66.54	0.67
60º	80.36	80.36	80.36	0.63
90º	115.24	115.24	115.24	0.50

It can be seen from table that harmonics generated are increased by increasing firing angle and current and voltage harmonics are same due to resistive load. Also, Input power factor decreases by increasing firing angle as shown in Fig. 5.
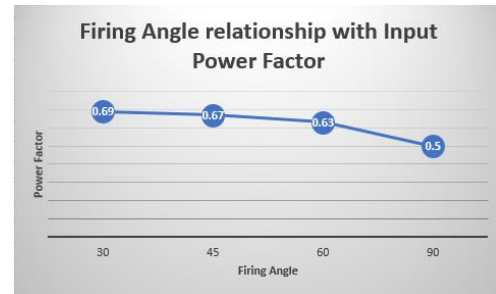
Fig. 5. Relationship of Firing angle and Input Power Factor.

3.2. Single Phase Half Wave Controlled Rectifier with RL Load

Input current and voltage with resistive-inductive load is shown in Fig.6.
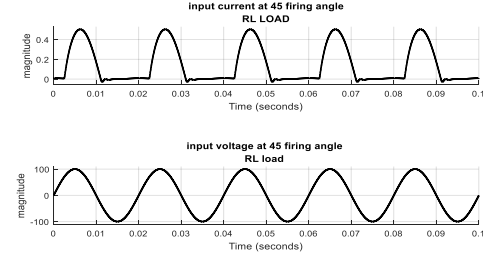
Fig. 6. Input Current and Voltage with RL load.

It can be seen that keeping all parameters same, current harmonics in resistive-inductive load is reduced than resistive load as shown in Fig. 7. Inductor works as a filter for current harmonics and therefore current waveform becomes smoother.
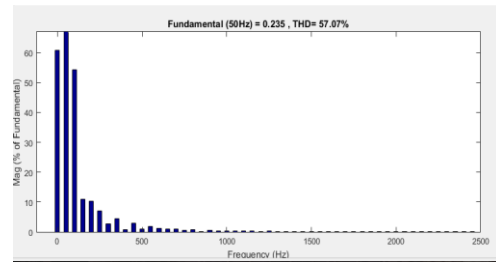
Fig. 7. Input Current THD with RL load at firing angle of 45º.

Output current and voltage with resistive-inductive load is shown in Fig. 8. Voltage and current waveform are different due to resistive-inductive load.
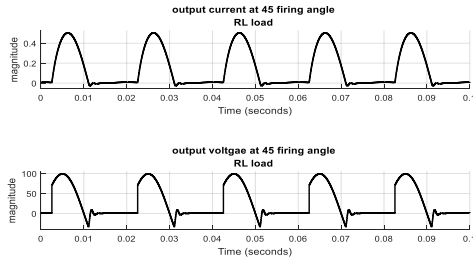
Fig. 8. Output Current and Voltage with RL load.

TABLE II. Input, Output, Voltage THD, Current THD and Power Factor with R Load at different Firing Angles.

Firing Angle	Input Current THD %	Output Current THD %	Output Voltage THD %	Input Power factor
30º	48.9	48.9	60.97	0.65
45º	57.07	57.07	72.39	0.62
60º	67.56	67.56	87.43	0.57
90º	93.73	93.73	127.5	0.42

In the above table it can be seen that the THD at the input side is increasing with the increase in the firing angle, also due to resistive-inductive nature of the load, the current ripples are filtered as an inductor opposes the change in current and due to this the current harmonics at the output is less than the voltage harmonics. It is observed that input power factor decreases with increase in firing angle as shown in Fig. 9.

**Fig. 9.** Relationship of Firing angle and Input Power Factor.

4. Single Phase Full Wave Controlled Rectifier

A full-wave controlled rectifier converts both the positive as well as negative half cycle of input waveform and converts both polarities of the input waveform to pulsating DC. The desired value at the output can be achieved by varying the firing angle α of the thyristor [8].

4.1 Single Phase Full Wave Controlled Rectifier with R Load

Fig. 10. shows the single phase full wave controlled rectifier with resistive load. This topology is also known as 2-pulse rectifier.
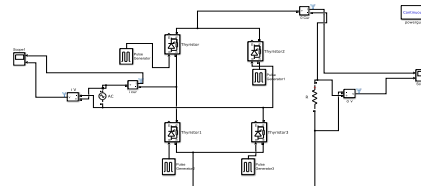
Fig. 10. Full Wave Controlled Rectifier with R load.
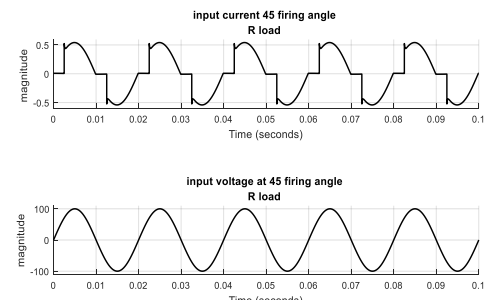
Fig. 11. Input Current and Voltage with R load.

Input voltage and current waveform at firing angle of 45º is shown in Fig. 11. Input current is distorted sinusoidal and Fig. 12 shows input current harmonics at firing angle of 45º.
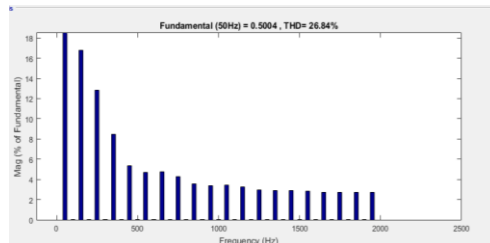
Fig. 12. Input Current THD with R load at firing angle of 45º.

Output current and voltage with resistive load is shown in Fig. 13. It can be seen from waveform that output is still not a pure dc and it contains ac components along with dc components but it has less ripple factor as compared to single phase half wave controlled rectifier.
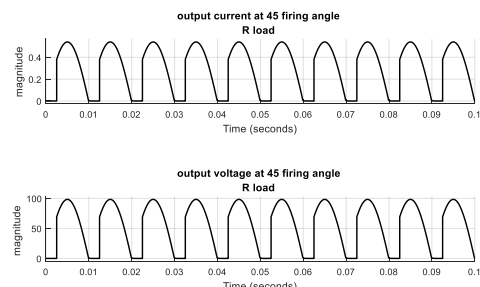
Fig. 13. Output Current and Voltage with R load.

It can be seen form table that harmonics generated are increased by increasing firing angle and current and voltage harmonics are same due to resistive load. Also Input power factor decreases by increasing firing angle as shown in Fig. 14.

TABLE III. Input, Output, Voltage THD, Current THD and Power Factor with R Load at different Firing Angles.

Firing Angle	Input Current THD %	Output Current THD %	Output Voltage THD %	Input Power factor
30º	16.32	30.57	30.57	0.98
45º	26.8	33.47	33.47	0.95
60º	40.4	37.1	37.1	0.89
90º	70.39	57.5	57.5	0.70

**Fig. 14.** Relationship of Firing angle and Input Power Factor.

4.2 Single Phase Full Wave Controlled Rectifier with RL Load

Input current and voltage with resistive-inductive load is shown in Fig. 15.
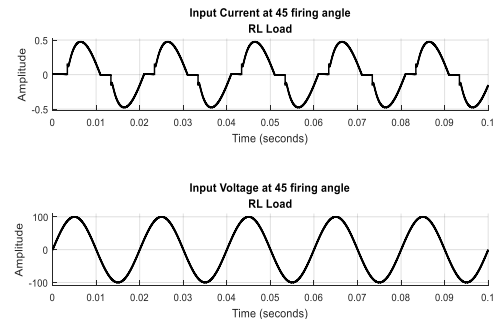
Fig. 15. Input Current and Voltage with RL load.

It can be seen that keeping all parameters same, current harmonics in resistive-inductive load is reduced than resistive load as shown in Fig. 16.
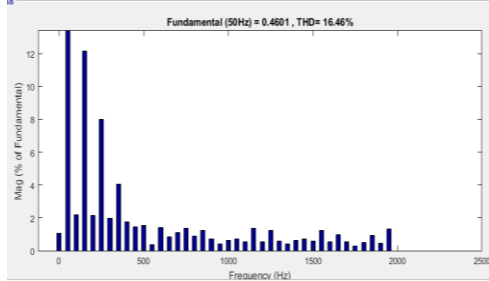
Fig. 16. Input Current THD with RL load at firing angle of 45º.

Output current and voltage with resistive-inductive load is shown in Fig. 17. Voltage and current waveform are different due to resistive-inductive load.
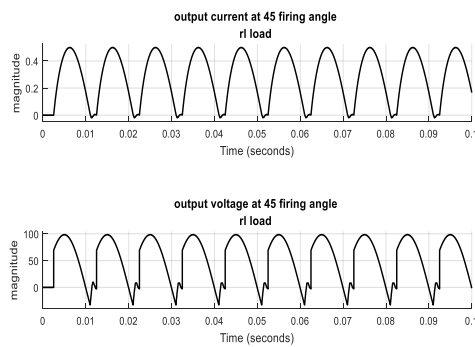
Fig. 17. Output Current and Voltage with RL load.

Table IV. Input, Output, Voltage THD, Current THD and Power Factor with RL Load at different Firing Angles.

Firing Angle	Input Current THD %	Output Current THD %	Output Voltage THD %	Input Power factor
30º	9.49	26.85	31.16	0.93
45º	16.4	21.51	33.47	0.89
60º	25.25	19.67	37.14	0.82
90º	49.39	37.22	56.65	0.62

It is observed that input power factor decreases with increase in firing angle as shown in Fig. 18. Harmonics increases due to increase in firing angle, thereby input power factor decreases.
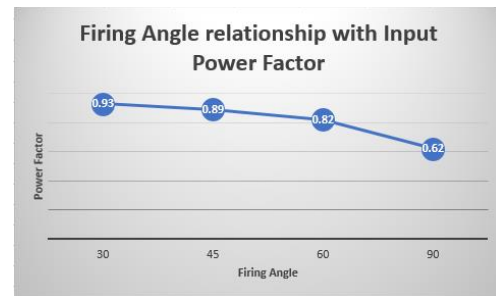
Fig. 18. Relationship of Firing angle and Input Power Factor.

5. Three Phase Full Wave Controlled Rectifier

In industrial applications where three phase AC voltages are available it Is preferred to use three phase rectifiers, as it gives us multiple benefits like high power handling, low ripple factor which reduces the filter size as well as low distortion at the input [9].

Application of higher pulse rectifiers are found at various points like for pipeline pumps in petrochemical industry, for steel rolling mills in metal industry, for pumps in water pumping stations, for fans in cement industry, for traction in locomotive industry etc [10].

5.1 Three Phase Full Wave Controlled Rectifier with R Load

Fig. 19. shows three phase full wave controlled rectifier with resistive load. This topology is also known as 6-pulse rectifier.
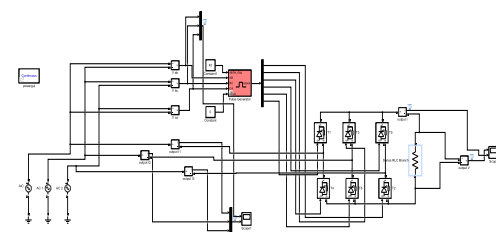
Fig. 19. Full Wave Controlled Rectifier with R load.
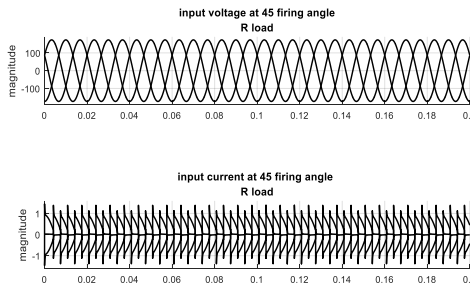
Fig. 20. Input Current and Voltage with R load.

Input voltage and current waveform at firing angle of 45º is shown in Fig. 20. Input current is no more a pure sinusoidal and Fig. 21. shows input current harmonics at firing angle of 45º.
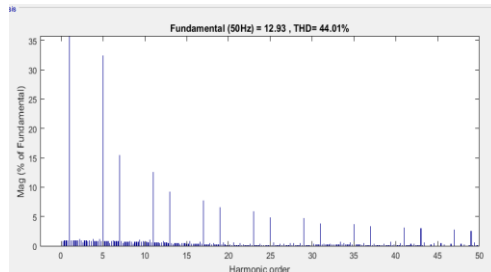
Fig. 21. Input Current THD with R load at firing angle of 45.

Output current and voltage with resistive load is shown in Fig. 22. Six pulse rectifier has less ripple factor and thus requires smaller filter size.
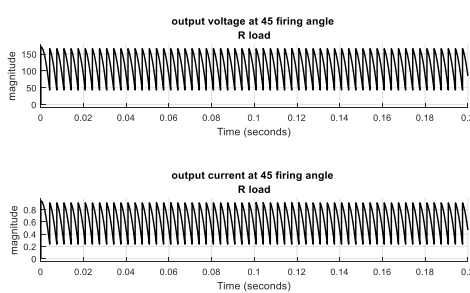
Fig. 22. Output Current and Voltage with R load.

TABLE V. Input, Output, Voltage THD, Current THD and Power Factor with R Load at different Firing Angles.

Firing Angle	Input Current THD %	Output Current THD %	Output Voltage THD %	Input Power factor
30º	35.55	75.62	75.62	0.51
45º	44.01	77	77	0.32
60º	62.09	78	78	0.13

It can be seen from the results that power quality of three phase rectifiers is better than single phase, also Input power factor decreases by increasing firing angle as shown in Fig. 23.
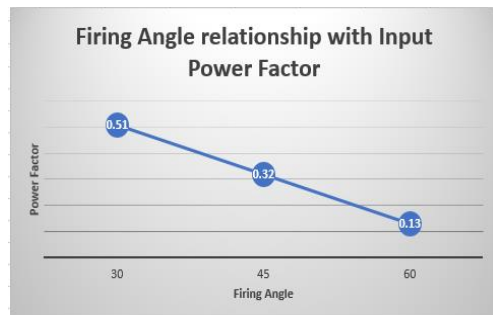
Fig. 23. Relationship of Firing angle and Input Power Factor.

5.2 Three Phase Full Wave Controlled Rectifier with RL Load

Input current and voltage with resistive-inductive load is shown in Fig. 24.
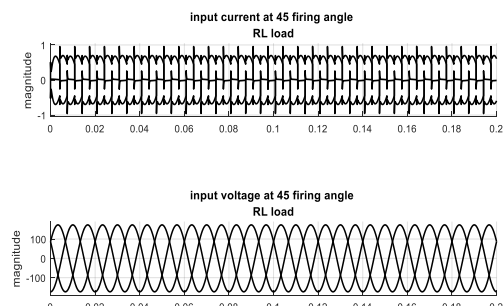
Fig. 24. Input Current and Voltage with RL load.

It can be seen that keeping all parameters same, current harmonics in resistive-inductive load is reduced than resistive load as shown in Fig. 25.
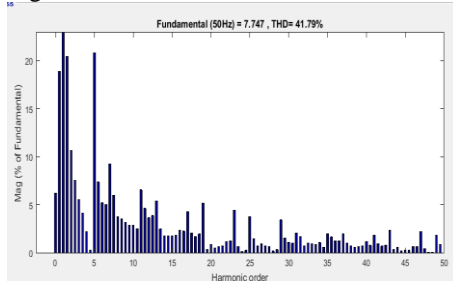

Fig. 25. Input Current and Voltage with RL load.

Output current and voltage with resistive-inductive load is shown in Fig. 26. Voltage and current waveform are different due to resistive-inductive load.
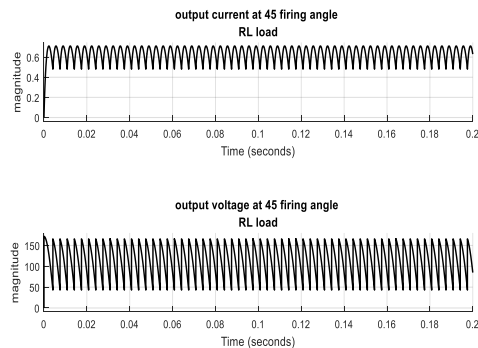

Fig. 26. Output Current and Voltage with RL load.

TABLE VI. Input, Output, Voltage THD, Current THD and Power Factor with RL Load at different Firing Angles.

Firing Angle	Input Current THD %	Output Current THD %	Output Voltage THD %	Input Power factor
30º	38.65	56.40	75.64	0.47
45º	41.79	58	77.35	0.24

The results of six pulse rectifier for resistive-inductive load are shown in above table. The relationship of input power factor with firing angle is also demonstrate in Fig. 27.
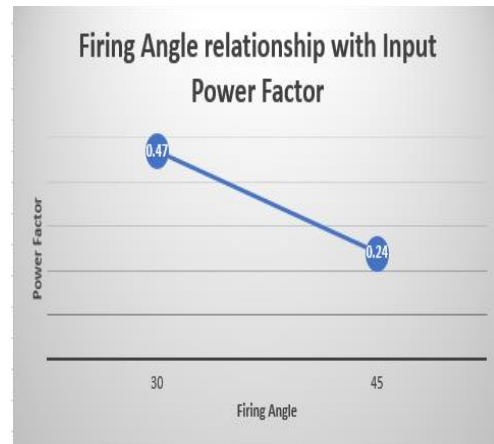
Fig. 27. Relationship of Firing angle and Input Power Factor.

6. Conclusion

From the comparison of above results and relationship of higher pulses with THD it can be concluded that as we move towards the higher pulses, the THD at the input is decreased or simply the input supply distortion decreases with the increase in the number of pulses. Another advantage is that filter size will reduce and filter losses will be minimized as we move towards higher pulses rectifiers. Thus, ripple factor at the output of the higher pulse rectifiers (i.e. 12-pulse, 18-pulse and 24-pulse) will be very less. The power factor is also less disturbed which also saves our economy as the disturbed power factor would increase the copper losses in the system as well as it would increase the stress on the switching devices, insulators and heating effect. In HVDC Transmission System higher pulses rectifiers are preferred because of their huge advantages like economy, minimum losses and reliability.

REFERENCES

[1] B. K. Bose, "Recent Advances in Power Electronics," *IEEE Transactions on Power Electronics,* vol. 7, no. 1, pp. 2 – 16, 1992.

[2] T. Tanaka, S. Fujikawa, and S. Funabiki, "A New Method of Damping Harmonic Resonance at the DC Link in Large-Capacity RectifierInverter Systems Using a Novel Regenerating Scheme", *IEEE Transaction on Industry Applications,* vol. 38, no. 4, Page(s):1131 – 1138, July/August 2002.

[3] O. Garcia, M. D. Martinez-Avial, J.A. Cobos, J. Uceda, J. Gonzalez, and J. A. Navas, "Harmonic Reducer Converter," *IEEE Transactions on Industrial Electronics,* vol 50, no. 2, pp. 322 – 327, April 2003.

[4] Baharom, R., Hashim, N. and Hamzah, M.K., 2009, November. Implementation of controlled rectifier with power factor correction using single-phase matrix converter. *In Power Electronics and Drive Systems, 2009. PEDS 2009. International Conference on* (pp. 1020-1025), IEEE.

[5] F II, I., 1993. IEEE recommended practices and requirements for harmonic control in electrical power systems. New York, NY, USA.

[6] Mahar, M.A., Larik, A.S., and Shah, A.A., "Impacts on power factor of ac voltage controllers under non-sinusoidal conditions," *Mehran University Research Journal of Engineering and Technology,* vol. 31, no. 2, pp.297-300, 2012.

[7] Solanki, A., "Simulation & Performance Parameters Analysis of Single-Phase Full Wave Controlled Converter using PSIM," *International Journal of Engineering Research and General Science,* vol. 2, no. 3, pp.410-414, 2014.

[8] Mahobia, S.K. and Kumrey, G.R., "Study and Performance of Single-Phase Rectifiers with Various Type of Parameter," *International Journal in Engineering Technologies and Management Research,* vol. 3, no. 1, pp. 9-14, 2016.

[9] Mohan, N. and Mohan, T.M., 1995. Power electronics (Vol. 3). *New York: John wiley & sons.*

[10] Pyakuryal, S. K., "Control of harmonics in 6-pulse rectifiers *(Doctoral dissertation, University of Denver),"* 2013.

Design and Control of an Unmanned Ground Vehicle for Search and Rescue Missions

Kamran Shahani[1], Hong Song[1], Chaopeng Wu[1], Syed Raza Mehdi[1], Kazim Raza[1], Noorudin Khaskheli[2]

Abstract:

This paper focuses on the design and control of the unmanned ground vehicle for search and rescue missions. It is operated manually by using Xbee remote controller and arduino Uno is utilized to guide signals to UGV. This robot has innovations such as to move on rocky surfaces, a robotic arm is fixed on it which will perform pick and place tasks according to the inputs from the operator. The camera is attached for live vision feedback. The custom model designed was experimented with various situation scenarios to test its fidelity. This project is suitable for multiple purposes like monitoring and for military exploration missions.

Keywords: *Xbee module; UGV; Arduino; Wireless Control; DC motor; Manipulator.*

1. Introduction

An Unmanned Ground Vehicle (UGV) is a vehicle running in touch with the ground, transporting devices, without a human operator presence. The robot can move on the rough grounds and in order to perform various farm duties where the presence of human being inside the area/place is unsafe [1]. To evade trailing of human life, this is more suitable to use the robot for a related job. Mostly UGV's are useful for nowadays for the armed forces especially in the battlefield or war, now a day's these are also used in different industries for loading and unloading purpose, in nuclear power plants for filling and wasting purpose and in homes, these robots are used as servants [2]. The aim is to get the wireless live visual feedback of the accident cities, find the presence of enemy's positions, weapons, obstacles and much more information without any distressing they can get it control [3].The UGV can work as rescue robot in rescue organization, rescue organization will quickly and securely receive data of the accident cities, a duty that is both tough and terrible.

A review of the development of unmanned ground vehicles in Japan from the1970's to 1990's is presented in [4].The Unmanned Ground Vehicle for fumigation purpose which designed by the National Space Research and development agency, Abuja Nigeria [5]. The vehicle consists of four wheels, uses Bluetooth as communication channel and can operated around 8 meters of radius.

[1]Ocean optics and automation lab, Institute of ocean technology, Ocean College, Zhejiang University Hangzhou 310058, China;
[2] Institute of Coastal engineering, Ocean College, Zhejiang University
Corresponding Email: 21634142@zju.edu.cn

2. Proposed System

Figure 1 shows the entire proposed system block diagram where the Arduino Uno microcontroller saves the C code that commands the vehicle, the manipulator drive and the camera. The two direct current (DC) motors drive the vehicle forth, backward, left and right directions, the servo motor controls the movements of manipulator and camera. L298 driver module works as the direct current (DC) motors driver board and the Xbee module builds a wireless connection between the surface controller and the vehicle [6].
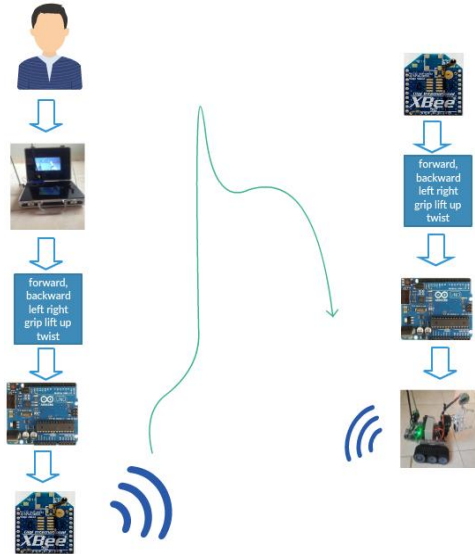
Fig. 1. Proposed System block diagram.

2.1. Versa Chassis Body

We have built essentially the frame of our vehicle from Versa (VEX) apparatus [7]. These components are made of a lightweight aluminum sheet. We use this because it saves our lot of time all parts are available we have to just assemble and build the body of a robot. Other parts are also available such as a shaft, gears, bearings gripper and many more. On aluminum sheets there are already holes and squares available; the size of these holes is about 0.8cm. For assembling the robot we do not need any welding machine for fixing of components done by using nuts and bolts.

Figure 2 shows the U, L and C shapes sheets provided by the versa robotics. Our vehicle consists of two main parts one is crawler body and the second one is the three degrees of freedom (3-DOF) manipulator arm with the gripper. Crawler which is the main frame of the vehicle holds tracked wheels, in order to move on the coarse surfaces easily without any difficulty facing.
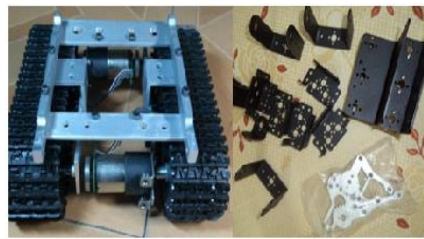
Fig. 2. Crawler robot and manipulator parts.

2.2. Dc Geared Motor

Source of moving the vehicle is motor. Our UGV consists of two dc gear motors, track wheel drive based robot. Dc geared motors are used because they have low speed but high torque [8]. Always DC geared motor is used in that type of crawlers or tanks because at hilly or inclined surfaces more torque is needed instead of speed. Crawlers motor cannot allow the direct drive to the tracked- wheels because these motor's shaft is a lock or not compatible. In this type of robot special type of wheels are used named as spikey-wheels [9]. Table 1 shows the direct current (DC) motor specification of motors.

TABLE I. DC Motor Specifications.

Specification	Explanation
Voltage Rated	12 V
Stall Current	5.5 A
No load current	0.16 A
Torque Rated	0.53 Nm
Speed Rated	327 rpm
Current Rated	1.5 A
Stall Torque	2.15 Nm

Fig. 3. 3-DOF manipulator robot arm.
Source: www.sainsmart.com/products/3-axis-desktop-robotic-arm.

2.3. Manipulator Arm

Manipulator's assembly is made of aluminum U and L shapes plates. Purpose of placing manipulator in the robot is to pick and place the objects from the surface or ground [10].

This manipulator consists of shoulder, wrist, and gripper. Shoulder joint which is revolute and rotates about 90 degrees, wrist joint which is twisted joint rotate about 180 degree and last one is gripper whose angle of opening and closing is about 160 degree. Joints of manipulator robot are driven by 3 MG 996 Servo motors. There are 3 links in this manipulator robot each link is connected with the joint. Measurements of links are given below.

Distance between link 0 to link1 = 96mm (3.7 inch) this part is called shoulder.

Distance between links 1 to link 2 = 105mm (4.1 inches) this part is called wrist. With link 2 end effector is connected whose opening distance is about 55mm (2.16 inch) Figure 3 shows the three degree of freedoms manipulator arm.

2.4. Main Controller Arduino Uno

This is the main controller of the vehicle. Consist of a microcontroller which saves the program which we write. This main board is operated at 5V dc; we can supply it by 3 methods, through USB cable connected with PC, plug the 5V DC input at its VIN pin and connect the ground must and last one which is through external 5-12 Dc adapter to a power socket of the Arduino. You can give maximum supply 12V dc, 1A current. Inside the Arduino, there is 7805 voltage regulator used which prevent the board from any damages. Figure 4 shows the input and output ports of the Arduino Uno. No need of soldering the wires user can easily plug the male connecting wires to the female header of Arduino UNO for communication.
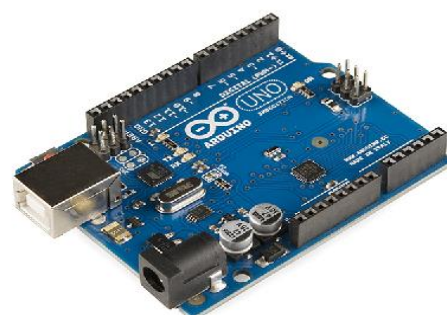
Fig. 4. Arduino Uno Main Controller.
Source https://www.arduino.cc/

2.5. Xbee Pro S1 Module

This is a very interesting wireless device used for wireless communication between two points through buildings or any place. There are many Xbee modules such as Xbee S1 and Xbee S2, we are using Xbee Pro S1 this is the advanced version of the remaining XBee modules. Figure 5 shows the front view of xbee pro S1. This device is the product of Digi Tech [11]. It has a built-in antenna which makes the better communication, increase the distance of communication. These modules allow a very reliable and simple communication between microcontrollers, computers, systems, really anything with a serial port! Point to point and multi-point networks are supported with a range of 1500 meter coverage.

The Xbee Pro S1 module in this vehicle is used to provide the wireless communication between the unmanned ground vehicle and the surface controller.

Fig. 5. Xbee Pro module.
Source. https://www.digi.com

2.6. Xbee X-CTU

X-CTU is software used to configure a connection between pc and xbee module. First we have to make the connection between pc and device. After this we select COM port where xbee is connected with the laptop port. After this we have to select correct baud rate which you set in the arduino, matching of baud rate is very important if there is no matching wireless system can't work. Figure 6 shows the interfacing window of the X-CTU.

From this software xbee input and output ports are initialized. After declaring of the ports proper selecting of sample rate is important in our case 20 is set.
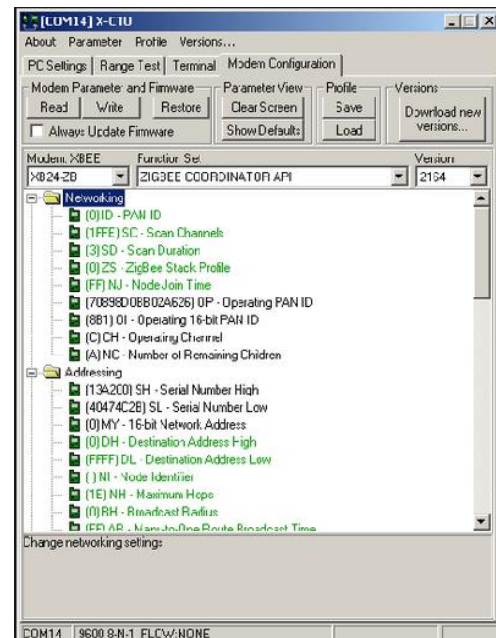
Fig. 6. Xbee X-CTU.
Source. https://www.digi.com

3. Controlling The Robot Movement

A controller is made for the controlling of UGV movements and manipulation of arm and camera, in which different switches and knobs are used. When user from the controller send the command through buttons or knobs, signal will be generated in the xbee and xbee sends the signal to the controller where signal is processing, then these signals transmitted to the UGV to perform the desired tasks. Figure 7 shows the controller of the robot. , Table 1 show the input commands which sense the robot for specific movement and table 2 shows the main specifications of the UGV.

Fig. 7. Main controller of the robot.

TABLE II. Robot Commands.

Input character	Command
F	Move forward
B	Move backward
L	Turn left
R	Turn right
K1-Gripper	Open or Close
K2- Shoulder	Lower or upper
K3- Wrist	Twist clock wise or anti clockwise

TABLE III. UGV Specifications.

Specification	Explanation
UGV size (L x W x H)	170 x 167 x 80 mm
Crawler treads (width)	50 mm
Manipulator arm	200 mm
Controlling range	1000 meter (open area)
Weight	2 kg

4. Results

The execution of the unmanned ground vehicle (UGV) for search and rescue mission hardware model experimented throughout the real-time experiment. Figure 8 shows the experimental results of the unmanned ground vehicle with no load and full load torque, current and speed. It was affirmed that the model was flawlessly towing on both glossy and irregular surfaces. The dynamic strength of the crawling vehicle while transporting the objects was kept. The vehicle can operate remotely via Xbee from up to the boundary of 1000 meters coverage. The manipulator is proficient of grasping objects up to 1000 meters radius with live video feedback. The battery can serve for 8 hours outwardly renewing. Figure 9 shows the main model of the UGV.
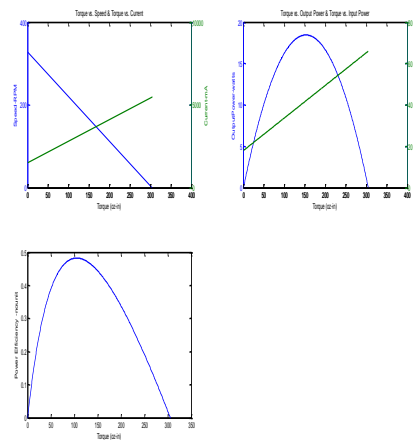
Fig. 8. UGV Load and No load results.

These figures are formulated in MATLAB version R2014b. Figure 8 shows the no load and full load speed, current, and torque of the unmanned ground vehicle on the ground. Therefore from figure we can see that slope of Torque Vs Current is 13.114754. The reciprocal is 0.076250. Maximum output mechanical power is 18.450975(watts). This happens at the

Torque load of 152.5 (oz-in), with Current 3500 (mA).
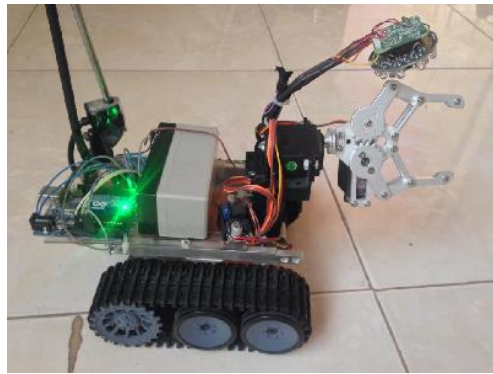
Fig. 9. Main model of the robot.

5. Conslusion

This article confers a scientific overview of the implementation of an unmanned ground vehicle with the three degree of freedom (3-DOF) manipulator arm for search and rescue missions. A model was created for an apparent induction of the method and it has been decided that by this sort of system invented, search and rescue operations can be done with less human through appearance while rescuing, through keeping the human from dangers. The design method advised in this article is cost-effectively applying a full-duplex transmission and suitable for military search and monitoring missions.

REFERENCES

[1] J. Pyo, "Future Unmanned System Design for Reliable Military Operations," International Journal of Control and Automation. Korea, vol. 5, pp. 173-186, September 2012.

[2] A. Bouhraoua, N. Merah, M. AlDajani and M. ElShafei, " Desing and Implementation of an Unmanned Geound Vehicle fo Security Applications", Proceedings of the 7th International Symposium on Mechatronics and its Applications. Saudi Arabia, vol. 4, pp. 20-22, April 2010.

[3] D. Voth, "A New Generation of Military Robots", IEEE Intelligent Systems. USA, vol. 19, pp. 2-3, Jul-Aug 2004.

[4] S. Tsugaw, "Vision-based Vehicles in Japan: machine vision system and driving control systems", IEEE Transactions on Industrial Electronics. Vol. 41, pp. 398-405, 1994.

[5] A. Bugaje, A. Loko, A. Ismail, A. Samuel, "The Unmanned Ground Vehicle for fumigation purpose". International Journal of Engineering Trends and Technology. Nigeria, vol 30, December 2015.

[6] S. Singh and P. Ranjan, "Towards a new low cost, simple implementation using embedded system wireless networking for UAVs", Proceedings of the IEEE 5th International Conference on Advanced Networks and Telecommunication Systems. India, pp. 18-21, December 2011.

[7] T.Gillespie, "Fundamentals of Vehicle Dynamics" SAE Interational, 1992.

[8] Y.Ali, S. Noor, and S. Bashi, "Microncontroller Performance for Dc Motor Speed Control System", Proceedings of Power Engineering Conference.Malaysia, December 2003.

[9] A. Mohebbi, S. Safaee, M. Keshmiri and S. Mohebbi, "Design, Simulation and Manufacturing of a Tracked Surveillance Unmanned Ground Vehicle", Proceedings of the IEEE International Conference on Robotics and Biomimetices. China, December 2010.

[10] B. Binoy, T. Keerthana, P. Barani, S.Aswathy, " A GSM based Versatile Unmanned Ground Vehicle", Proceedings of International Conference on Emerging Trends in Robotics and Communication Technologies. India, December 2010.

[11] D. Vidhya, N. Mapari, " Wireless Control and Transmission of Data for Underwater Robot", International Journal for Innovative Research in Science and Technology. India, vol. 2, pp. 364-369, May 2016.

Design of artificial neural network based power split controller for hybrid electric vehicle

Engr.Aqsa KK[1], Noor U Zaman Laghari[2]

Abstract:

The progress of a society and degree of civilization is increasing, major factor behind it is a said developing cars. Due to this increasing numbers of cars the pollution because of emission of internal combustion engine (ICE) in environment is increased and also fuel consumption is increased. To reduce the said fuel consumption and said environment pollution Hybrid Electric Vehicle (HEV) attracted many researchers to work on it. In this research paper, work presented to minimize the said fuel consumption a power spilt controller is designed based on artificial neural network (ANN) between two propelling source electric motor (EM) and ICE the data is taking through dynamic programing-the research is done to achieve better said fuel economy in nonlinear parallel hybrid electric vehicle (PHEV).In the ANN controller one input layer, one output layer, and two hidden layers are used. The matlab-simulation is used for the implementation and numpy-library is used for the training of the data. All the simulation result are discussed. The trained data is used. The data is tested on three driving cycle named NEDC, US06 and FTP-75 for both the thermal and hybrid vehicles.

1.Introduction

From many years a big attention has been inclined to the problems of automobiles consumption of fuel reduction and more highway vehicles. Concomitantly very ample concentration has been paid on emission pollutants reduction through automobiles and other vehicles. At higher temperatures if operated an engine then it can be realized the fuel consumption reduction and increased in the efficiency of thermodynamics. In engines substantial interest has been erected of ceramic materials endure higher combustion temperatures than those in active now [1]. On the other hand higher combustion temperatures in engines fuelled with gasoline cause to increase in certain undesirable pollutants, typically NOx.

One proposal is vehicles use should be limited which is powered by said ICE and instead employs the EM which are powered electric vehicles (EV) powered by said rechargeable batteries for reducing the pollution in the cities. All such electric cars (EC) have no more than 150 miles typically limited range, for hill climbing and acceleration having an insufficient power

[1] *Department of Mechatronics Engineering ,Mehran UET Jamshoro , Pakistan*
[2] *Department of Computer Systems Engineering, Mehran UET Jamshoro, Pakistan*
Corresponding Email: aqsa.kk@unifiedcrest.com

other than when the batteries are charged fully, and require ample time for the re-charging battery. Thus the finite range and extended batteries recharge time would not be an inconvenience in many circumstances and for all the travel necessity of most individuals such cars are not suitable [2]. Accordingly, for most users an electric car (EC) would have to be an supplementary vehicle, arranging a substantial economic deterrent. Moreover, coal-fired power plants is the source of generation of most electricity in the US (United States) and it will be appreciated, so using electric vehicles (EV) merely moves the point of supply of the pollution, but doesn't eliminate it .The respective net costs comparison of driving per mile, ethanol-fuelled vehicles (EFV) are not competitive with EV, with conventional gasoline-fuelled vehicles (GFV) [3].create these components, incorporating the applicable criteria that follow.

- Drive torque is supplied by a power unit to said output shaft and two or more drive wheels receiving torque for propelling said vehicle from an output shaft.

- A controllable torque transfer unit (TTU) adapted to receive torque from two sources through first and second input shafts and transmit the torque to said output shaft.

- An engine adapted to consume combustible fuel and supply torque to said torque transfer unit.

- An electric motor (EM) supply torque to said torque transfer unit and from a battery adapted to receive electricity.

- A stored electric energy in a battery is supplied to said motor and when motor is operated as a generator the storing electric energy received from a motor.

- For controlling the operation of electric motor (EM), engine and torque transfer unit (TTU) a controller is used, such that torque transfer unit (TTU) receives said torque.

- from either or both of electric motor (EM) and internal combustion engine (ICE) through first and second input shafts and transmit the torque from drive wheels by way of output shaft, For controlling the relative contributions of the EM and ICE to the said torque driving the wheels.

Where in the relative ratio of the rate of rotation of a said output member of torque transfer unit (TTU) to the rate of rotation of driven wheels, and the relative ratios of the rates of rotation of engine and EM to input shafts are fixed [4].

In many application of control system artificial neural networks (ANN) have been favorable used. But the learning algorithm based on ANN shows a great accomplishment when used off-line it means that before implementation they have to be fully trained.

"AN networks have extensively parallel distributed processor and have an natural propensity for storing developmental knowledge and making this knowledge accessible for use" by Haykin (1994).

The AN networks also resemble to the brain of the human in two aspects, they having a network similar to human brain networks and acquires a knowledge via a learning process and second they have an synaptic weights which is used to store these acquire knowledge. Similar to black box model AN networks require no detail information of the system. Instead, by studying the previous record data these neurons learn the relationships among the various input parameters. The AN networks have an ability that it can handle enormous and complex system with many interrelated parameters.AN networks concentrates on the more substantial inputs and ignores the input data having minimum significance. Our aim is to design a controller strategy which is based on AN networks in which controller takes substantial input and give it to the vehicle for the desired output [5-6].

The problem statement is:

1. The problem considered is to minimize the fuel consumption of an HEV that reconciles the drivers demanded vehicle velocity, by designing a controller for the Parallel Hybrid Electric Vehicle.
2. Many researchers worked on dynamic programing and neural network for energy management individually.
3. To our best knowledge combine the both strategies for the better energy management and fuel economy that are presented in this research, have not been addressed.

The aim of this research work is

- To compute the optimized fuel optimization and power split between ICE and EM using dynamic programing (off-line).
- To develop an artificial intelligence based power-split controller for real time driving condition.
- To train and test the design controller using the data from off-line optimization result.
- Test and simulate the designed controller for real time condition.
- Compare and contrast the results with existing strategies/controller for slandered driver cycle.

2. Literature review

Chan, C.C [7] developed rules based on heuristics, intelligence of the humans and math's model generally without prior knowledge of a drive cycle. These implementation rules are executed through lookup tables to share the demand of power between ICE and electric traction motor to meet driver requirements and other peripherals (electrical loads, battery) in the most effective technique. A good fuel economy as well as at the same time drivability and dynamic performance is also improved.

Hofman et al [8] research based on Rule-Based and Equivalent Consumption Minimization Strategies (RB-ECMS). Only one main design parameter is used and of many threshold control values and parameters no tuning is required. This design parameter represents the secondary power source maximum propulsion power (i.e. electric machine/battery) during pure electric driving. Comparison of RB-ECMS with the strategy based on DP. In this paper The RB-ECMS proposed requires significantly inferior computation time with the result similar as DP (within §1% accuracy).

Jhun Hana et al [9]-[10] the equivalent consumption minimization strategy (ECMS) is often considered as practical avenue while driving in the real world situation with uncertainties such as rugged road ECMS is used to control parameter as stated in rugged road so that the state of charge (SOC) is maintain inside the boundary and give the distinct improvement in fuel economy.

Jinming Liu and Huei Peng [11] developed THS power train dynamic model and then apply it for model-based control development. Introduced 2 control algorithms: one based on the stochastic dynamic programming method, and the second based on the ECMS. Both approaches determine the engine power depend on the overall vehicle efficiency to optimize engine operation apply to the electrical machines. These 2 algorithms performance is evaluate by comparing against the dynamic programming results, which are non-causal but provide theoretical benchmarks for more implementable control algorithms.

3. Model of parallel hybrid electric vehicle

3.1. Vehicle Parameter

TABLE I. Electric motor parameters.

S:NO	Components	Components Parameters	quantity
1	Said Internal Combustion Engine (SI)	Said Cylinders	4
		Said Litres	2.2
		Said peak power	84 kW
		Said mass	250 kg
2	Said Permanent Magnet Electric Motor (brushless)	Said peak power	53 kW
		Said peak torque	248 N.m
3	Said Nimh Ovonic Battery	Said capacity	28 Ah
		Said number of modules	50
		Said nominal voltage	6 V/module
		Said Energy density	48.6 Wh/kg
		Said Power density	444.4 W/kg
4	Said Vehicle Body	Said Mass	800 kg
		Said Wheel radius	0.27 m
		Said Veh. Drag Coeff.	0.48 Ns2/ m2
		Said Surf. Fric. Coeff.	0.3 (wet road)

3.2. Model (Equation of Motion)
3.2.1 Traction force
$F_Z = mg = F_{Z1} + F_{Z2}$ (1)

TABLE II. Vehicle parameters.

S:NO	Parameter	Value
1.	Said imax,mot	475 A
2.	Said Pmax,mot	53 kW
3.	Said ω max,mot	8000 rpm

Where,

$$F_{Z1} = mg \frac{l_2}{l} \ , F_{Z2} = mg \frac{l_1}{l} \quad (2)$$

3.2.2 Longitudinal forces

(F_x = actual wheel force)

$$| F_{xi} | \leq |F_{xi,max}| = F_{zi}, for \, i = 1, 2$$

3.2.3 Vehicle's acceleration

$$a_{veh} = \frac{F_{x1} + F_{x2} - F_d}{m} = \frac{F_x}{m} \quad (3)$$

3.2.4 Weight transfer due to acceleration

$$F_{Z1} = F_g \frac{l - l_1}{l} - \frac{(ma_{veh} + F_d)}{l}$$

$$F_{Z2} = F_g \frac{l_1}{l} + \frac{(ma_{veh} + F_d)}{l} \quad (4)$$

3.3. Power train Torques

3.3.1 Thermal engine torque

$$T_{engine} = T_{eng} - \frac{P_{loss,eng}}{eng} \quad (5)$$

3.3.2. Electric motor torque

$$T_{max,elec} = P_{map,motor}^{-1} (P_{max,elec}, _{mot}) \ (11)$$

3.4 Electrical Systems modelling
3.4.1. Open circuit voltage of battery

$$V_{oc} = \frac{q_{batt}}{C_{batt}} \quad (6)$$

3.4.2. Output voltage of battery

$$V_{output} = V_{oc} - \frac{d(q_{batt})}{dt} R_{batt} \qquad (7)$$

3.4.3 State of charge

$$SOC = \frac{V_{oc} - V_{min}}{V_{max} - V_{min}} \qquad (8)$$

where V_{min} and V_{max} represent the minimum and maximum allowable voltages of the battery. These minimum and maximum values are used as 250 and 400 V, respectively, compatible with the electric motor used in the simulation model.

TABLE III. ANN controller.

No	Component	Specification
1	Input Layer	1(Vehicle speed, Engine RPM)
2	Output Layer	1(2-Nodes, Split ratio, gear number)
3	Hidden layers:	2(each with 55 nodes)
4	Activation function	Rectified Linear Unit (RELU)
5	Learning method	Backward Propagation
6	Training Tool	Python, (Numpy library)
7	Implementation Tool	(Matlab-Simulink)

## 4. Artifical neural network controller

Specification for artificial neural network used in this research are given in table III.

5. Implementation of model phev in matlab –simulink

Following steps take place for the implementation of the model in Simulink

I. calculation of total torque from the Said EM and engine
II. Using an integrated transfer case (ITC) unit model block the distribution of total torque to the rear and front axles.
III. Said Rear model blocks and said front axles are separated from each other.
IV. For appropriate demand calculations the sensor information is passing to the said controller.
V. The simulation model contains a driver block, which selects appropriate driver commands (acceleration and braking) given a time-based drive cycle.

Simulation model Block diagram
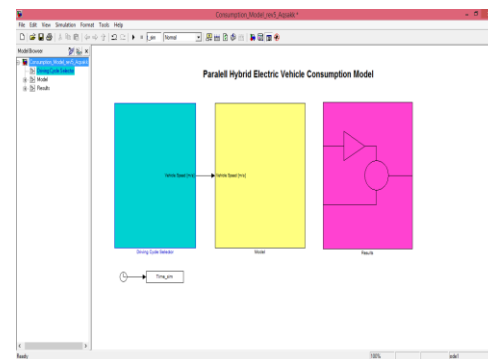
Fig. 1. PHEV model.

6. Results and Discussion

NEDC (New European Driving Cycle)

The graphs and result obtained from the NEDC driving cycle in order to obtained better said fuel economy by implementing dynamic programming and artificial neural network controller 1 strategies are discussed below.

In table 4 thermal engine vehicle having said average fuel economy ICE (start/ stop) mode has 13.89km/l. For Hybrid electrical vehicles average fuel economy for dynamic programing controller (DPC) is 20.57 km/l

and for artificial neural network controller is 19.71 km/l both are higher than thermal engines fuel economy. Battery SOC compensation supply is 20.73 km/l this increased compensation shows that from its present initial value battery SOC has raised final SOC becomes 51% whereas 50%. The initial present value. Overall DPC improvement and ANN is 48.09% and 49.24% respectively.in ANN Battery SOC compensation provided is 19.34 km/l this increased compensation hence the final SOC becomes 49.7 % less than the present value 50 %.where as in each option the overall improvement is 41.9% and 39.237%.

Fig. 2. Controller in Model.

Fig. 3. NEDC cycle.

FTP-75 (Federal test procedure)

The graphs and result obtained from the FTP-75 driving cycle on said conventional and hybrid both drivetrain in order to obtain improved said fuel economy and less emission are discussed below.

TABLE IV. Result of NEDC.

Driving cycle = NEDC (Initial SOC: 50%)	UNIT	THERMAL	HYBRID	
		ICE (start/stop)	DPC	ANN
Average fuel economy	[Km/l]	13.89	20.57	19.71
Average fuel economy with battery SOC compensation	[Km/l]	13.89	20.73	19.34
Final battery SOC	[-]		51	49.7
		% Difference in each option		
			48.09 %	41.9 %
			49.24 %	39.237 %

Fig. 4. FTP cycle.

In table V final result of FTP-75 The Said average fuel economy and having ICE only start/stop supplied by the base model consisting of thermal engine vehicle is 12.64 km/l. Hybrids embedded with dynamic programming based control strategy gives Average fuel economy with battery SOC compensation is of 18.49 km/l with battery SOC is 50%. The net improvement battery SOC compensation and in the fuel economy is 46.28% in each. Average fuel economy given by the artificial neural network controller is 17.66 km/l Battery SOC compensation supplied is 17.78 km/l this increased compensation shows that battery SOC has raised from its present initial value hence the final SOC becomes 49.7 % less than the present value 50 %.where as in each option the overall improvement is 39.71% and 40.664%. US06 DRIVING CYCLE

The graphs and result obtained from the US06 driving cycle are discussed.
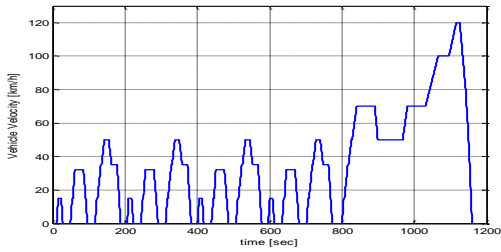
Fig. 5. US06 cycle.

US06 driving cycle in table VI, average fuel economy provided by The thermal embedded base model is 13.49 km/l . In hybrid electric vehicle with DPC the average fuel economy provided is 19.61 km/l with final SOC of a battery to 52% and with ANN controller average fuel economy to 19.79 km/l upgrading final battery SOC =52%.

TABLE V. Result of FTP.

Driving cycle = FTP (Initial SOC: 50%)	UNIT	THERMAL	HYBRID	
		ICE (start/stop)	DPC	ANN
Average fuel economy	[Km/l]	12.64	18.49	17.66
Average fuel economy with battery SOC compensation	[Km/l]	12.64	18.49	17.78
Final battery SOC	[-]		50	49.7
		% Difference in each option		
			46.28 %	39.71 %
			46.28 %	40.664 %

Improvement in fuel economy in both controller is 45.36% and 46.70% respectively. In DPC battery SOC compensation is 19.61 km/l and in Said ANN controller and Said

battery SOC compensation to 18.88 km/l, the improvement in compensation of SOC battery is 45.36% and 39.95% respectively with both controllers. Average fuel economy given by the artificial neural network controller is 17.66 km/l higher than Said fuel economy provided by thermal engines.

Battery SOC compensation provided is 17.78 km/l this boost compensation shows that battery SOC has raised from its present

TABLE VI. Result of US06.

DRIVING CYCLE: US06 (Initial SOC: 50%)	UNIT	THERMAL	HYBRID	
Average fuel economy	[Km/l]	13.49	19.61	19.79
Average fuel economy with battery SOC compensation	[Km/l]	13.49	19.61	18.88
Final battery SOC	[-]		50	52
% Difference in each option				
			45.36 %	46.70 %
			45.36 %	39.95 %

initial value hence the final SOC becomes 49.7 % less than the present value 50 %.where as in each option the overall improvement is 39.71% and 40.664%.

For study of US06 driving cycle in table IV, 50% SOC of a battery. Average fuel economy provided by the thermal embedded base model is 13.49 km/l. In case of dynamic programing HEV, the average fuel economy provided is 19.61 km/l and average fuel economy with battery SOC compensation is 19.61 km/l., 50% final battery SOC, The net productivity for both fuel economy and SOC compensation of battery is 45.36%.

7. Conclusion

The results of simulated PHEV are follows: An online Artificial Neural Network based power split controller was implemented within Hybrid vehicle fuel consumption model. The ANN optimization was achieved used the data from Dynamic Programming based offline controller. The ANN controller offers promising results as seen from the tabular data above. The proposed ANN controller slightly deviates in terms of consumption figures due to under-fitting. ANN control has also been found to have proper gear shifting during the simulation test runs (i.e. too frequent shifting, as exhibited by many other algorithms such as ECSM, is not observed).Battery SOC is appropriately maintained and utilized as depicted by results. Proposed controller Performance need to be further tried and tested for combination of multiple driving cycles.

REFERENCES

[1] J. M. Miller, "Propulsion Systems for Hybrid Vehicles," London: The Institution of Electrical Engineers, 2004.

[2] Gao and M. Ehsani, "An investigation of battery technologies for the Army's hybrid vehicle application," in Proc. of the IEEE 56th Vehicular Technology Conference, 2002.

[3] M. Ehsani, Y. Gao, S. E. Gay, and A. Emadi, "Modern Electric, Hybrid Electric, and Fuel Cell Vehicles":

Fundamentals, Theory, and Design, Boca Raton: CRC Press, 2005.

[4]   Gheorghe Livinţ, et al, "Control of Hybrid Electrical Vehicles." Technical University of aşi Romania,2011.

[5]   Vivek yadav mr. manish kashyap, "Neural Networks and their application" http://seminarprojecttopics.blogspot.com/2012/07/neural-networks.html, 21 ,APRIL , 2011.

[6]   ARTIFICIAL NEURAL NETWORK Seminar Report, [Accessed: 29 june, 2016].

[7]   Chan, C.C "The state of the art of electric ,hybrid and fuel cell vehicles", proceedings of the IEEE (Vol: 95, issue: 4), 2007

[8]   T. Hofman, M. Steinbuch, R.M. van Druten, and A.F.A. Serrarens "Rule-Based Equivalent Fuel ConsumptionMinimization Strategies for Hybrid Vehicles", Technische Universiteit Eindhoven, Dept. of Mech. Eng., Control Systems Technology

[9]   Cristian Musardo, Giorgio Rizzoni, Fellow, IEEE and Benedetto Staccia, "A-ECMS: An Adaptive Algorithm for Hybrid Electric Vehicle Energy Management", Proceedings of the 44th IEEE Conference on Decision and Control,2005.

[10] Jihun Hana, Young jin Parak, Dongsuk kumb, "Optimal adaptation of equivalent factor of equivalent consumption minimization strategy for fuel cell hybrid electric vehicles under active state inequality constraints ", vol 267, 2014.

[11] Jinming Liu and Huei Peng, "Modeling and Control of a Power-Split Hybrid Vehicle", Control Systems Technology , IEEE Transactions on (Vol:16 , Issue: 6), 2008.

An Experimental and Comparative study about the engine Emissions of conventional Diesel Engine and Dual Fuel engine

Ghazanfar Mehdi[1,2], Syed Asad Ali Zaidi[1,3], M.Mustafa Azeem[4], Salman Abdu[1]

Abstract:

Because of the high thermal effectiveness, consistency, flexibility and economical cost diesel engines are extensively used all around the world. Diesel engine emissions are producing serious environmental pollution which consists of oxides of nitrogen (NO_X), carbon monoxide (CO) and particulate matter (PM). So it's necessary to find the alternate solution to control diesel emissions. Natural gas is a highly attractive due to its clean burning, low cost, and wide availability. In this experimental work, single cylinder (8.6 Hp LA186F) four-stroke conventional diesel engine was studied. Natural gas is the major gaseous fuel used in dual fuel method which is up to 80% while diesel is used as a pilot fuel for the source of ignition up to 20%. In comparison with the conventional diesel method, it was observed that the dual fuel method significantly reduces the NO_X maximum up to 72.5%, carbon dioxide (CO_2) 34.5% and CO 59.8%. However, Hydrocarbon (HC) increased 66.76% in contrast with normal diesel combustion. During dual fuel mode, the emissions of HC and NO_X shows the inverse relation.

1. Introduction

Diesel engines are extensively used in the public transportation because of their higher stability and thermal effectiveness. Meanwhile, greenhouse gases are produced by transportation sector is about 30% of the world which leads to global warming [1]. Therefore, diesel engine is more responsible for the serious atmospheric hazards [2]. NO_X and PM are the main harmful components of diesel engine. NO_X emission produces photochemical smog which is a major source of acid rain [3]. It has been proved by numerous studies that these gases can be enormously harmful to the environment, especially living beings as health hazard [4]. Hence, emission regulations become stricter to reduce this environmental pollution. At the same time, energy consumption is growing rapidly and the fossil fuels are dwindling. In this regard, use of alternative fuels is necessary to meet the requirement of energy consumption and standard emission regulations. In public transport, natural gas is more environmental friendly among the various alternative fuels. Because of its clean burning, widely spread distribution stations, and lower cost [5].

[1] College of Power and Energy Engineering, Harbin Engineering University, Harbin, PR China.
[2] Faculty of Engineering Science and Technology, Indus University, Karachi, Pakistan
[3] Department of Engineering Sciences, PN Engineering College, National University of Sciences and Technology, Karachi, Pakistan.
[4] College of Nuclear Science & Technology, Harbin Engineering University, Harbin 150001, PR China.
Corresponding Email: ghazanfarmehdi22@gmail.com

1.1. Natural gas used as a substitute fuel

In comparison by means of other alternative methods, the more attractive source of energy is natural gas used in the internal combustion engines[6]. Natural gas has desirable advantages including low emission of greenhouse gases and reduction of capital costs. Currently, due to environmental issues and energy shortage problems, governments of the worldwide are looking to the natural gas as a substitute fuel for conventional diesel engine [7].

1.2. Physiochemical properties of natural gas

Methane is the major part of natural gas which is near about 90%.

TABLE I. Typical components of natural gas [8].

Content	Typical investigation (Vol. %)	Range (Vol. %)
Methane	94.9	87.0-96.0
Ethane	2.5	1.8-5.1
Propane	0.2	0.1-1.5
Isobutane	0.03	0.01-0.3
n-butane	0.03	0.01-0.03
Isopentane	0.01	Trace to 0.14
n-pentane	0.01	Trace to 0.14
Hexane	0.01	Trace to 0.06
Nitrogen	1.6	1.3-5.6
Carbon dioxide	0.7	0.1-1.0
Oxygen	0.02	0.01-0.1
Hydrogen	Trace	Trace to 0.02

But with methane, it also consists of many numbers of gases namely ethane, propane, pentanes, n-butane and lightweight alkanes. Nitrogen, carbon dioxide and traces of water vapors are also the components of natural gas. Natural gas properties vary according to the composition, source of production, and process used.

Table 1 shows the composition of natural gas [8]. Mostly, Natural gas consists of 87–96% of methane. Due to this reason, natural gas has same physical and chemical characteristics like methane.

Table 2 represents fuel properties of gasoline and diesel in comparison to natural gas [9–10]. In contrast with other fossil fuels, natural gas consists of less carbon per unit energy, therefore for public transport natural gas is environmental attractive as it produces low CO_2 emissions per mile. Although, because of the higher auto-ignition temperatures of natural gas it is intricate to used it in diesel engines. However, for spark ignition engines natural gas is very favorable because of anti-knock quality. Further, Natural gas is used in diesel engines without auxiliary modifications.

TABLE II. Physical and chemical characteristics of gasoline, natural gas and diesel [9–10].

Fuel Properties	Natural gas	Diesel	Gasoline
Low Heating Value(MJ/kg)	48.6	42.5	43.5
Heating value of stoichiometric mixture (MJ/kg)	2.67	2.79	2.78
Cetane number	-	52.1	13-17
Octane number	130	-	85-95
Auto-ignition temperature (°C)	650	180-220	310
Stoichiometric air-fuel ratio (kg/kg)	17.2	14.3	14.56
Carbon content (%)	75	87	85.5

2. Dual fuel concept

According to the dual fuel methodology, the intake manifold is used to mix the air stream and natural gas uniformly then it is introduced into the combustion chamber and pilot fuel with high

cetane number is used for ignition [11–12]. A systematic diagram of dual fuel mode is shown in Fig. 1.

In dual fuel mode, no serious modification is required. It is very easy to put in practice like a conventional diesel engine. However, this technology reduces more than 80% of diesel fuel [13]. The natural gas is introduced as a major gaseous fuel while diesel is only used for ignition purpose. Hence the performance of dual fuel has been increased.

With the use of dual fuel technology, the engine emissions decreased NOx, CO and PM emissions in comparison with a conventional diesel engine. Meanwhile, some type of problems related to the dual-fuel mode such as thermal efficiency relatively low during operation of the engine at the small and moderate loadings. Also, with the use of dual fuel emission of unburned hydrocarbon is increased considerably [14].
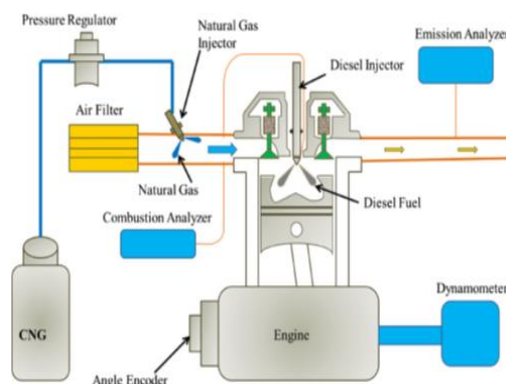

Fig. 1. The systematic diagram of dual fuel mode [15].

Fig.1 is a schematic representation of dual-fuel engine with its components highlighted in different colors.

3. Engine Emission Characteristics

3.1. Nitrogen Oxides (NOₓ)

In diesel engines, NO_x emissions are very harmful. It consists of nitrogen dioxide (NO_2) and nitrogen monoxide (NO). There are usually two mechanisms involved in the combustion mode which results in the NO_x formation namely as prompt mechanism (Fenimore mechanism) and thermal mechanism (Zeldovich mechanism).

Thermal NO_X depends upon the combustion temperature and amount of oxygen. In the thermal mechanism, if the engine in-cylinder temperature is higher than the 1800K, NO_x formation starts and it increases gradually with the increase of temperature [16].

In the prompt mechanism, during the fuel combustion hydrocarbon fragments especially CH_2 and CH reacts with N_2, resulting in the formation of prompt NO, which is the C-N species [17].

Thermal mechanism is accepted to be as the major contributor of NO_X during normal diesel engine operating conditions [18].

3.2. Carbon Monoxide(CO)

CO is the most detrimental emissions from a diesel engine. It is formed due to the presence of unburned fuel and in-cylinder combustion temperature. CO is mostly produced because of oxygen shortage in the fuel rich area. Also if the in-cylinder temperature is lower than 1450 k, CO can be increased in the fuel lean area [19].

3.3. Hydrocarbon (HC)

HC is also the outcome of unburned fuel in the combustion temperature. But for the entire oxidation, the temperature of HC is low. With the autonomy of actual fuel form, it has been observed to be near about 1200 K [20].

3.4. Carbon dioxide (CO₂)

CO_2 is produced due to complete burning of fuel during the combustion process. However, the fuel is first oxidized into CO, then due to the increase of combustion temperature and existence of oxygen concentration the fuel is further oxidized into CO_2. Therefore, CO_2 highly rely on in-cylinder temperature and oxygen presence.

4. Experimental Procedure

A single cylinder four stroke engine (8.6 Hp LA186F) has been used. In this experiment, the engine emission effects of the diesel engine and dual-fuel engine are investigated.

Initially, diesel fuel is used for five minutes only without any load until the engine reaches to stable operating state. Later engine speed is set at 1600 rpm through a throttle valve of the engine.

A TRICOR mass flow meter, Bronkhorst mass flow meter, and turbine mass flow meter were used for measuring the diesel fuel, natural gas, and air respectively. A portable gas analyzer (Autologic Company) was used to measure the exhaust emissions of the engine such as NO_X, CO, CO_2, and HC.

The calibration of the gas analyzer is necessary for obtaining the accurate measurements after each measurement. Primarily, all the experiments conducted at maximum operating load, then with moderate operating loads and keeping same engine speed.

The experiment was performed on three operating engine speeds 1600, 1800 and 2000rpm for efficient comparison. The engine was loaded till the maximum condition obtained for every speed. After finishing measurement on a diesel engine, it is necessary to cool engine for re-operation for accurate results.

In the dual fuel mode, initially, it is very essential to warm the engine by supplying the pilot fuel for five minutes. Then, natural gas is allowed to the cylinder, passing through the gas regulator. The pilot fuel remains unchanged throughout the experiment. But the flow of natural gas is increased only for obtaining and controlling the particular engine speeds.

5. Results and Discussion

5.1. Exhaust Emission for Maximum and Moderate Load Operating Conditions

5.1.1. Oxides of Nitrogen (NO_x)

It has been proved that in the dual fuel engine, NO_x emissions are reduced in both moderate and maximum operating loading conditions in comparison with conventional diesel fuel engine. In both conventional diesel mode as well as dual fuel mode NO_x emission increases with the rise of engine speed which also results in the rise of exhaust temperature. This can be represented in Fig. 2.

Natural gas possesses a high value of specific heat capacity as compared with air. Since with the use of natural gas overall heat capacity rises due to this reason mean temperature reduces close to the ending of the compression stroke and throughout the whole combustion practice.

The NO_X formation is directly associated with the increase of engine in-cylinder temperature. However, the result is more efficient because at lower engine load combustion temperature is always reduced as the quantity of air and oxygen concentration lessen by means of natural gas. When the speed of the engine increases there is lesser time for the formation of NO_X because of which the emission of NO_X decreases.

In dual fuel engine, ignition delay occurs because of the poor burning of natural gas. Due to this in-cylinder temperature decreases which result in a reduction of NO_X emission.

According to the dual fuel mode, NO_x emissions are reduced up to an average of 73% at maximum operating conditions and 72% at moderate operating conditions. Consequently, overall NO_x reduction throughout the experiment is 72.5% that can be clearly seen in Fig 2.
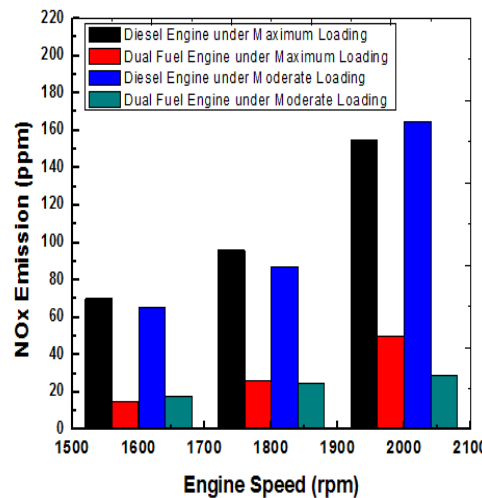
Fig. 2. Exhaust NO_X Emission for Maximum and Moderate Loading with different engine speeds.

5.1.2. Carbon Dioxide

It has been found that in the dual fuel mode, CO_2 emissions are reduced for both moderate and maximum operating loading conditions as compared with conventional diesel fuel engine as seen in Fig. 3.

In dual fuel mode, CO_2 emissions are lower because natural gas is low carbon content as compared with the diesel fuel. In dual fuel process, there is a problem of poor combustion because little amount of the fuel is not completely oxidized to CO and flow out from the exhaust valve, which leads to the decrease of CO_2 emission.

With the increase of engine speed, the amount of CO_2 emission also increases because the engine required more fuel. Therefore the number of carbon contents increases in the combustion chamber. Due to the larger carbon content chains in the diesel fuel, the range of CO_2 is higher at all speeds of engine.

According to the dual fuel mode, CO_2 emissions are reduced up to an average of 37% at maximum operating conditions and 32% at moderate operating conditions. Consequently,
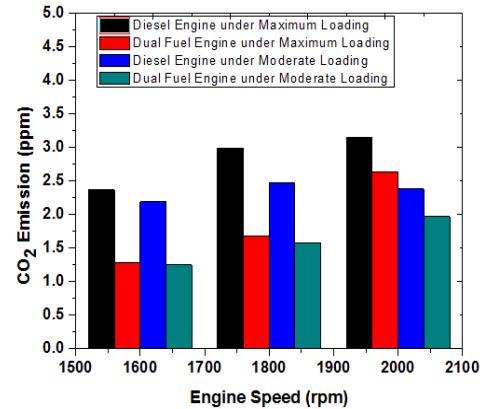

Fig. 3. Exhaust CO_2 Emission for Maximum and Moderate Loading with different engine speeds

overall CO_2 reduction throughout the experiment is 34.5% that can be clearly seen in Fig. 3.

5.1.3. Carbon Monoxide

It has been proved that in the dual fuel mode the CO emissions are reduced in both moderate and maximum operating loading conditions in comparison with conventional diesel fuel engine as shown in Fig.4. However, if the engine is running at lower speed, CO reduction is more noticeable.

CO is produced because of the incomplete fuel combustion, engine coldness and lacking of air concentration in the cylinder. With the decrease of air to fuel ratio, the amount of CO increases, if the mixture is rich with fuel.

In dual fuel mode, emissions of carbon monoxide decreased as compared with normal diesel engine with varying engine speeds. Due to the better combustion efficiency of natural gas produces less amount of CO, because natural gas is a gaseous fuel generally contains little quantity of contaminants than diesel fuel.
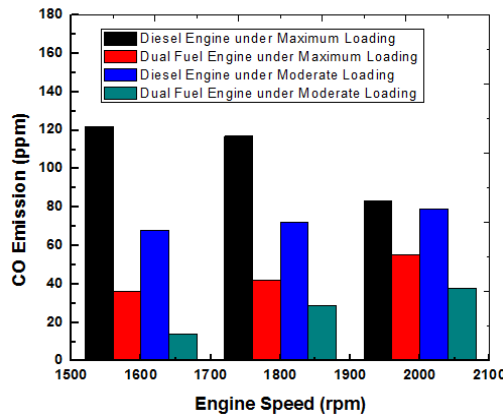
Fig. 4. Exhaust CO Emission for Maximum and Moderate Loading with different engine speeds.

With the increase of engine speeds, CO emission increased in dual fuel method. However, when engine speed increases the dwelling time of fuel inside the cylinder shorten, resulting in superior CO formation.

According to the dual fuel mode, CO emissions are reduced up to an average of 56% at maximum operating conditions and 63.66% at moderate operating conditions. Consequently, overall CO reduction throughout the experiment is 59.8% that can be clearly seen in Fig.4.

5.1.4. Hydrocarbons

It has been observed in the dual fuel mode the amount of HC emissions are much more increased in both moderate and maximum operating loading conditions in comparison with normal diesel engine as shown in Fig.5.

However, the HC increased several times in comparison with normal diesel combustion. This is due to the incomplete combustion and remains of unburned fuel in the combustion chamber.

In dual fuel mode, it shows trade-off connection in between HC and NO_X emission, due to less air to fuel ratio oxygen concentration is not enough for combustion process.

The level of HC emissions are reduced when load increases, resulting in better efficiency for the combustion. Due to this, it is observed that

HC emission level is lower during maximum loading conditions. It has been found that in dual fuel method HC reduced when the engine speed is increased since the combustion process is better when the engine operates at high speeds.

Due to the scavenging process during the valve opening time, a small amount of air and natural gas mixture directly passed through the exhaust valve, which results the increase of HC.
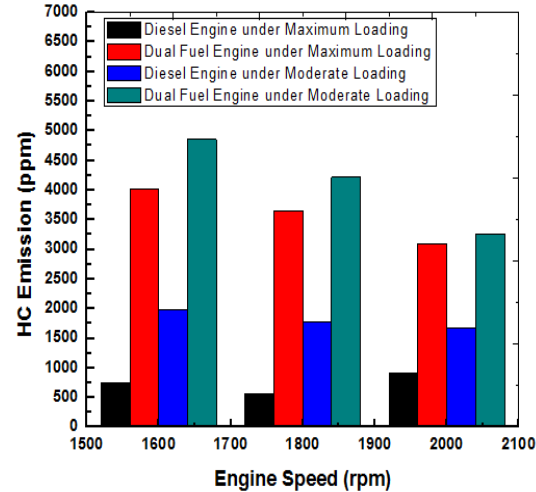

Fig. 5. Exhaust HC Emission for Maximum and Moderate Loading with different engine speeds.

According to the dual fuel mode, HC emissions are increased up to an average of 78.5% at maximum operating conditions and 55% at moderate operating conditions. Consequently, overall HC increment throughout the experiment is 66.76% that can be clearly seen in Fig.5.

6. Conclusion

In this study, it has been established that a significant reduction takes place in NO_X, CO_2 and CO emissions with the use dual fuel mode in comparison with the normal diesel engine. However, HC emission is increased several times in comparison with diesel fuel engine. In dual fuel mode, it shows the trade-off link in between HC and NO_x emission. Therefore our investigation concludes that dual fuel engine is

more environmental friendly in contrast with diesel engine.

REFERENCES

[1] Pan HS, Pournazeri S, Princevac M, et al. Effect of hydrogen addition on criteria and greenhouse gas emissions for a marine diesel engine. Int J Hydrog Energy;39:11336–45, 2014.

[2] W. Tutak, K. Lukács, S. Szwaja, Á. Bereczky, Alcohol–diesel fuel combustion in the compression ignition engine, Fuel. 154,196–206. 2015.

[3] L. Stayner, D. Dankovic, R. Smith, K. Steenland, Predicted lung cancer risk among miners exposed to diesel exhaust particles,Am. J. Ind.Med. 34 (3) 207–219. 1998).

[4] J.D. McDonald, M.D. Reed, M.J. Campen, E.G. Barrett, J. Seagrave, J.L. Mauderly.

[5] A. Demirbas, Methane gas Hydrate: Springer Science & Business Media, 2010.

[6] Korakianitis T, Namasivayam AM, Crookes RJ. Natural-gas fueled spark ignition (SI) and compression-ignition (CI) engine performance and emissions. Prog Energy Combust Sci;37(1):89–112. 2011.

[7] Jin K, Takashi O, Yasuhiro D, Ryouji K, Takeshi S. Combustion and exhaust gas emission characteristics of a diesel engine dual fueled with natural gas. JSAE Rev;21(4):489–96,2000.

[8] A. Demirbas, Methane gas Hydrate: Springer Science & Business Media, 2010.

[9] Q.C. Zhang, G.S. Chen, Z.Q. Zheng, H.F. Liu, J. Xu, M.F. Yao, Combustion and emissions of 2,5-dimethylfuran addition on a diesel engine with low temperature combustion, Fuel 103 730–735. 2013.

[10] B.B. Yang, M.F. Yao, W.K. Cheng, Z.Q. Zheng, L. Yue, Regulated and unregulated emissions froma compression ignition engine under low temperature combustion fuelled with gasoline and n-butanol/gasoline blends, Fuel 120 ,163–170. 2014.

[11] O.M.I. Nwafor, Effect of choice of pilot fuel on the performance of natural gas in diesel engines, Renew. Energy 21 (3–4),495–504. 2000.

[12] A. Paul, R.S. Panua, D. Debroy, P.K. Bose, Effect of compressed natural gas dual fuel operation with diesel and Pongamia pinnata methyl ester (PPME) as pilot fuels on performance and emission characteristics of a CI (compression ignition) engine, Energy 68 ,495–509, 2014.

[13] R.G. Papagiannakis, D.T. Hountalas, C.D. Rakopoulos, Theoretical study of the effects of pilot fuel quantity and its injection timing on the performance and emissions of a dual fuel diesel engine, Energy Convers. Manag. 48 (11) 2951–2961, 2007.

[14] Liu H, Wang Z, Long Y, Xiang SZ, Wang JX, Scott , Wagnon W. Methanol-gasoline Dual-fuel Spark Ignition (DFSI) combustion with dual-injection for engine particle number (PN) reduction and fuel economy improvement. Energy;89:1010–7, 2015.

[15] Wang-Helmreich H, Lochner S. The potential of natural gas as a bridging technology in low-emission road transportation in Germany. Therm Sci;16(3)729–46, 2012.

[16] J.B. Heywood, Internal Combustion Engine Fundamentals: Mcgraw-Hill New York, 1988.

[17] S.K. Hoekman, C. Robbins, Review of the effects of biodiesel on NOx emissions, Fuel Process. Technol. 96, 237–249, 2012.

[18] C.T. Bowman, Kinetics of pollutant formation and destruction in combustion, in: N.A. Chigier (Ed.), Energy and Combustion Science (Student Edition One).,33–45 (Pergamon1979).

[19] T. Kitamura, J. Senda, H. Fujimoto, Mechanism of smokeless diesel combustion with oxygenated fuels based on the dependence of the equivalence ratio and temperature on soot particle formation, Int. J. Eng. Res. 3 (4) 223–248. 2002.

[20] J. Liu, F. Yang, H.W. Wang, M.G. Ouyang, S.G. Hao, Effects of pilot fuel quantity on the emissions characteristics of a CNG/diesel dual fuel engine with optimized pilot injection timing, Appl. Energy 110,201–206, 2013.

0.7" ↕ Margin Top

Paper Formatting Guidelines

Title: 14ᵖᵗˢ Bold

Author Name: 11ᵖᵗˢ Bold

Affiliation: 11ᵖᵗˢ Italic

Abstract: Single Paragraph (Min: 150 – Max: 250 words)

Paper Length: Formatted as guided (Min: 4,000 – Max: 8,000 words)

Font: Times New Roman 10ᵖᵗˢ

Font Color: Black

Line Spacing: 1.0 (single line space throughout the paper)

Indentation: Justify

References & In-text Citations: Follow the IEEE & Use EndNote X7 for In-text citations and Bibliography.

Headings: 12ᵖᵗˢ Bold

1. **12ᵖᵗˢ Bold**
   1.1. **11ᵖᵗˢ Bold**
      1.1.1.   *11ᵖᵗˢ Bold Italic*

Margin Left
0.8" ←→

Margin Right
0.5" ←→

6.5"x10"

Page Size: 6.5" (Width) x 10" (Height)

Submission: Formatted paper as guided can be submitted through our online submission system at http://sjcms.iba-suk.edu.pk

1.9" ↕ **Margin Bottom**

Sukkur IBA
Journal of
Emerging Technologies

Sukkur
IBA
University

SUKKUR IBA UNIVERSITY
Merit - Quality - Excellence